Project funded by the European Commission under the 6th (EC) RTD Framework Programme (2002- 2006) within the framework of the specific research and technological development programme “Integrating and strengthening the European Research Area”

Project UpWind

Contract No.:
019945 (SES6)

“Integrated Wind Turbine Design”

CONCEPT REPORT on GENERATOR TOPOLOGIES, MECHANICAL & ELECTROMAGNETIC OPTIMIZATION

(Deliverable No.: D 1B2.b.1)

Part 1 (TUD, AAU) – Page 1 - 51

Part 2 (EDIN) – Page 52 - 79

Part 1

AUTHOR:	Henk Polinder[1], Deok-Je Bang[2], H. Li[3], Z. Chen[4]
AFFILIATION:	Delft University of Technology[1, 2], Aalborg University[3, 4]
ADDRESS:	Mekelweg4, 2628CD Delft, the Netherlands[1, 2], Aalborg East DK-9220, Denmark[3, 4]
TEL.:	+31 15 27 818441[1, 2],
EMAIL:	h.polinder@ewi.tudelft.nl[1], d.bang@ewi.tudelft.nl[2], lih@iet.aau.dk[3], zch@iet.aau.dk[4]
FURTHER AUTHORS:	
REVIEWER:	Project members
APPROVER:	

Document Information

DOCUMENT TYPE	Deliverable
DOCUMENT NAME:	Deliverable_1B2.b.1.pdf
REVISION:	1
REV.DATE:	4/12/2007
CLASSIFICATION:	R1: Restricted to project members
STATUS:	

Comment on structure of deliverable report:

This deliverable report is divided into two parts: the first part reporting on the activities and results of Delft University of Technology and of Aalborg University, the second part reporting the milestone of University of Edinburgh, which is part of this deliverable.

Abstract:

Wind energy is currently the most cost-effective energy source to produce electricity among various renewable energy sources with significant growth of power capacity installed worldwide, and with rapid development of technology. During last two decades, various wind turbine concepts with different generator systems have been developed and built to maximize the energy capture, to minimize costs, to improve power quality, and others. Therefore, an overview of wind turbine technologies and a comparison of different generator topologies in literature and on the market is necessary. This report surveys the trend of wind turbine technology including various control concepts, various generator systems, and market states in literature. Secondly, promising direct-drive permanent magnet machines, which are the axial, radial and transverse flux machine, are also surveyed in literature to find the most suitable generator type for direct-drive large scale (offshore) wind turbine. The advantages and disadvantages of each type are investigated and discussed. Finally, the comparison of different generator topologies based on the technical data and market aspects is introduced with comparison criteria.

Contents

STATUS, CONFIDENTIALITY AND ACCESSIBILITY											
Status				**Confidentiality**				**Accessibility**			
S0	Approved/Released			**R0**	General public			Private web site			
S1	Reviewed			**R1**	Restricted to project members			Public web site			
S2	Pending for review			**R2**	Restricted to European. Commission			Paper copy			
S3	Draft for commends			**R3**	Restricted to WP members + PL						
S4	Under preparation			**R4**	Restricted to Task members +WPL+PL						

PL: *Project leader* **WPL:** *Work package leader* **TL:** *Task leader*

1. Introduction

The need for renewable energy source as wind energy, solar energy, wave energy, and others has increased during the 20th century, since limited fossil fuel and environmental concern have made it necessary to find renewable energy. The oil crises in the 1970s encouraged the need for renewable energy. Among different renewable energies, wind energy has achieved the fastest growth in the world because of its high potential as the wind exists everywhere on the earth and the wind is the most cost-effective way to produce electricity.
The average annual growth rate of wind energy is around 30% during last ten years [131][132]. Global wind electricity-generating capacity increased by 24% in 2005 to 59,100 megawatts (MW). This represents a twelve-fold increase from a decade ago, when world wind-generating capacity stood at less than 5,000 MW (See Fig.1-1 [132]). By the end of 2020, it is expected that this figure will be increased to over 1,260,000MW, which will be sufficient for 12% of the world's electricity consumption [127][133]. Fig. 1-2 depicts the annual wind power installed capacity of different countries. It can be seen that Europe continues to lead the world in total installed capacity with over 40,500MW, or two-thirds of the global total. The European Wind Energy Association (EWEA) has set a target to satisfy 23% European electricity needs with wind by 2030 [132]. Therefore, the global market for the electrical power produced by wind turbine generators has been increasing steadily, which directly pushes the wind technology into a more competitive area.

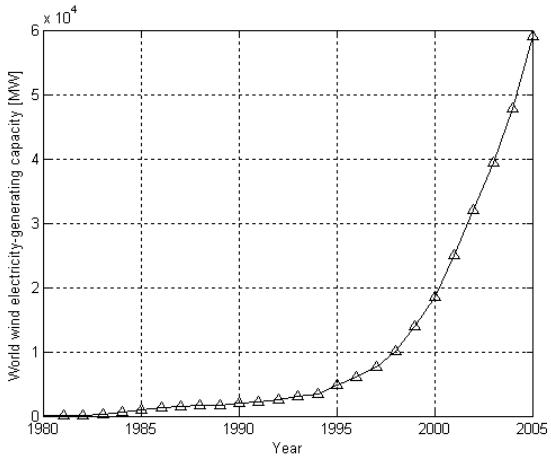

Fig. 1-1: *World wind electricity generating capacity during 1980-2005*

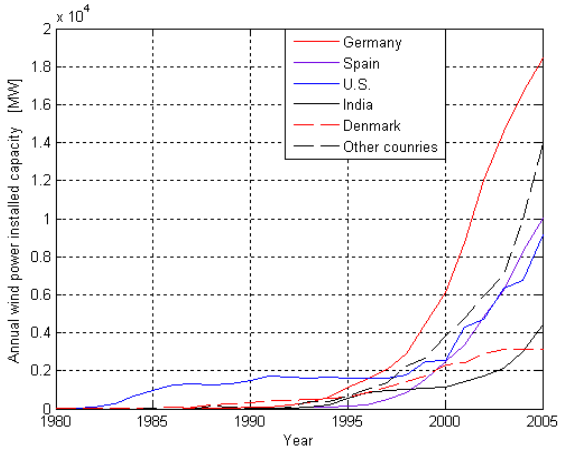

Fig. 1-2: *Annual wind power electricity generating capacity by different countries during 1980-2005*

Various wind turbine concepts have been developed and built to maximize annual energy capture, minimize costs, provide consistent dynamic response, improve power quality, and ensure safety together with the growth of wind energy during last two decades [5].
The three main types of typical generator systems for large wind turbines are the following [127][133][134][135]. The first type is a fixed-speed wind turbine system using a multi-stage gearbox and a standard squirrel-cage induction generator (SCIG), directly connected to the grid. The second type is a variable speed wind turbine system with a multi-stage gearbox and a doubly fed induction generator (DFIG). The power electronic converter feeding the rotor winding has a power rating of approximately 30% of the rated power; the stator winding of the DFIG is directly connected to the grid. The third type is also a variable speed wind turbine, but it is a gearless wind turbine system with a direct-drive generator. It uses a low-speed high-torque synchronous generator and a full-scale power electronic converter for the grid connection. For increasing power levels and decreasing rotor speeds, these direct-drive wind generators are becoming larger and more expensive. An interesting alternative may be a mixed solution, a single-stage gearbox and a smaller low speed permanent magnet synchronous generator (PMSG), which is the multibrid system [1][72][135]. Considering various types of existing wind generators and new generator topologies being developed for wind turbines, how to design and choose the more cost-effective generator topologies for large wind turbines is an interesting issue, because each type has its strengths and weaknesses.
On the other hand, the scale of wind turbine installed in the world is increasing, and the installation location of the turbine is moving to offshore in recent years, because of space limitation to install onshore, higher wind speed and less turbulence offshore.
The growth of wind turbine size is presented in Fig. 1-3 and Fig. 1-4. The annual average wind turbine sizes installed worldwide during 1995-2004 is presented in Fig. 1-3 [127]. The average size installed in 1995 was around 400 kW, and the average size in 2003 and 2004 was over 1.2 MW which is three times larger than the size in 1995. The scale growth of wind turbines on the market during 1980-2005 is also presented in Fig. 1-4. Currently 5 MW wind turbines are commercially available [128]. Larger (offshore) wind turbines are currently being developed.

As mentioned above, the trend of wind turbines including concept, generator system, scale and installation location has been improved and changed on the market during last two decades.
Therefore this report investigates wind turbine technology, generator systems, and direct-drive PM machines for large scale (offshore) wind turbines as an early step to find the most suitable generator system.

This report is organized as follows. First, it gives an overview of wind turbine technology including various control concepts, generator systems, and trends on the market. Secondly, a literature survey on promising direct-drive PM machines as axial, radial and transverse flux machine is presented. Finally, the comparison of different generator systems is described considering quantitative comparisons and comparison criteria.

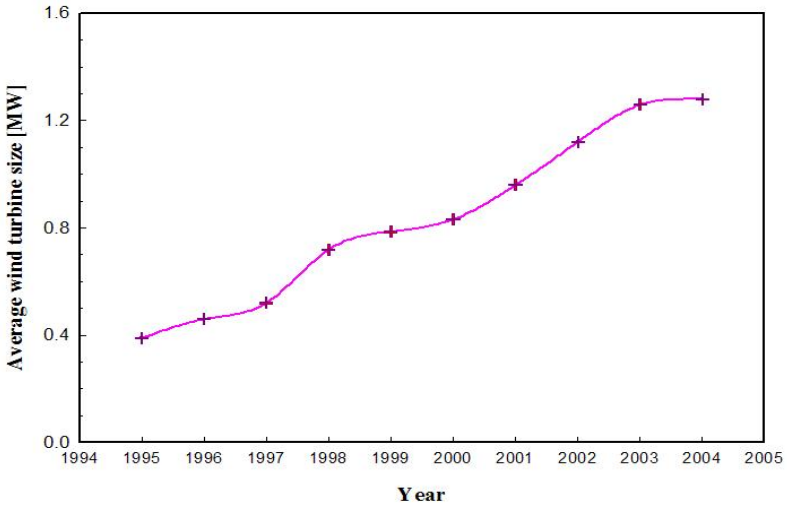

Fig. 1-3: *Annual average wind turbine size installed worldwide during 1995-2004*

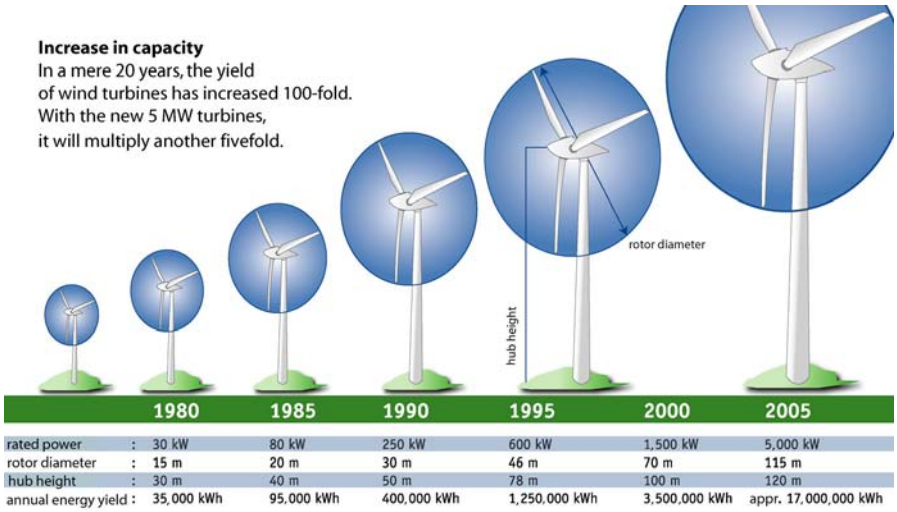

Fig. 1-4: *Development of power and size of wind turbines (Source: Bundesverband WindEnergie e.V.)*

2. Overview of wind turbine technology

Various wind turbine concepts have been rapidly developed during last two decades. When the rotation speed is considered, these concepts can be classified into fixed speed (F.S.), limited variable speed (L.V.S.), and variable speed (V.S.). When the power regulation is considered, these concepts can be classified into stall and pitch control. When the drive train is considered, these concepts can be classified into geared drive and direct-drive systems.
In case of the fixed speed wind turbine concept, the stall, active stall and pitch control have been developed and used with a squirrel cage induction generator (SCIG) and a gearbox. The limited variable speed wind turbines have used a wound rotor induction generator (WRIG) with a gearbox. In the variable speed wind turbines, the pitch control has been used with different generator systems.
Among various wind turbine concepts, the fixed speed stall control wind turbines were mostly manufactured with a SCIG and a multiple-stage gearbox during the 1980's and 1990's. Since the late 1990's, most wind turbines, of which power level was increased above 1.5 MW, have been changed to the variable speed control concept because of the grid requirement for good power quality. Generator systems of variable speed wind turbines mostly used consist of a doubly-fed induction generator (DFIG), a multiple-stage gearbox and a power electronic converter. Since 1991, direct-drive wind turbine systems have been built to reduce failures in the gearbox and to lower maintenance problems [1, 2].
This chapter describes features of three different wind turbine concepts as F.S. concept, L.V.S. concept, and V.S. concept including power regulation method, drive train and generator type. Table 2-1-1 shows the concepts which have been used and built on the market, and the details of each concept are described in next subsections.

Table 2-1-1: *Different wind turbine concepts*

	F.S. concept			**L.V.S. concept**	**V.S. concept**						
Power regulation method	Stall	Active stall	Pitch	Pitch	Pitch						
Drive train type	GD	GD	GD	GD	GD					DD	
Generator type	SCIG	SCIG	SCIG	WRIG	DFIG	SCIG	PMSG	PMSG	PMSG	EESG	PMSG
Gearbox	3 stage	3 stage	3 stage	3 stage	3 stage	3 stage	3 stage	1 stage	2 stage + Hydro	-	-
Speed	2 speed	2 speed	2 speed	Optislip	Variable speed	Variable speed	Variable speed	Variable speed	Variable speed	Variable speed	Variable speed
Subsection for each concept	2-1	2-1	2-1	2-2	2-3	2-3	2-3	2-5	2-6	2-4	2-4

2.1 Fixed speed concept

2.1.1 Stall control

The fixed speed stall control concept includes single speed and two speed stall control concepts. The wind turbine with the fixed speed stall control concept consists of mainly a tower and foundation, nacelle and yaw system, rotor blades, bearings, brakes, a multiple-stage gearbox, and a squirrel cage induction generator (SCIG) directly connected to the grid through a transformer as illustrated in Fig. 2-1-1. It is known as “Danish concept”. The rotor blades have simple construction because the blade is directly fixed on the hub. The angle of the rotor blades of this concept is adjusted only once when the turbine is erected. The power limitation over the rated wind speed is achieved by the stall effect of the rotor blades. The wind turbine with this concept is completely passive while the wind causes the power regulation by itself. Therefore this concept is called a passive stall control concept or shortly a stall control concept. This concept is very simple, robust and old concept on the market. Wind turbines of this concept were mostly manufactured during the 1980’s and 1990’s.
However, this concept is not very flexible because the performance of rotor blades is optimal only at one wind speed. Therefore the efficiency of rotor blades is not constant over wide range of the wind speed. This concept also causes varying amounts of active and reactive power from the grid, resulting in flicker. During the 1980’s this concept was extended with a capacitor bank for reactive power compensation and with a soft-starter for smoother grid connection.
The two speed stall control concept has been developed to overcome a disadvantage of single speed stall control concept by using a pole changeable SCIG. A pole changeable SCIG, which leads two rotation speeds, has been used for both the fixed speed (active) stall control concept and the fixed speed pitch control concept with a multiple-stage gearbox. A pole changeable SCIG is useful to increase the efficiency of rotor blades and to reduce the audible noise at low wind speeds.
This concept has been used by the manufacturers as Neg-Micon (currently Vestas), Made, and Nordex on the market.
The fixed speed geared generator concept with a pole changeable SCIG has been also used in the active stall control and the pitch control. Therefore the details of SCIG system are described in this subsection. The features of both the active stall control and the pitch control are described in subsection 2.1.2 and 2.1.3.
In general, the pole pair number is mostly equal to 2 or 3 in this type commercial fixed-speed wind turbine with SCIG, so that the synchronous speed in a 50Hz-grid is equal to 1500 or 1000 rpm. Therefore, a three-stage gearbox in the drive train is usually required.
The advantages of SCIG are well-known and robust technology; easy and relatively cheap mass production of the generator. In addition, there is no electrical connection between stator and rotor system. Furthermore, it enables stall regulated machines to operate at a fixed speed when it is connected to a large grid which provides a stable control frequency, which is the most common type of generator used for the grid connected wind turbines [24][137].
The disadvantages of SCIG are as follows:

- The speed is not controllable and variable only over a very narrow range. Any wind speed fluctuations are directly translated into electromechanical torque variations, rather than rotational speed variations. This causes high mechanical and fatigue stresses on the system (turbine blades, gearbox and generator), and may result in swing oscillations between turbine and generator shaft. Also the periodical torque dips due to the tower shadow and shear effect are not damped by speed variations, and result in high flicker values. Fluctuations in power output are hardly damped, compared with wind speed fluctuations [137]. The turbine speed cannot be adjusted to the wind speed to optimize the aerodynamic efficiency. It must be mentioned however that many commercial wind turbines can switch between two pole-pair numbers, e.g. p=2 or 3, by a rearrangement of the stator windings connection. This

allows setting up one turbine speed for low wind speeds (p=3 or higher) and one for high wind speeds (p=2), but it does not provide continuous speed variations.
- In general, a three-stage gearbox in the drive train is necessary. Gearboxes represent a large mass in the nacelle, and also a large fraction of the investment costs. They are relatively maintenance intensive and a possible source of failures.
- It is necessary to obtain the excitation current from the stator terminals. This makes it impossible to support grid voltage control. In most cases, capacitors are grid-connected parallel to the generator to compensate for the reactive power consumption.

2.1.2 Active stall control

The fixed speed active stall control concept can supply the power to the grid as good as possible by turning the rotor blades which cause or delay the stall effect.
This concept has been used by the manufacturers as Bonus (currently Siemens) and Neg-Micon (currently Vestas) on the market.

2.1.3 Pitch control

The fixed speed pitch control concept has the opposite turning direction of the rotor blades compared to the fixed speed active stall control concept in regulating wind turbine power.
This concept needs more powerful pitch drives than the fixed speed active stall control concept, and has problems to apply into large wind turbines because of the late turning of rotor blades by the high inertial of the blades.

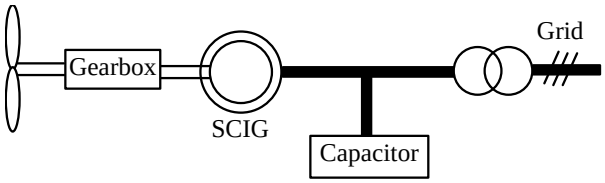

Fig. 2-1-1: *Scheme of a SCIG system*

2.2 Limited variable speed concept

The limited variable speed concept is known as the OptiSlip concept, which was applied by Vestas since the mid 1990's [24]. The basic idea of this concept is to control the rotor resistance using a variable external rotor resistance by means of a power electronic converter, as shown in Fig. 2-2-1. It is basically a single-fed induction generator with the same characteristics as a SCIG. With the power electronic converter mounted on the rotor shaft, it is possible to control the slip (by controlling the external rotor resistance) over a 10% range [131]. The most suitable torque-speed characteristic can be chosen to obtain the optimal speed at the operating point. Only speeds higher than synchronous speed are possible for generator operation, and the rotor power is not fed back into the grid.

The manufacturers as Vestas and Suzlon are using this concept on the market.

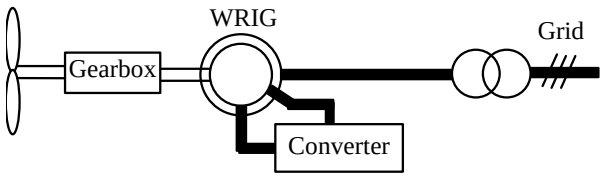

Fig. 2-2-1: *Scheme of a WRIG system (OptiSlip)*

2.3 Variable speed concept with multiple-stage gearbox

Since the late 1990's, most wind turbines over 1.5 MW output power have been changed to the variable speed control concept because of the grid requirement of good power quality. A wind turbine with fixed speed is operated at its highest efficiency only within a narrow range of wind speed as discussed above. The variable speed control is necessary to maximize the efficiency of the turbine, to dampen the power and torque peaks cause by wind gust, to let the turbine accelerate and to store energy in it during gust [2].
A wind turbine with variable speed pitch control mostly has a multi-stage gearbox, a generator, a power electronic converter and a blade pitch system. The frequency of the generator is varied for the grid connection by the converter. This concept has been applied successfully to large wind turbines although the cost of power electronics is a disadvantage compared to fixed speed systems.
Variable speed pitch control concept has two methods for operation as speed changes and blade pitch changes. Between the cut-in wind speed and rated wind speed, the wind turbine of this concept is operated at fixed pitch with a variable rotor speed to maintain an optimal tip speed ratio. When the rated power is reached, the generator torque controls the electrical power output, while the pitch control is used to maintain the rotor speed within acceptable limits. During gusts the generator power can be maintained at a constant level, while the rotor speed increases. The increased energy in the wind is stored in the kinetic energy of the rotor blades. If the wind speed is decreased, the decreased aerodynamic torque results in a deceleration of the rotor blade while the generator power is kept constant. If the wind speed remains high, the rotor blade pitch can be changed to reduce the efficiency of rotor blades and torque, once again reducing the rotor speed [5].

The reasons for the variable speed control can be summarized as follows [8, 9]:

- improved output power quality
- increased energy capture
- reduced noise
- reduced mechanical stress of the drive train

2.3.1 DFIG system

The doubly fed induction generator (DFIG) is the popular generator type for large wind turbines, since the rating of a power electronic converter could be reduced to roughly 30% of full scale. The connection scheme of a DFIG is shown in Fig. 2-3-1. The stator is constructed in the same way with a SCIG. The rotor is equipped with a three-phase winding and connected to the grid through the power electronic converter. The basic operation principle is same as a SCIG. However, the rotor active power can be controlled by the current of the rotor side converter. Typically, by controlling the rotor active power flow direction, a speed range $\pm$ 30% around the synchronous speed can be obtained. Instead of dissipating the rotor energy, it can be fed into the grid. The choice for the rated power of the rotor converter is a trade-off between costs and speed range desired. Moreover, this converter performs reactive power compensation and smooth grid connection.
It is the advantage of a DFIG that the speed is variable within a sufficient range with limited converter cost. The stator active and reactive power can be controlled independently by controlling the rotor currents with the converter. Furthermore, the grid-side converter can control its reactive power, independently of the generator operation. This allows the performance of voltage support towards the grid.

According to the trends on the market, the variable speed pitch control concept with both DFIG and a multiple-stage gearbox seems to be a most attractive concept because many manufacturers have used this concept. However DFIG system has disadvantages as follows:

- heat dissipation by friction of gearbox
- regular maintenance of gearbox
- audible noise from gearbox
- high torque peaks in the machine and large stator peak currents under grid fault conditions
- the brush-slip ring set to bring power to the rotor needs maintenace
- external synchronization circuit required between the stator and the grid to limit the start-up current
- In case of grid disturbances, the ride-through capability of DFIG is required so that the control strategies may be very complex. Detailed transient models and good knowledge of the DFIG parameters are required to make a correct estimate of occurring torques and speeds [138].

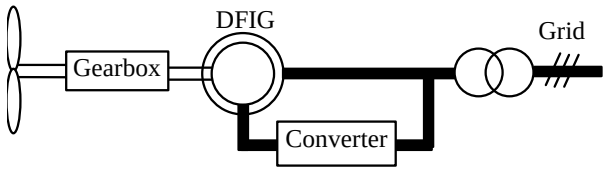

Fig. 2-3-1: *Scheme of a DFIG system*

2.3.2 SCIG system

In order to fulfill variable speed operation with a SCIG, the capacitor bank and soft-starter are replaced by a full scale converter (approximately 120% of nominal generator power), which enables variable speed operation at all wind speeds and does not need to have its output frequency the same as the grid frequency, as shown in Fig. 4. This configuration is other types of wind turbines with a traditional SCIG. However, compared with the “Danish concept”, its drawback is the high cost of the full scale converter.

Siemens is using this concept in the model of Bonus 107-3.6 MW on the market.

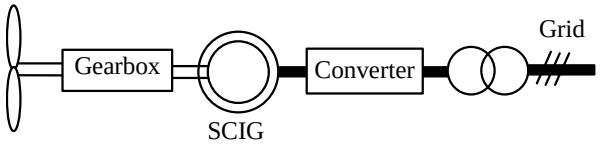

Fig. 2-3-2: *Scheme of SCIG system with full-scale converter*

2.3.3 PMSG system

An alternative generator system that might replace DFIG system in geared wind turbines is PMSG with a full scale converter. Compared to the DFIG this generator system has the following advantages:

- the generator has a better efficiency,
- the generator may be slightly cheaper,
- the generator can be brushless,
- it can be used both in 50 Hz and 60 Hz grids,
- the grid-fault ride through capability is less complex,

and the following disadvantages:

- larger, more expensive converter (100% of rated power instead of 30%), and
- the losses in the converter are higher because all power is processed by the converter.

The decreasing cost of power electronics (roughly a factor 10 over the past 10 years) and the absence of brushes make this system attractive.

On the market, this system have been used in Spanish manufacturer Made, GE multi-megawatt series. The 2.5 MW Clipper Liberty turbine type, which features four 660 kW PMSGs, has also used this concept.

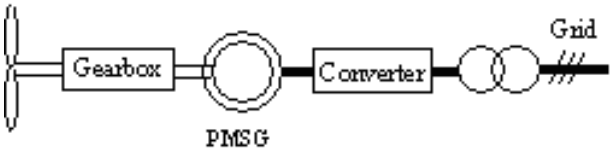

Fig. 2-3-3: *Scheme of PMSG system with full-scale converter*

2.4 Variable speed direct-drive concept

The most important difference between the geared generator and the direct-drive generator is the rotation speed of the generator. The direct-drive generator rotates at low speed, because the rotor of generator is directly connected on the hub of rotor blades. This low speed makes it necessary to produce a very high rated torque in the direct-drive generator, since the size of this generator depends on the rated torque rather than the rated power. The direct-drive generator mostly used in the market can be classified to two concepts: the electrically excited synchronous generator (EESG) and the permanent magnet synchronous generator (PMSG).

The advantages of the direct-drive generator compared to the geared generator can be summarized as follows:

- simplified drive train by omitting the gearbox
- high overall efficiency and reliability
- high availability
- low noise of the drive train

However direct-drive generators have disadvantages as follows:

- large weight and large diameter of the generator
- high cost

A direct-drive generator is usually heavier than a geared generator because it has to make a high rated torque as mentioned above. To increase the efficiency, to reduce the weight of the active parts, and to keep the end winding losses small, the direct-drive generator is usually designed with a large diameter and small pole pitch.

In the considerations of the energy yield and reliability, direct-drive systems seem to be more powerful than the geared systems, especially for offshore. Direct-drive systems, which are operated in low speed, also have disadvantages as the large diameter, large weight, and high cost compared to geared systems [1, 3, 7, 8, 9, 73].

A direct-drive synchronous generator is presented in Fig. 2-4-1. In this section, direct-drive EESG and PMSG system are described.

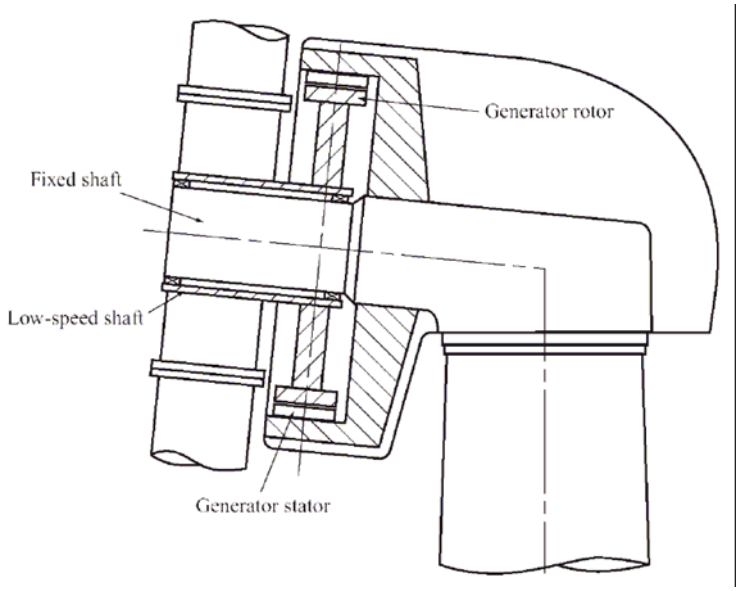

Fig. 2-4-1: *Direct-drive synchronous generator*

2.4.1 EESG

The EESG is usually built with a rotor carrying the field system, provided with a DC excitation. The stator carries a three-phase winding quite similar to that of the induction machine. The rotor may have salient poles, or may be cylindrical. Salient poles are more usual in low speed machines, and may be the most useful version for application to wind turbine generators. The grid connection scheme of a SG for direct-drive wind turbine is shown in Fig. 2-4-2. All power of the generator is processed through a power electronic converter, the interface between generator and grid. At the generator side of the converter, amplitude and frequency of the voltage can be fully controlled by the converter, independently of the grid characteristics. The generator speed is fully controllable over a wide range, even to very low speeds. The gearbox can thus be omitted. The generator is directly driven by the turbine, hence the denomination 'direct drive'. This is advantageous because the gearbox normally has a non-negligible manufacturing cost, generates some acoustic noise, requires regular maintenance (lubrication) and is also a potential cause of mechanical failure. In addition, the other advantage is that the converter permits very flexible control of the entire system. The generator speed, active and reactive power can be fully controlled in case of normal and disturbed grid conditions [3]. Compared to the PMSG, the EESG has the most opportunities for control of the flux, thus allowing to minimize loss in different power ranges. Furthermore, it does not require the use of permanent magnets, which would represent a large fraction of the generator costs, and might quickly suffer from performance loss in harsh atmospheric conditions. Therefore, it is the most used generator type by the manufacturers of large direct-drive wind turbines [137].
The main drawbacks are that the converter costs are considerable, as it has to process all the generator power: this requires more expensive power electronic components and needing intensive cooling. On the other hand, the generator needs a specific design: compared with normal electrical machines, it has to supply high electrical torques at low speeds. The diameter of the EESG in large wind turbines will be large. Direct-drive EESG typically has a large rotor diameter (nearly 12 m for the Enercon E-112 direct drive 4.5 MW turbine, see Fig. 2-4-3 [139]). The pole pitch must be large enough for this specific design in order to arrange space for the excitation windings and pole shoes. So the larger number of parts and windings probably

makes it an expensive solution. In addition, it is necessary to excite the rotor winding with DC, using slip rings and brushes, or a brushless exciter, employing a rotating rectifier [137].

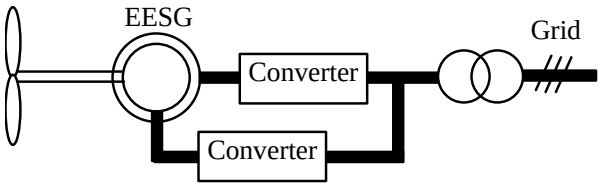

Fig. 2-4-2: *Scheme of a direct-drive EESG system*

Fig. 2-4-3: *Enercon E-112, 4.5MW*

2.4.2 PMSG

The direct-drive generator system has high potential for the wind turbines because of its reduced failure, increased energy yield and reliability. The grid connection scheme of a PMSG for direct-drive wind turbines is shown in Fig. 2-4-4. Fig. 2-4-5 shows 2 MW direct-drive system of Zephyros (currently Harakosan). The advantages of PM machines over electrically excited machines can be summarized as follows according to literature:

- higher efficiency and energy yield
- no additional power supply for the magnet field excitation
- improvement in the thermal characteristics of the machine due to absence of the field losses
- higher reliability due to the absence of mechanical components as slip rings
- lighter and therefore higher power to weight ratio

However, PM machines have disadvantages and it can be summarized as follows:

- high cost of PM
- difficulties to handle in manufacture
- demagnetization of PM at high temperature

In recent years, the use of PMs is more attractive than before, because the performance of PMs is improving and the cost of PM is decreasing. Additionally the cost of power electronics is decreasing. Therefore these trends make PM machines with a full-scale power converter more attractive for the direct-drive wind generators. According to [7], the variable speed pitch control concept with the direct-drive PMSG produces 5-10% more energy than the fixed (two) speed concept, or 10-15% more than the fixed (single) speed concept drive (both concepts had SCIG system with multi-stage gearbox) [7].
Zephyros (currently Harakosan) and Mitsubishi are using this concept in 2 MW wind turbines on the market.

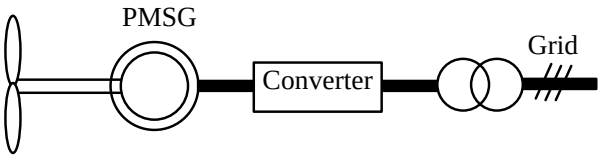

Fig. 2-4-4: *Scheme of a direct-drive PMSG system*

Fig. 2-4-5: *Zephyros Z72-2MW*

2.5 Variable speed concept with single-stage gearbox

The variable speed pitch control concept has a single-stage planetary gearbox that increases the speed by a factor of roughly 10 and a low-speed permanent-magnet generator. The grid connection scheme of this concept is shown in Fig. 2-5-1. This concept, which was introduced as the Multibrid, has gained the attention because it has the advantages as both a higher speed than the direct-drive concept and a lower components amount than the concept of DFIG with a multiple-stage gearbox. Fig. 2-5-2 shows a PM synchronous generator with a single-stage gearbox of the drive train.

Wind turbine manufacturers as Mulibrid (see Fig. 2-5-3) and WinWind are using this concept on the current market.

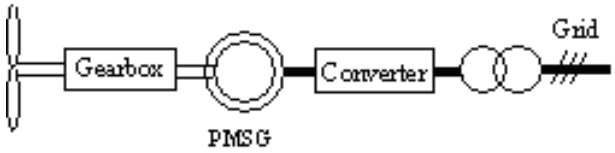

Fig. 2-5-1: *Scheme of PMSG system with a single-stage gearbox*

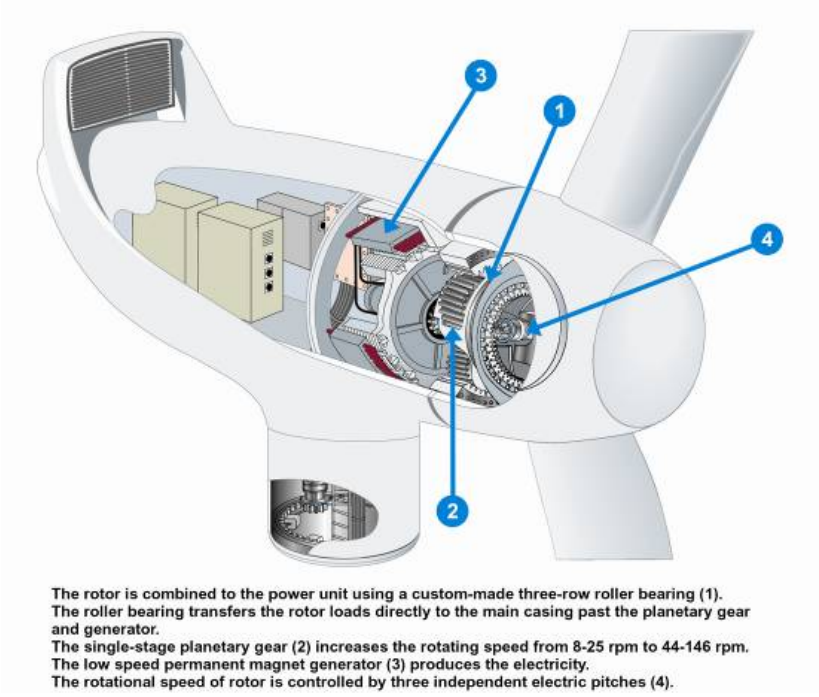

Fig. 2-5-2: *PM synchronous generator with a single-stage gearbox*

Fig. 2-5-3: *Multibrid M5000, 5MW*

2.6 Variable speed concept with hydraulic gearbox system

To develop a new wind technology solution, DeWind has used Voith Turbo's WinDrive technology in D8.2 (2 MW, see Fig. 2-6-1) model. The drive system of D8.2 model is made up of a 2-stage gearbox, a hydrodynamic WinDrive gearbox, and a fixed-speed 13.8 kV 4-pole synchronous generator. This generator is directly grid connected (or depending on grid voltage by means of a medium-voltage transformer), meaning that a frequency converter is no longer needed. As the WinDrive gearbox hydraulics functionally decouple the mechanical gearbox output shaft from the generator input shaft, drive train vibrations are dampened. Shocks and peak loads are substantially reduced. DeWind are expecting that this technology offers the potential for drive train weight reductions of up to 20% and nacelle weight reductions of up to 10% in the future [130]. Fig. 2-6-2 shows the schematic diagram of this system [21].
A wind turbine manufacturer, Windflow, has also introduced a hydraulic variable speed concept which allows rotor speed to vary independently of the fixed electrical grid frequency and as a result provide smooth power output. Conventional fixed speed turbines must be significantly over-designed to cope with torque fluctuations. This results in increased fatigue loads and necessitates the gearbox being far heavier and more expensive than hydraulic variable speed system [129]. Fig. 2-6-3 shows power qualities of the wind turbine before and after applying Windflow's concept.

Fig. 2-6-1: *Dewind D8-2, 2MW*

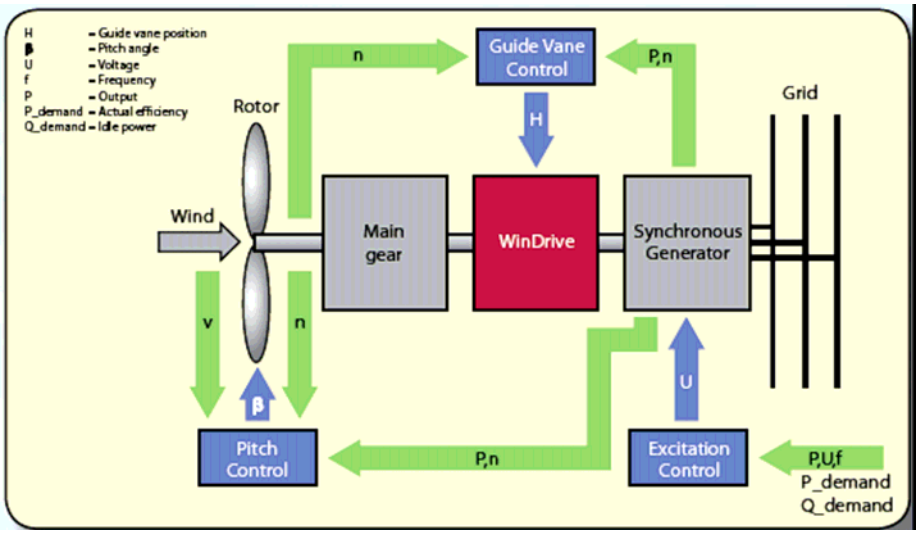

Fig. 2-6-2: *Schematic diagram of D8.2 model of DeWind*

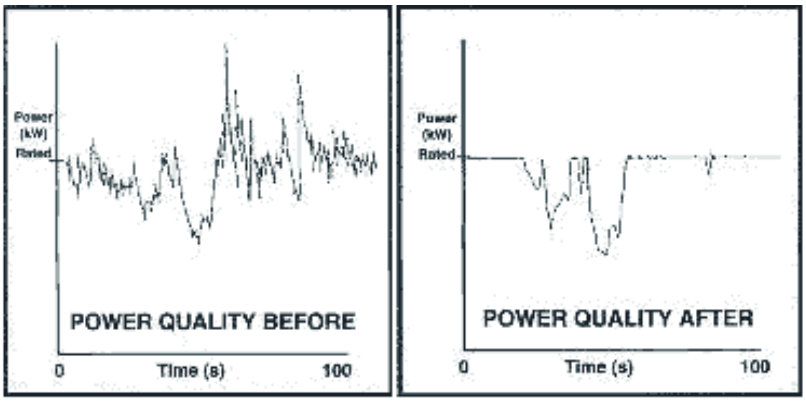

Fig. 2-6-3: *Comparison of power quality*

2.7 Other potential concepts

Many other types of wind generators are also mentioned in literatures, such as linear induction generators [145]; switched reluctance generators [146]; claw pole generators [145][146]; brushless doubly fed induction generators (BDFIGs) [145][137][147]. Amongst them, the BDFIG is the most innovative type. It has two separate three-phase windings on the stator, amongst which one directly grid-connected and one through a power electronic interface, and a double-cage rotor. The machine has the similar properties as a DFIG concerning speed range, active and reactive power control, with the additional advantage not to have electrical connections between the fixed and rotating system and it is brushless in the rotating system. However the machine operation principle and its assembly are very complex. In addition, as some authors presented in [145][137], experiences with the DFIG have shown that the slip rings and brushes are not the most critical components of the generator. Technical solutions to avoid them are thus not a prior concern of manufacturers. Therefore, the BDFIG is not likely to be a commercial success within the years to come [137].

2.8 Wind turbine trend

2.8.1 Market status

The generator systems of large scale wind turbines over 2 MW are surveyed to comprehend the trends of generator systems on the market as Table 2-8-1, in which the concept, generator type, rated power and manufactures are summarized by referring the websites of different manufacturers [10-22]. Different kinds of wind turbines have been built on the market by manufacturers because of the advantages of each generator system. In recent years, the rated power of the largest wind turbine on the market is almost 5 MW, which are manufactured by Enercon of Germany, Vestas of Denmark, Repower of Germany and Multibrid of Germany. Several manufactures are also producing wind turbines over 2 MW of the rated power as Nordex of Germany, GE Wind of USA, Gamesa of Spain, Ecotecnia of Spain, DeWind of Germany, Siemens of Denmark, Suzlon of India, Zephyros and Mitsubishi of Japan. Most manufactures are using a gearbox in the generator system. The wind turbines produced by Vestas, Repower, Nordex, GE, Gamesa, Ecotecnia and Dewind are using DFIG with a multiple-stage gearbox. According to this survey, it is clear that the wind market is still dominated by DFIG with a multiple-stage gearbox, and the mostly used generator type is still the induction generator (DFIG, SCIG and WRIG). Two companies such as Multibrid and WinWind use PMSG with a single-stage gearbox. DeWind uses an EESG with two-stage gearbox and a hydro-controlled gearbox. The direct-drive wind turbines are used in Enercon, Zephyros and Mitsubishi. Enercon have applied EESG, and Zepyros and Mitsubishi have applied PMSG.

In addition, Fig. 2-8-1 depicts the market penetration and share of the different wind turbine concepts based on recorded world suppliers' market data over a 10 year period (1995–2004) [127][142]. As it can be seen, market interest in the fixed speed wind turbine concept (SCIG) has decreased about threefold over 10 years, from almost 70% in 1995 to almost 25% in 2004. The small market share increase of SCIG experienced in 2004 is believed to be only temporary [127]. Market penetration of the OptiSlip concept (WRIG in Fig. 2-2-1) has declined since 1997 in favor of the more attractive variable speed concept (DFIG). The trend depicted in Fig. 2-8-1 clearly indicates that the WRIG type is being phased out of the market. Incorporation of the DFIG wind turbine concept has increased from 0% to almost 55% of the yearly installed wind power over 10 years, with it clearly becoming the most dominant concept at the end of 2004. Market penetration of the SG concept (EESG or PMSG) has altered little over 10 years, with no dramatic changes as observed for SCIG, WRIG and DFIG. There is, however, a slight increasing trend over the last 3 years (2002–2004). During the 10 years, the direct-drive SG (EESG and PMSG) has ranked third or fourth (Fig. 2-8-1). The increasing trend of the DFIG and the direct-drive SG, as result of their better grid support capabilities, indicates that the system will compete with DFIG system with a multiple-stage gearbox for first and second positions in the future [127][137].

Table 2-8-1: *Large wind turbine concepts on the market over 2 MW*

Drive train	Generator Type	Power / Rotor diameter / Speed	Manufacturer
Multiple-stage gearbox	DFIG	4.5 MW / 120 m / 14.9 rpm	Vestas
		5 MW / 126 m / 12.1 rpm	Repower
		2.5 MW / 90 m / 14.85 rpm	Nordex
		3.6 MW / 104 m / 15.3 rpm	GE
		2 MW / 90 m / 19 rpm	Gamesa
		3 MW / 100 m / 14.25 rpm	Ecotecnia
		2 MW / 90 m / 20.7 rpm	DeWind
	SCIG	3.6 MW / 107 m / 13 rpm	Siemens
	WRIG	2 MW / 88 m / rpm	Suzlon
	PMSG	2.x MW / 88 m / 16.5 rpm	GE
Single-stage gearbox	PMSG	5 MW / 116 m / 14.8 rpm	Multibrid
		3 MW / 90 m / 16 rpm	Winwind
Hydro-controlled Multi-stage gearbox	EESG	2 MW / 90 m / 20.7 rpm	DeWind
Direct-drive	EESG	4.5 MW / 114 m / 13 rpm	Enercon
	PMSG	2 MW / 71 m / 23 rpm	Zephyros
	PMSG	2 MW / m / rpm	Mitsubishi

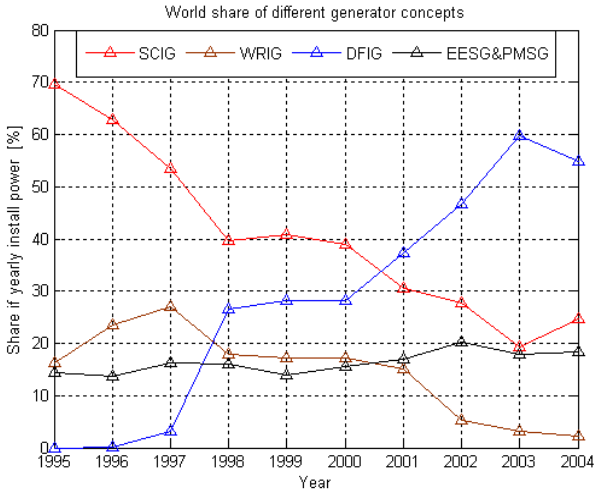

Fig. 2-8-1: *World market share of yearly installed power for different wind turbine generator types*

According to the survey on the world market share of the Top 10 wind turbine manufacturers worldwide in 2004 [127], different generator systems have been used on the market. Between these different systems, geared generator systems have been usually used on the market around 82%. In consideration of the generator type, five different types have been operated on the market as the doubly fed induction generator (DFIG), the squirrel cage induction generator (SCIG), the wound rotor induction generator (WRIG), the EESG, and the PMSG. Among different generator systems, DFIG system has recorded the highest share on the market as around 55%. A few companies have used the direct-drive concept with EESG and PMSG.
Fig. 2-8-2 shows the world market share of the Top 10 wind turbine manufacturers in 2004 [127]. According to Fig. 2-8-2, the largest markets in the world have been headed by Germany, Spain, USA and Denmark. The Danish company Vestas Wind Systems maintains its position as the world's largest manufacturer, followed by the Spanish company Gamesa Eolica. The German company Enercon and the US company GE Wind are in third and fourth positions respectively. The major 10 manufacturers have dominated the world wind turbine market at the end of 2004 with account for more than 95% of the total world market. The most used generator system is the induction generator with a gearbox, which have occupied the world wind turbine market over 70%.

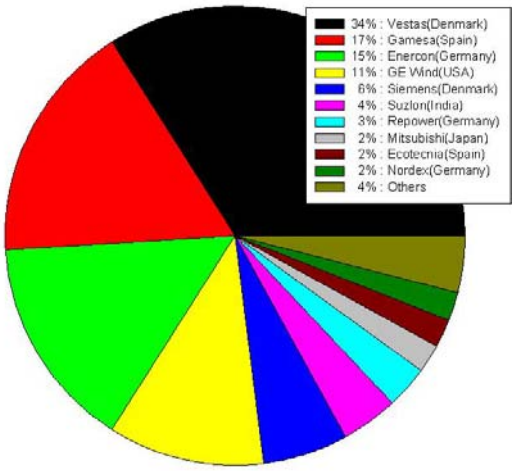

- **World market : 100%**
- **Top 10 manufacturers : > 95%**
- **Geared generator system : > 80%**
  - Induction G. + gearbox : 70%
  - DFIG + gearbox : 55%
- **Direct-drive generator system : < 20%**
  - Direct-drive EESG : > 15%
  - Direct-drive PMG : < 5%

Fig. 2-8-2: *World market share of wind turbine manufacturers in 2004*

2.8.2 Technology trend

Control concept

Variable speed concept is mostly used on the market.

Scale and install location of wind turbines

It is expected that the increase in power levels will continue because this reduces the cost of placing wind turbines, especially offshore.

Two important reasons to build offshore wind farms are the following. Firstly, in densely populated regions (like the Netherlands), there is hardly space for wind energy on shore, while these countries have their obligations towards the environment (Kyoto). Secondly, offshore, wind speeds are much higher than on shore, so that higher energy yields can be expected.

Technically speaking, permanent-magnet direct-drive generators are suitable for offshore wind turbines. These machines do not have brushes and gearboxes that require maintenance. Further, the large size of direct-drive generators is not a large disadvantage offshore.

Grid requirements

Wind turbines are usually connected to a 50 or 60 Hz grid. To enable large-scale application of wind energy without compromising power system stability, wind turbines should stay connected and contribute to the grid in case of a disturbance such as a voltage dip. They should – similar to conventional power plants – supply active and reactive power for frequency and voltage recovery, immediately after the fault has been cleared.

A number of grid operators already require voltage-dip ride-through capability, especially in places where wind turbines provide for a significant part of the total power supply. Examples are Denmark and parts of Northern Germany. The requirements concerning immunity to voltage dips as prescribed by E.ON Netz, a grid operator in Northern Germany, is shown in Fig. 2-8-3. Only when the grid voltage drops below the curve (in duration or voltage level), the turbine is allowed to disconnect. When the voltage is in the shaded area the turbine should also supply reactive power to the grid in order to support grid restoration [128].

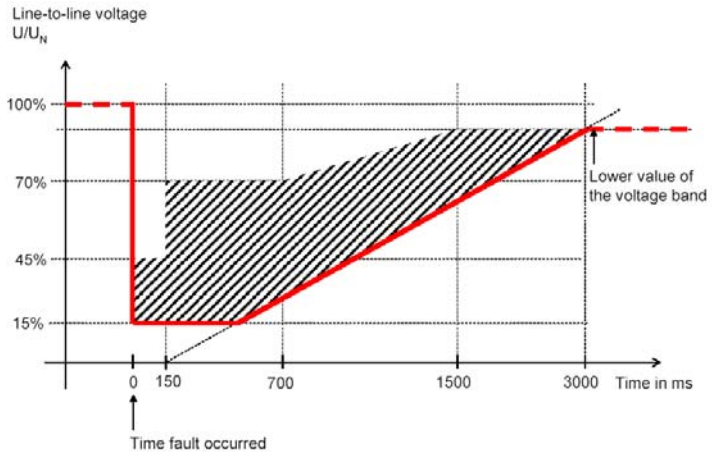

Fig. 2-8-3: *Voltage dip that wind turbines should be able to handle without disconnection (E.On Netz)*

Generator systems

As investigated above, DFIG with a multiple-stage gearbox system is still dominant on the current market. On the other hand, the interest of PMSG with a multiple-stage gearbox, and single-stage gearbox system is also increasing on the market.

The SCIG with a multiple-stage gearbox and a full-scale power converter is used over 3 MW wind turbine, which is Bonus 107 3.6 MW model of Siemens wind power.
A PMSG with two-stage gearbox and hydraulic gear have been used in D8.2 model of DeWind.

Decreasing cost of PE and PM

In recent years, the performance of PMs is improving and the cost of PM is decreasing. Additionally the cost of power electronics is decreasing roughly a factor 10 over the past 10 years. Therefore these trends make PM machines with a full-scale power converter more attractive for the direct-drive wind generators.

3. Literature survey on promising direct-drive PM machines

Direct-drive PM machines have advantages, which were described in subsection 2.4.2 including reduced failures, increased energy yield and reliability compared to electrically excited (EE) machines. Additionally, the performance of PMs is improving and the cost of PM and power electronics is decreasing in recent years. Therefore the direct-drive PM machine can be more attractive in application for large scale (offshore) wind turbines, and promising direct-drive PM machines are surveyed in this chapter.
Promising PM machines for direct-drive can be classified by both the direction of flux pass and the structure as follows, which can be combined to sixteen concepts.

- the longitudinal and transverse flux machine
- the radial and axial flux machine
- the slotted and slotless machine
- the surface mounted and flux concentrating machine

However, this report mainly classifies the promising PM machines to three concepts as follows, and the subdivisions of each concept are presented in Table 3-1.

- the axial flux PM machine
- the radial flux PM machine
- the transverse flux PM machine

According to the survey on PM machines, the slotted and slotless surface mounted PM machines, which are *(1)* and *(2)* in Table 3-1, have been mostly discussed among the references of axial flux PM machines.
The slotted surface mounted PM machine and the slotted flux concentrating PM machine, which are *(3)* and *(4)* in Table 3-1, have been mostly discussed in the references about the radial flux PM machines.
In cases of the transverse flux PM machines, the axial and radial flux, slotted, surface mounted PM machine and flux concentrating PM machine, which are *(5), (6), (7) and (8)* in Table 3-1, have been mostly discussed in the references.
More details of these three different machines are discussed in Section 3-1, 3-2, and 3-3 of this chapter.

Table 3-1: *Different PM machines for direct-drive*

Machine type		Longitudinal flux		Transverse flux	
		Surface mounted PM	Flux concentrating PM	Surface mounted PM	Flux concentrating PM
Axial flux	Slotted	(1)		(5)	(6)
	Slotless	(2)			
Radial flux	Slotted	(3)	(4)	(7)	(8)
	Slotless				

3.1 Axial-flux PM machine

The axial-flux permanent magnet (AFPM) machine is a machine producing magnetic flux in the axial direction with permanent magnets. AFPM machine can be classified into slotted machines and slotless machines as mentioned in Table 3-1. Many references have discussed about AFPM machines because of the advantages compared to RFPM machines as follows:

- simple winding
- low cogging torque and noise (in slotless machine)
- short axial length of the machine
- higher torque/volume ratio

However, the disadvantages of AFPM machines have been also discussed compared to RFPM machines as follows [8, 9]:

- lower torque/mass ratio
- larger outer diameter, large amount of PM, and structural instability (in slotless machine)
- difficulty to maintain air-gap in large diameter (in slotted machine)
- difficult production of stator core (in slotted machine)

AFPM machines discussed in references [27-39, 54, 61, 66, 67, 123, 125] are surveyed to review their possibility and potential for large scale direct-drive wind turbines in this section.
A slotless, toroidal-stator, permanent-magnet generator was discussed with several advantages as the lightness, the compactness, the short axial length, the suitable integration with the engine and others by Spooner and Wu *et al*. This machine's short axial length tends to give it a high power to weight ratio [37, 38, 39].
Chalmers et al presented an axial flux PM generator named Torus for a direct-drive variable speed wind turbine application. They described the perceived advantage of the Torus configuration and discussed the design characteristics of a 5 kW at 200 rpm. The Torus machine is a slotless, toroidal-stator, double-sided, axial, disc-type, permanent magnet, brushless machine [33].

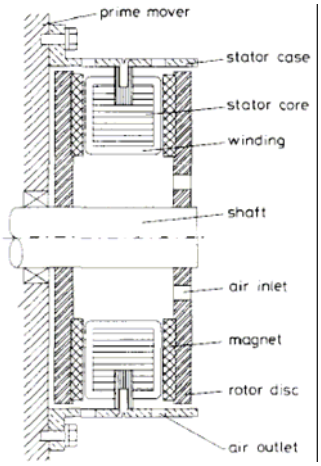

Fig. 3-1-1: *Spooner, Wu et al [37, 38, 39]*

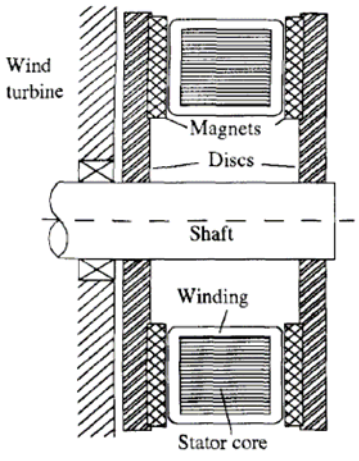

Fig. 3-1-2: *Chalmers et al [33]*

Söderlund et al proposed a direct-drive, low-speed, axial flux PM synchronous wind power generator, of which stator is toroidal with the iron sheet core to avoid eddy currents, and the winding is wound directly on the toothless stator core. Both mechanical and electromagnetic designs of a 100 kW machine were described [27, 28].

Boccaletti et al analyzed the algorithms and the relevant numerical optimisation techniques for the design of axial flux PM machines. They described some numerical optimisation algorithms, and their applications to the design technique. Objective functions to be minimized were discussed, such as mean torque, power losses and total weight [31].

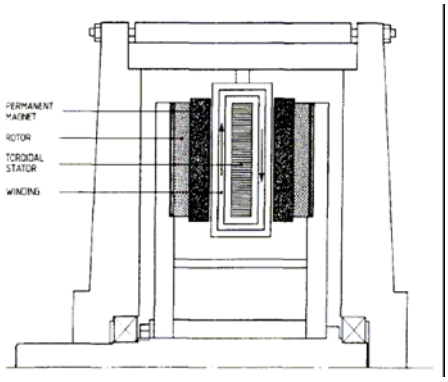

Fig. 3-1-3: *Söderlund et al [27, 28]*

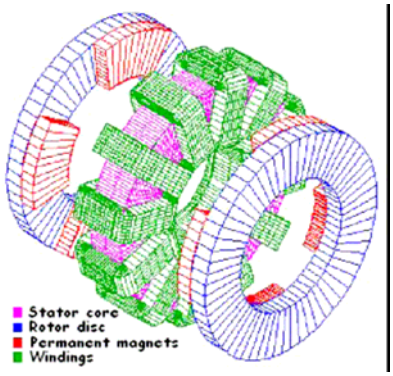

Fig. 3-1-4: *Boccaletti et al [31]*

Bumby et al described the design and development of an axial-flux PM generator for use as a direct-drive generator with small-scale wind turbine. The generator consists of two rotor discs each with PM located around its periphery. The stator is made of non-magnetic non-conducting material and has a number of bobbin-wound armature coils located around its periphery. The generator produces 1 kW at 300 rpm or 2 kW at 500 rpm with an electrical efficiency substantially greater than 90% [29].

Caricchi et al proposed a new axial flux PM machine topology to apply to the ship propulsion. In designing an axial flux PM machine devoted to ship propulsion systems, the machine weight should be particularly taken into consideration, since the achievement of a high machine torque-to-weight ratio results in a great saving of active materials and reduces the machine costs. The machine proposed by Caricchi et al is characterized by the synchronous counter-rotation of the two machined rotors, to apply to the ship propulsion. Such a new machine topology can find application in the direct driving of two counter-rotating propellers, which may be used in ship propulsion systems to recover energy from the rotational flow of the main propeller slip stream. The use of an axial flux PM machine having counter-rotating rotors allows an improvement in terms of weight and efficiency, since the epicyclic gear otherwise required for the motion reversal can be avoided. Significant design characteristics were evaluated for the axial flux PM machines having the rated power in the range from 1 MW to 20MW [32]. Caricchi et al proposed slotless axial flux PM machines in references [123, 125].

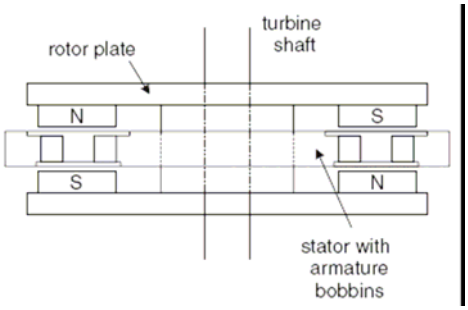

Fig. 3-1-5: *Bumby [29]*

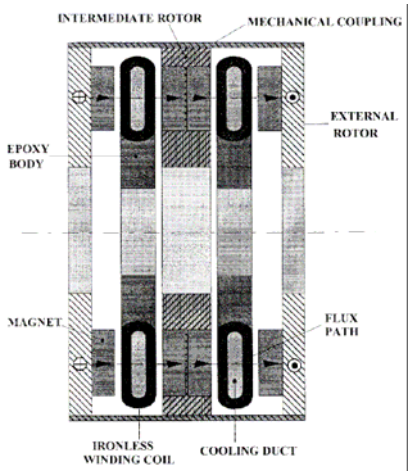

Fig. 3-1-6: *Caricchi et al [123]*

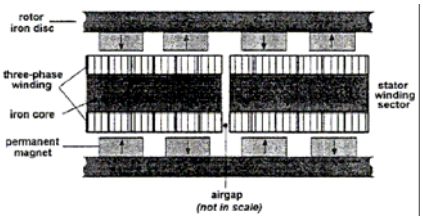

Fig. 3-1-7: *Caricchi et al [125]*

Sahin described a high speed, slotted, double-stator, internal rotor type axial flux machine [61].
Eastham et al proposed a novel direct-drive brushless PM axial flux machine for aircraft drive. This machine must have the best possible power-to-weight ratio together with the conflicting attribute of high efficiency. One form of machine under consideration for the drive follows the multiple surface ideas that have been proposed for machines with high power density. Conventional machines use only one cylindrical surface within the machine to generate torque. However, machines such as the ship propulsion under development generate torque on coaxial cylindrical surfaces within the machine volume. Multiple disc machines are also possible and again produce a larger total torque producing surface. They have been applied to gas turbine generators and versions having two discs are in use for wind turbine applications [34].

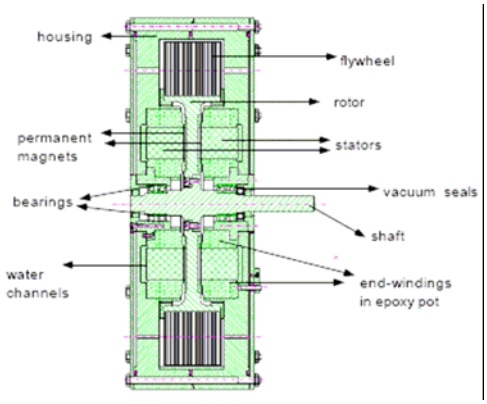

Fig. 3-1-8: *Sahin [61]*

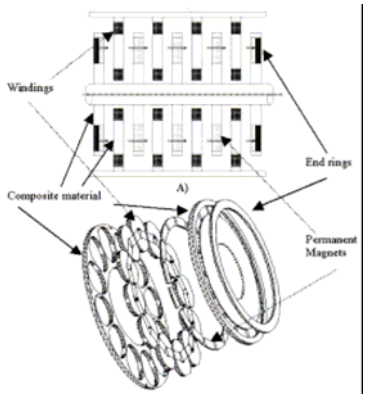

Fig. 3-1-9: *Eastham et al [34]*

The potential application of soft magnetic composite (SMC) material was discussed to apply to the low speed, direct-drive, axial flux PM wind generators by Chen *et al*. Comparative design studies were conducted on PM generator for wind turbines of different configurations with both lamination core and SMC core [35].
Parviainen discussed about an analytical method to perform the preliminary design of surface mounted, low speed, PM axial flux machines with one-rotor-two-stators configuration. A performance and construction between the low speed radial flux and axial flux PM machine were compared in the power range from 10 kW to 500kW at 150-600 rpm [36].

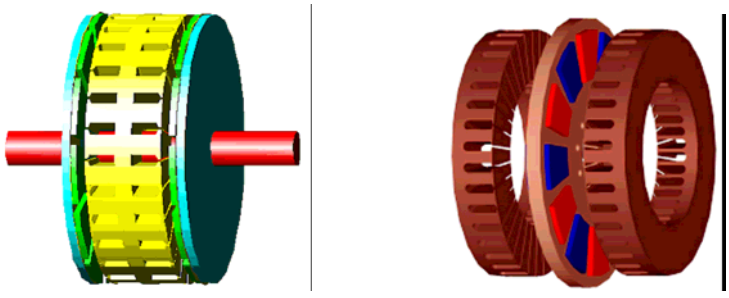

Fig. 3-1-10: *Chen Y. et al [35]* **Fig. 3-1-11:** *Parviainen [36]*

Vizireanu *et al* studied a 9-phase, 2.7MW axial flux generator with two PM outer rotors and one interior 9-phase stator [66]. Vizireanu *et al* also presented a comparative study for different configurations of a 9-phase concentrated winding PM synchronous generator for direct-drive wind turbines of 5MW output power [67].
The structural mass of axial flux PM machines for a range of typical wind turbine ratings was analyzed and discussed in a reference [54].

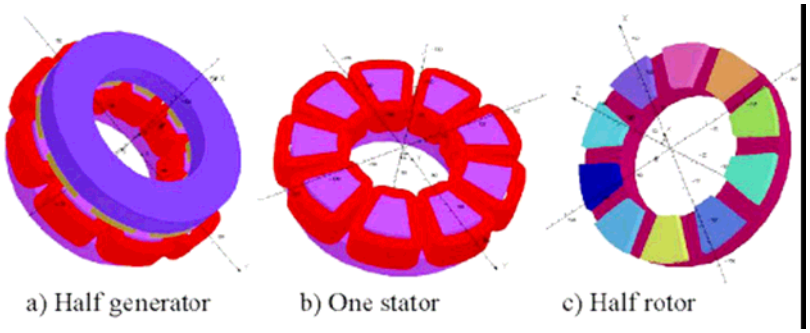

Fig. 3-1-12: *Vizireanu et al [66, 67]*

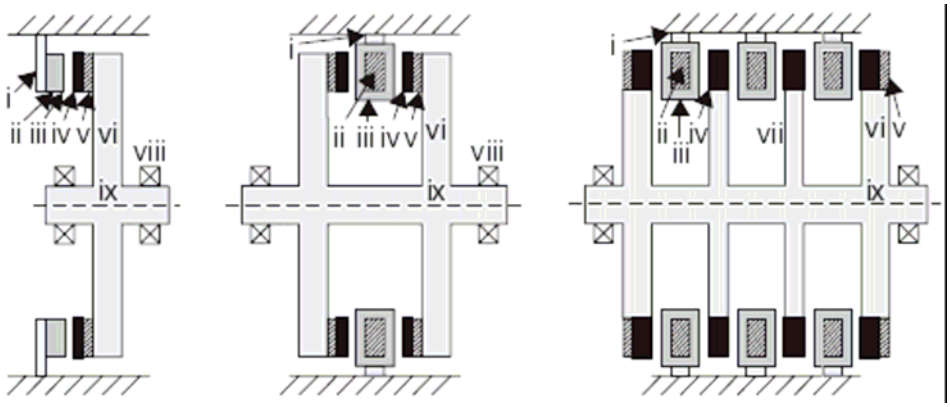

Fig. 3-1-13: *Mueller et al [54]*

Okazaki et al have proposed the axial flux motor for the ship propulsion. This motor is a liquid nitrogen cooled high-temperature superconducting motor, and it has a shape of stacked disks as Fig. 3-1-14. Each disk contains several coils those are used as the rotor or the stator [30].

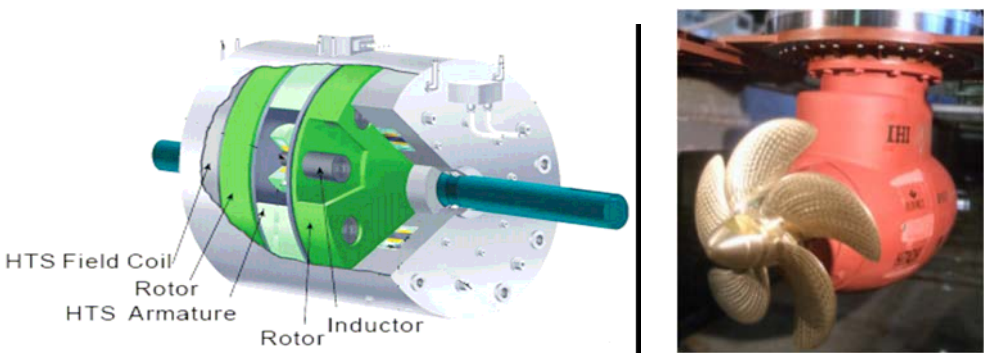

Fig. 3-1-14: *Okazaki et al [30]*

3.2 Radial-flux PM machine

Most of the radial flux (RF) machines have a conventional inner rotor design but some outer rotor designs have also been presented in literature. The permanent magnets (PMs) of RF machines are radially oriented. The design of RF machines is simple and widely used. The structural stability of RF machines is easy to make sufficient. Most of the low-speed megawatts wind generators are RF machines and these RF machines seem to be the most interesting machine type for the large scale direct-drive wind turbines. When using permanent magnets (PM) for the direct-drive generators, the generators can operate with good and reliable performance over a wide range of speeds. In manufacture, the simple way of constructing the machine with high number of poles is gluing PMs on the rotor surface. In RFPM machines, the length of the stator and the air-gap diameter can be chosen independently. If necessary, the radial-flux machine can be made with a small diameter by using a long stator.
The RFPM machines can be classified to the slotted surface mounted PM machine and the slotted flux concentrating PM machine as Table 3-1 presented above.

In this section, RFPM machines discussed in references [7, 9, 40-50, 52, 53, 55-58, 63, 68] are surveyed to review the possibility and potential of RFPM machines for large scale direct-drive wind turbines.
Reference [7], [9], [57] and [58] discussed the radial flux machines with surface mounted magnet. The radial flux machine is economically a better choice for large scale gearless wind turbines than the axial flux machine. The radial flux machine with surface mounted magnets seems to be a good choice for the design of a large scale direct-drive wind generator [7, 9]. The radial flux PM machine with flux concentration was discussed and compared to the machine with surface mounted PM in [8, 40].
A direct-drive modular PM synchronous generator for variable speed wind turbines was discussed with attractive features. The stator module of the generator is divided circumferentially into a large number of E cores, each carrying a coil which may be wound on a bobbin and fitted prior to assembly of the generator. Rotor module consists of a large number of blocks with permanent magnet and steel pole side [41, 42, 45]. The cancellation of the noise and vibration was discussed and an alternative damping system was described about this modular generator [43, 44]. A mathematical model of the modular machine was described and its predictions were compared with measured losses [46].
Wu et al also described a surface mounted PM machine, which is a small outer-rotor, direct-drive type for wind turbines. They discussed the optimisation techniques including the starting torque of the machine by using finite element analysis and with generator [49].

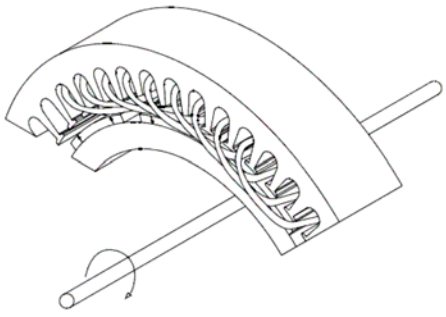

Fig. 3-2-1: *Radial flux surface mounted PM machine*

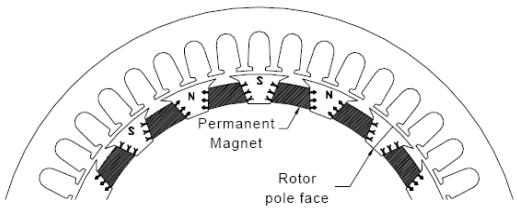

Fig. 3-2-2: *Radial flux PM machine with flux concentration*

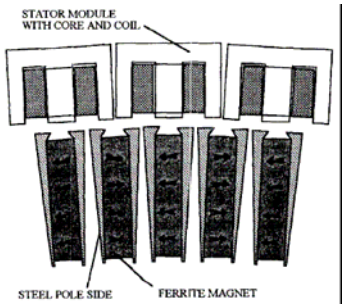

Fig. 3-2-3: *Chen, Spooner, Geng [41, 42, 43, 44, 45, 46]*

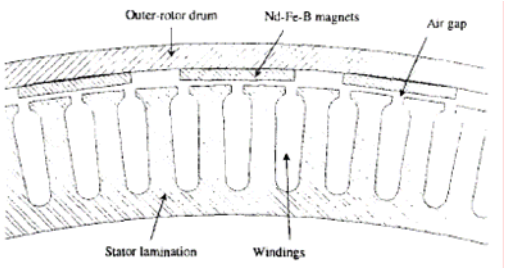

Fig. 3-2-4: *Wu et al [49]*

The design and finite element analysis of an outer-rotor PM synchronous generator were also presented for the direct-drive wind turbines by Chen et al in [52]. Several advantages of the outer-rotor machine were identified in this reference.
A direct-drive PM synchronous generator for the wind turbine of 1.5 MW output power was designed by conventional magnetic equivalent circuit method and analyzed by finite element method for verification of design [53].

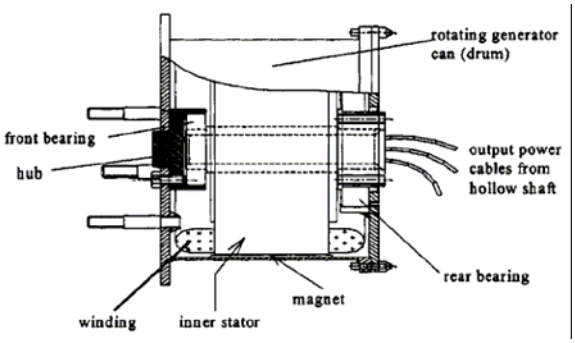

Fig. 3-2-6: *Chen J. et al [52]*

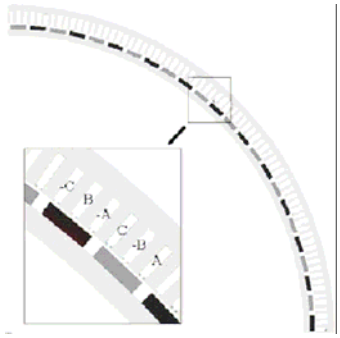

Fig. 3-2-7: *Kim et al [53]*

A direct-drive PM wind generator of 500 kW at 40 rpm was designed by Lampola, and its electrical performance was calculated by the finite element method [56].

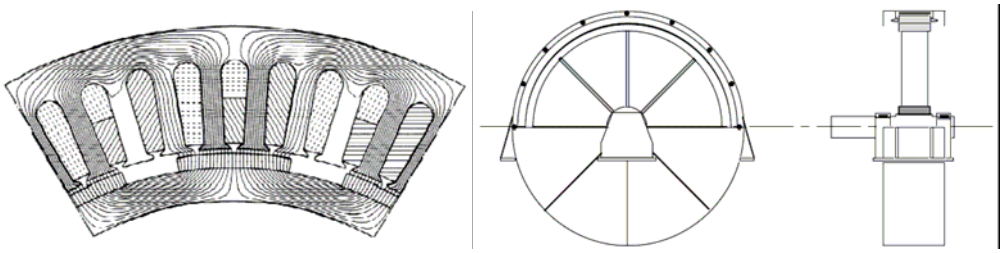

Fig. 3-2-8: *Lampola [56]*

Five different direct-drive PM machines, which are a surface mounted PM type, an inset surface mounted PM type, an outer rotor surface mounted PM type, a V-shaped buried PM type, and a tangentially magnetized PM type, have been investigated and compared to design the PM machines with better efficiency and less weight than the induction machine with its gearbox in [63]. According to [63], the rotor with V-shape magnets is not appropriate for design with high pole numbers. Outer rotor type is lighter than inner rotor type when comparing the active material weight as a function of the pole numbers. The inset PM type is slightly lighter than the

surface mounted PM type. The tangentially magnetized PM type gives the best performances in the consideration of application.

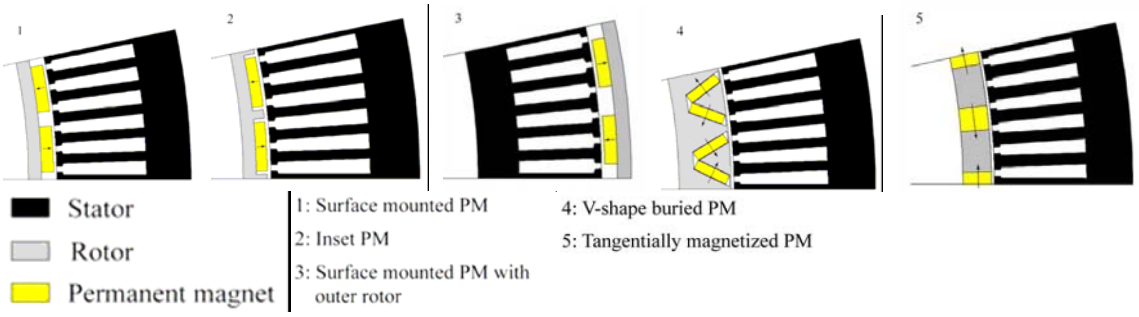

Fig. 3-2-9: *Libert et al [63]*

The design features of a direct-drive, surface mounted PM wind generator with the rated power in the region of 20 kW at 110 rpm were discussed in [68].
Hanitsch and Korouji have designed a rare-earth PM radial-flux wind-energy generator with new topology, which is constructed from two rotors and one stator and by short end windings. It improves the performance of the machine by reducing the weight, increasing the efficiency and reducing the cost of active materials [148].
The references of [47, 48, 55] have discussed about a new concept and an optimisation of the mechanical constructions.
A new PM generator, which is very light in weight, was proposed for direct-drive wind turbines. The proposed generator used a pair of spoked wheels to carry the rotor and stator of an air-gap winding radial flux PM machine by Spooner *et al* in [47].
Tavner et al described how the large number of pole pairs and air-gap radius affect the design of the large, low-speed, direct-drive machines. They discussed and compared the output torque with the ratio of structural/active component weight of different machines. The different machines include an induction machine, a wound rotor synchronous machine, a PM synchronous machine, a slotless armature machine and an ironless machine [48].

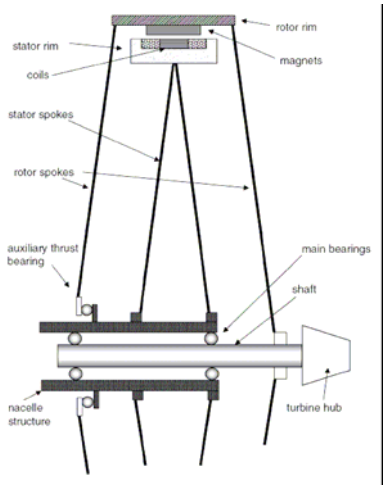

Fig. 3-2-10: *Spooner et al [47]*

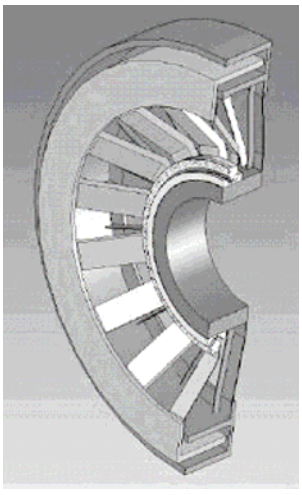

Fig. 3-2-11: *Tavner et al [48]*

RFPM machines (PMSG) have advantages as a better torque density than the RF electrically excited synchronous machine (EESG), so that these machines have been discussed in a number of literature. In this section, various kinds of RFPM machines have been surveyed as the surface mounted PM machine, the flux concentrating PM machine, the PM machine with modular stator and rotor, the outer rotor PM machine, the inset surface mounted PM, and the buried PM machine.

3.3 Transverse-flux PM machine

The transverse flux (TF) principle means that the path of the magnetic flux is perpendicular to the direction of the rotor rotation. There are also some different rotor structures for this technology, such as the rotor with single-sided surface magnets with single-sided flux concentration and with double-sided flux concentration. The nature of its operation is that of a synchronous machine, and it will function in principle in a similar manner to any other PM synchronous machine. The major difference of TFPM machine compared to RFPM or AFPM machine is that TFPM machine allows an increase in the space for the windings without decreasing the available space for the main flux, this allows for very low copper losses. TFPM machine can also be made with a very small pole pitch compared with the other types.
The transverse flux permanent magnet (TFPM) machines have been discussed in a number of references with the features, topologies, advantages, disadvantages and others [8, 9, 23, 24, 74-122].
TFPM machines surveyed in references can be mainly classified as Table 3-1 presented above. In this section, different TFPM machines are surveyed to review the possibility and potential of the machines to apply to the large scale direct-drive wind turbines.
According to the survey of references, the main advantages of TFPM machines can be summarized as follows compared to the longitudinal machines:

- higher force density
- considerably low copper losses
- simple winding

However the force density of TFPM machine with large air-gap is a little high or even low compared to the longitudinal machines [8]. The construction of TFPM machines is much more complicated than longitudinal flux machines. Therefore the mechanical design of TFPM machines seems very complicated.
In cases of [9, 93], the weight of 55 kW transverse flux machine is about half of the total weight of an asynchronous machine with a gearbox. Transverse flux machine seems to be suitable for direct-drive applications because of its high specific torque, although it has a large number of individual parts and special methods of manufacturing and assembly [24].
The surface-mounted TFPM machines have been discussed by Weh [75], Harris [77, 124], Bork and Henneberger [93] and others.
The flux-concentrating TFPM machines have been discussed by Weh [74, 75, 81, 87], Lange [82], Mecrow [83], Mitcham [85], Voyce [86], Maddison [88] and Blissenbach [89].
Dubois also have discussed about different topologies of TFPM machines in [8, 59, 60, 101].

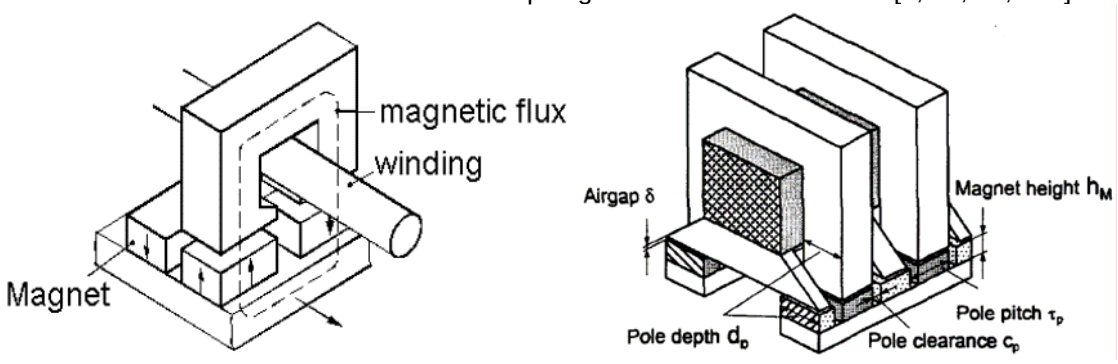

Fig. 3-3-1: *Surface mounted TFPM machine*

The double-side TFPM machine were discussed in [74, 75, 81, 82, 83, 85, 86]. E-core TFPM has been discussed in [81]. References as [87], [88] and [89] have discussed the claw pole TFM. Maddison has compared the single-sided, the single-sided bridged, and the double-sided TFM with the claw pole TFM in [25].

A new concept of a transverse flux machine was proposed by Henneberger and Bork in [93]. Dubois has reviewed various transverse flux permanent magnet machines as the surface-mounted TFPM machine and the flux-concentrating TFPM machine which have a radial air-gap configuration [8]. Dubois has proposed a new single-sided TFPM machine with flux-concentration, single-winding and toothed rotor [8, 101].

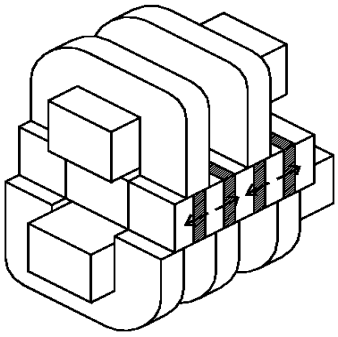

Fig. 3-3-2: *TFPM machine with double-sided with double-winding*

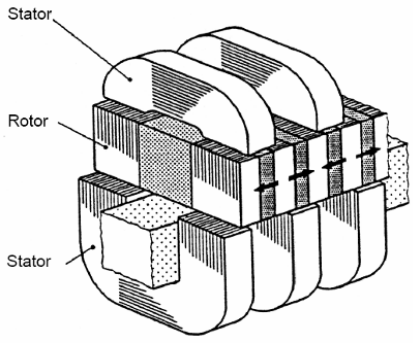

Fig. 3-3-3: *Double-sided TFPM machine with flux-concentration and single-winding in U-core arrangement*

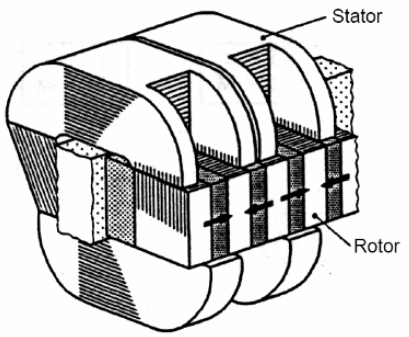

Fig. 3-3-4: *Double-sided, single-winding TFPM machine with C-core arrangement*

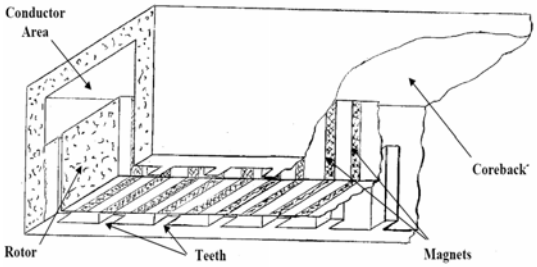

Fig. 3-3-5: *Double-sided, single-winding TFPM machine with C-core arrangement*

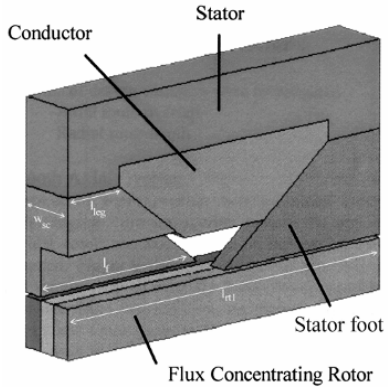

Fig. 3-3-6: *Claw pole TFM*

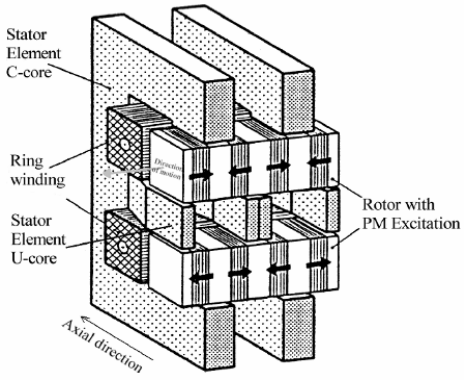

Fig. 3-3-7: *TFPM machine with E-core configuration, Weh [81]*

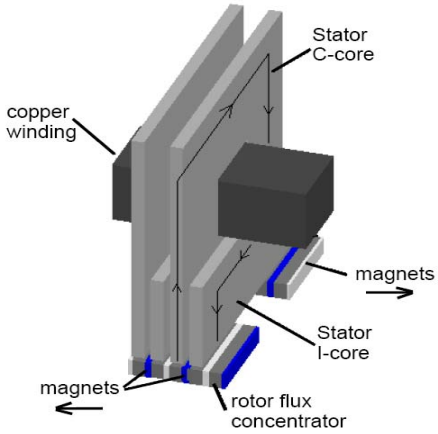

Fig. 3-3-8: *Single-sided stator version of Fig. 3-3-3 [93]*

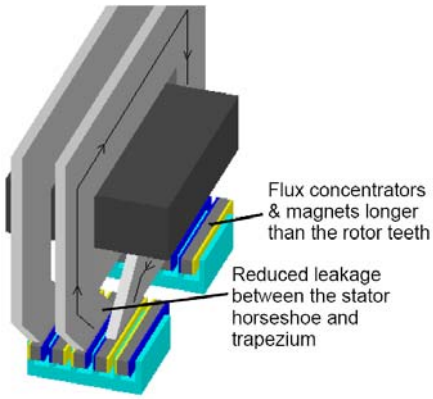

Fig. 3-3-9: *TFPM machine with toothed rotor version of Fig. 3-3-8 [8, 101]*

A combination of a modular, transverse flux, axial flux and toroidal stator winding was proposed to apply to a permanent magnet generator for wind turbines by Muljadi et al in [26]. The toroidal stator winding can be easily assembled and automated for production and the winding is exposed to open air, which improves cooling.
A modified design of the transverse flux machine, which offers a high torque density, was proposed for the electric propulsion of ships by Mitcham et al in [84, 85].
Rang et al discussed two typical topologies of TFPM, which are the double-sided double-winding type and the double-sided single-winding type with C-core stator in [104]. This reference also discussed an analytical design approach about the second topology. The topologies of this reference are same with what was discussed by Mitcham et al.

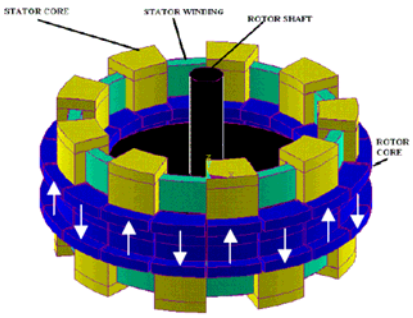

Fig. 3-3-10: *Mujaldi et al [26]*

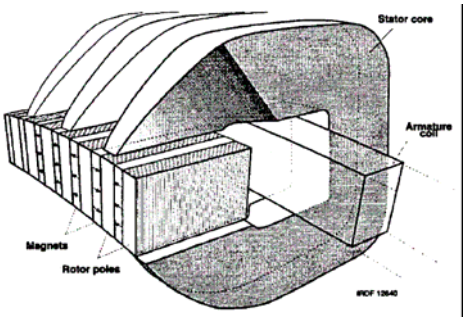

Fig. 3-3-11: *Mitcham et al [84, 85], Rang [104]*

The specific sizing and force density equations of the TFPM were discussed and the TFPM, of which topology is same with [74], was compared with the squirrel cage induction machine in [91, 92] by Huang et al.
Harris et al compare the relative advantages and disadvantages of three different topologies of TFPM machines, which include a single sided surface mounted PM machine, a single sided surface mounted PM machine with stator bridges, and a double sided flux concentrating PM machine [94]. They also discussed about power factor of the transverse flux machine in [95].
Hasubek et al proposed a transverse flux machine with the stator with PM and the passive rotor. The force density of the transverse flux machine was discussed and compared to different longitudinal machines [96]. They also discussed about an analysis of the design limitations of the machine in [97]. In this reference, useful pole pitches, PM widths, and rotor pole width were proposed.

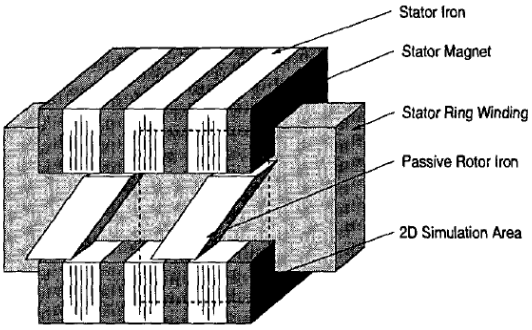

Fig. 3-3-12: *Hasubek et al [96]*

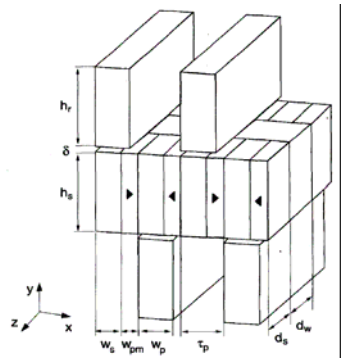

Fig. 3-3-13: *Hasubek et al [97]*

An analytical approach was proposed to dimension and analyze the performance of a transverse flux machine. The ratios of Torque/Active mass and Toque/Volume were compared to different transverse flux machines by Arshad et al in [98].
French et al discussed the TFM, which was an axial flux type, to apply to ships and an optimised torque control strategy was also presented in [99].
A configuration of TFM for the ship propulsion was proposed with discussions of a theoretical analysis and some experimental results. A condition monitoring technique for a TF machine was also proposed by Payne et al in [100].
In [102], an axial type TFPM to reduce the torque ripple was discussed by Kastinger et al.
A TFPM with intermediate poles, which was proposed by Zweygbergks in 1992, was discussed and compared to a conventional surface mounted TFPM in [103] by Arshad et al.
Husband et al introduced the transverse flux machine of 2 MW output power for ship propulsion. The TFPM was a type of the double-sided single-winding TFPM machine with C-core stator arrangement in [105].

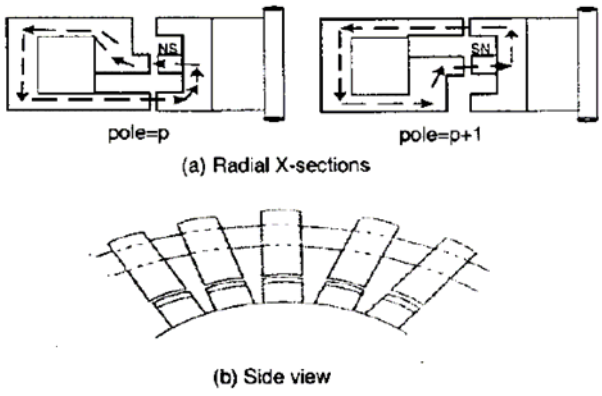

Fig. 3-3-14: *Arshad et al [103]*

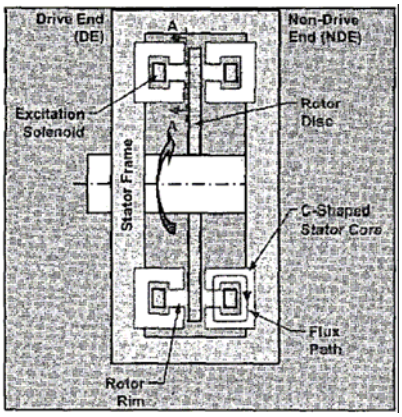

Fig. 3-3-15: *Husband et al [105]*

Njeh et al investigated of the cogging torque of a single-side claw pole TFPM machines [106].
Lu et al discussed a new torque equation, the estimation of inductance, an analytical model, and the power factor of a surface mounted PM transverse flux machines [107-110].
The principle, topologies, present research situations, and disadvantages of different TF machines were discussed by Shi et al in [111].
The design, performance analysis, and experimental results of the surface mounted PM transverse flux machine have been discussed by Guo et al. to investigate the potential of soft magnetic composite in [112, 113].

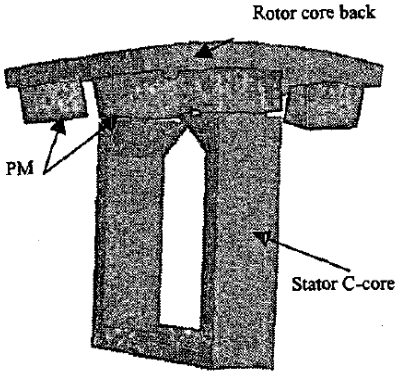

Fig. 3-3-16: *Lu et al. [107-110]*

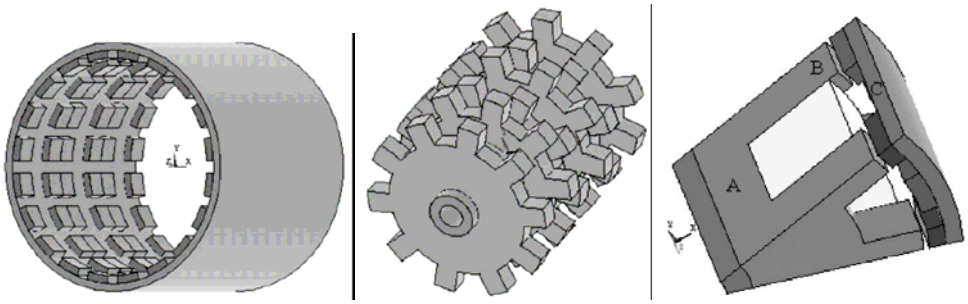

Fig. 3-3-17: *Guo et al. [112, 113]*

An optimisation of a single-sided claw pole TFPM machine was discussed about the overlap between adjacent stator teeth by Masmoudi et al. in [114]. The maximization of the output torque and the minimization of the cogging torque were discussed with considering the overlap.

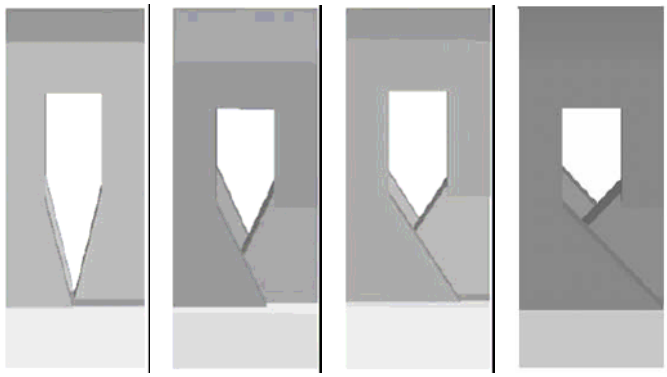

Fig. 3-3-18: *Masmoudi et al. [114]*

Bao et al discussed for cogging torque reduction of a double-sided, single-winding TFPM machine with C-core arrangement. A new double-sided single-winding TFPM machine with C-core stator was suggested with considering the reduction of power losses [115-117].
The cogging torque analysis of a transverse flux machine was discussed by Schmidt [119]. The concept of this machine is same with what was proposed in [81], which is a double-sided TFPM machine with flux-concentration and single-winding in U-core arrangement.
Wer et al presented about the reduction of the cogging torque of the TFPM machine by an optimal current control [122].

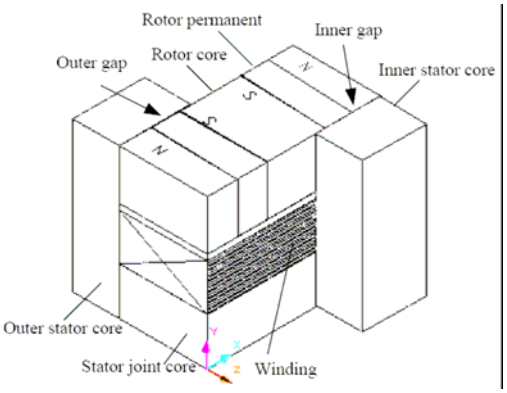

Fig. 3-3-19: *Bao et al [115-117]*

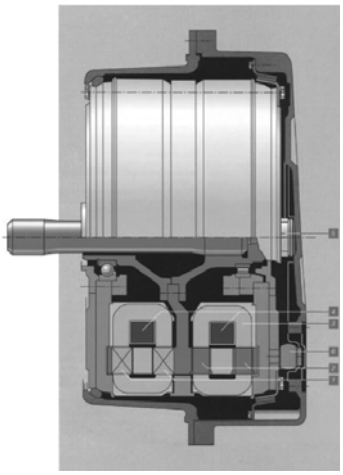

Fig. 3-3-20: *Schmidt [119]*

Gieras has discussed the analysis and performance characteristics of a three-phase single-sided flux concentrating TFPM with outer rotor in [120]. Power factor analysis of TFPM machine was discussed by Zhao et al [121].

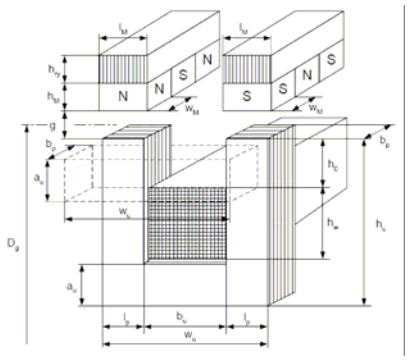

Fig. 3-3-21: *Gieras [120]*

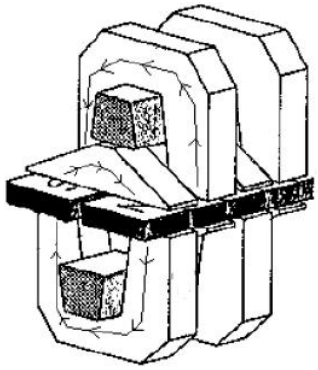

Fig. 3-3-22: *Zhao et al [121]*

A novel TFPM topology was proposed and analyzed for direct-drive wind generators, of which rated power are 3, 5, 7 and 10 MW, by Svechkarenko et al in [64, 65]. Its concept is same with the surface mounted TFPM topology.

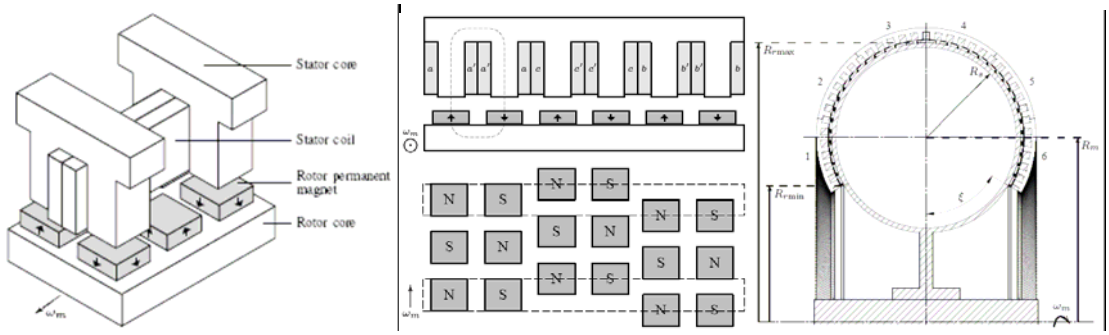

(a) (b) (c)

Fig. 3-3-23: *A novel TFPM topology for a direct-drive wind turbine, Svechkarenko [64, 65]*

Various kinds of TFPM machines have been proposed and discussed in a number of references. As discussed in references, TFPM machines have advantages such as high force density and simple winding with low copper losses compared to the RFPM and AFPM machines.

3.4 Discussion

To achieve the development of most suitable generator system for the direct-drive large scale wind turbines, it is required both to increase energy yield and decrease cost of the generator system.
In this chapter, promising PM machines as AFPM, RFPM and TFPM machine have been surveyed with advantages and disadvantages in literatures, because PM machines are more attractive and superior with higher efficiency and power to weight ratio compared to EE machine.
The disadvantages of AFPM machine as described in section 3.1 must be solved or even improved significantly, because these make the machine cost increase and manufacturing difficult according to the survey.
In case of RFPM machines, the electromagnetic design and optimisation with general topology have been discussed in a number of literatures. This means the machines are almost optimised electromagnetically, so that it is hard to reduce the active material weight and cost of the machines significantly.
TFPM machines have also disadvantages such as low force density in large air-gap, complicated construction in manufacturing, and low power factor although the machines have advantages as high force density and simple winding with low copper losses compared to the AFPM and RFPM machines. These disadvantages make TFPM machine more unattractive. However in a number of literatures, various topologies of TFPM machine have been proposed to solve or improve the disadvantages, since the machine is more flexible and attractive to design and invent new topology in the electromagnetic design. Each topology in section 3.3 has at least one advantage to make TFPM machine attractive. Therefore TFPM machine still has high potential to be most suitable generator type with new topology adopting and combining the advantages of different topologies.

4. Comparison of different generator systems

4.1 Survey of quantitative comparison

Some comparisons of different wind generator systems have been conducted by a number of authors in [1][3][6-9][24][50][59][71-73][126][127][133][136][137][140][141].
The 1.5 MW wind turbine with the electrically excited direct-drive generator system has been compared to the doubly fed induction generator system with a gearbox by Böhmeke and Siegfriedsen et al in [71, 72]. They conclude that the direct-drive system would be more expensive and heavier than the doubly fed induction generator system with a gearbox. The top masses of the direct-drive generator and the DFIG with a gearbox were also compared in [73].
However authors as Polinder [1], Bywaters et al [6], Grauers [7], Dubois [8], Lampola [9], and Poore et al [126] have discussed the benefits of direct-drive PM machines, which are the elimination of the excitation losses and the reduction of the weight of active material and others.
Grauers has presented a comparison between the direct-drive radial-flux PMSG connected to a forced-commutated rectifier and the three-stage geared-drive traditional SCIG for wind turbine systems. The rated power from 30kW up to 3MW is investigated. Some main comparisons for two-rated power 500kW and 3MW are shown in Table 4-1, respectively [7].

Table 4-1: *Comparison of the direct-drive PMSG and the geared drive SCIG*

Generators concepts	PMSG	SCIG	PMSG	SCIG
Rated power (kW)	500	500	3000	3000
Outer diameter of generator (m)	2.7	1.5	5	2.5
Length of system (inc. high speed shaft in SCIG)	1.2	3	2	6
Full-load efficiency (%)	90.3	93.7	91.4	94.3
Average efficiency (%)	90.7	88.4	91.6	90.0
Active material weight (inc. gearbox in SCIG) (ton)	2.7	7.7	14	53

As it can be seen, the outer diameter of the direct-drive PMSG is almost 2 times of the conventional geared-drive SCIG, however, the length is 2 to 3 times of SCIG system including the length of high-speed shaft. The SCIG system has larger efficiency at full rated load than PMSG (only considering the efficiency from the turbine shaft to the grid [7]), but it is less efficient on the average. The difference in average efficiency is 2.3 and 1.6% for the 500kW and 3MW systems, respectively. Due to the fixed-speed in the SCIG system, variable speed turbines can produce about 5 to 10% more energy, which will make the direct-drive PMSG more worthwhile than the geared-drive SCIG [7]. The increased energy production by means of the variable turbine speed is not included in the above full-load efficiency comparison. On the other hand, the total active weight of both gearbox and generator of SCIG system are 2.8 to 3.8 times of the active weight of the direct-drive PMSG.
Considering the components of wind turbines, Anon. has also described a comparison between the direct-drive PMSG and the geared-drive traditional SCIG at the commercial 500kW wind turbines. The detailed results are given in Table 4-2 [140][141].

Table 4-2: *Main data of a commercial 500 kW wind turbine with the direct-drive PMSG and the geared drive SCIG*

Generators concepts	PMSG	SCIG
Speed of wind turbines rotor (rpm)	18-38	30
Speed of generator rotor (rpm)	18-38	1500
Energy production at mean wind speed (kWh/a)		
--5 m/s	615	528
--10 m/s	2350	2189
Wind turbine rotor diameter (m)	40.3	38.2
Wind turbine weight (ton)		
--Rotor, including hub	20.5	9.2
--Nacelle	5.6	19.9
--Rotor + nacelle	26.1	29.0
--Tower	34.0	27.8
--Total	60.1	56.9

As it can be observed in Table 4-2, the annual energy production of the direct-drive PMSG is higher than that of the geared-drive conventional SCIG. Though the wind turbine rotor diameter of the direct-drive PMSG is bigger than that of the geared-drive SCIG, the total weight of the rotor and nacelle is lower. From the comparison of the 500 kW wind turbines with the PMSG and the conventional SCIG in Table 4-1 and Table 4-2, it may be concluded that the total weight of the direct-drive wind turbine with PMSG is only slightly higher than of the geared-drive SCIG system, even though the total weight of gearbox and generator of SCIG system are 2.8 times of the active material weight of the PMSG. That is, from the viewpoint of total weight for wind turbine systems, the direct-drive PMSG system maybe almost similar to the geared-drive SCIG system.

On the other hand, it is worthwhile to be mentioned, the study of Böh et al. (see Table 4-3) concludes that the electromechanical converter of a 1.5 MW wind turbine rotating at 19 rpm with a direct-drive EESG would be about 25% more expensive than the three-stage geared-drive DFIG solution [71][73]. Table 4-3 depicts the percentage of total turbine cost for the conventional geared-drive DFIG, the direct-drive EESG and PMSG.

Table 4-3: *Cost comparison between the geared drive DFIG, the direct-drive EESG and PMSG*

Parts considered	Percentage of total turbine cost		
	DFIG	EESG	PMSG
Gearbox, shaft, Bearing	25%	1%	1%
Generator	8%	36%	16%
Electrics (including converter)	11%	19%	22%
Total	44%	56%	39%

The results given by Table 4-3 may be not very accurate, because the total cost is derived from different sources [8][71][136][140], and the manufacturing and management overhead cost for the direct-drive PMSG is not taken into account. Once the manufacturing cost, management cost and profit are considered, the direct-drive PMSG technology will be more expensive than the geared-drive DFIG [140]. In addition, the comparison between the direct-drive PMSG and EESG shows the cost for active material of PMSG is lower. This is mainly due to the reduced pole pitch of PMSG. An increased number of poles can be set for a given diameter [7][8][140].
Polinder et al [1] have compared five different generator systems for wind turbines of 3 MW output power. Wind turbine characteristics and dimensions for the comparison are presented in Table 4-4 and Table 4-5. The five different concepts are defined as follows:

- *A - doubly-fed induction generator system with three-stage gearbox (DFIG 3G)*
- *B - electrically excited direct-drive synchronous generator system (EESG DD)*
- *C - PM excited direct-drive synchronous generator system (PMSG DD)*
- *D - PM excited synchronous generator system with single-stage gearbox (PMSG 1G)*
- *E - the doubly-fed induction generator system with single-stage gearbox (DFIG 1G)*

Fig. 4-1 shows the weight of the active material of five different generator systems. Fig 4-2 shows the cost of five different wind turbines. The annual loss and annual energy yield are presented in Fig. 4-3. According to the comparisons, the DFIG 3G system seems the lightest and low cost solution. That is why the DFIG 3G system is most widely used on the market. However this system has a low energy yield and has wearing components such as the gearbox, the brushes and the slip rings. These wearing components need frequent maintenance. The EESG DD system is the heaviest and the most expensive generator system. The PMSG DD system seems much more attractive because it has the highest energy yield and its active material weight is light compared to the EESG DD system. The active material weight of the PMSG DD is nearly half of that of the EESG DD. However the PMSG DD system is more expensive compared to the geared drive generator systems, although the cost of PMs and power electronics has decreased in recent years.

Table 4-4: *Wind turbine characteristics in [1]*

Rated grid power	3	[MW]
Rotor diameter	90	[m]
Rated wind speed	12	[m/s]
Rated rotating speed	15	[rpm]
Maximum aerodynamic rotor efficiency	48	[%]
Density of air	1.225	[kg/m^3]

Table 4-5: *Generator dimensions of different 3 MW wind turbines*

Generator concept	A (DFIG 3G)	B (EESG DD)	C (PMSG DD)	D (PMSG 1G)	E (DFIG 1G)
Stator air-gap diameter [m]	0.84	5	5	3.6	3.6
Stack length [m]	0.75	1.2	1.2	0.4	0.6
Air-gap length [mm]	1	5	5	3.6	2

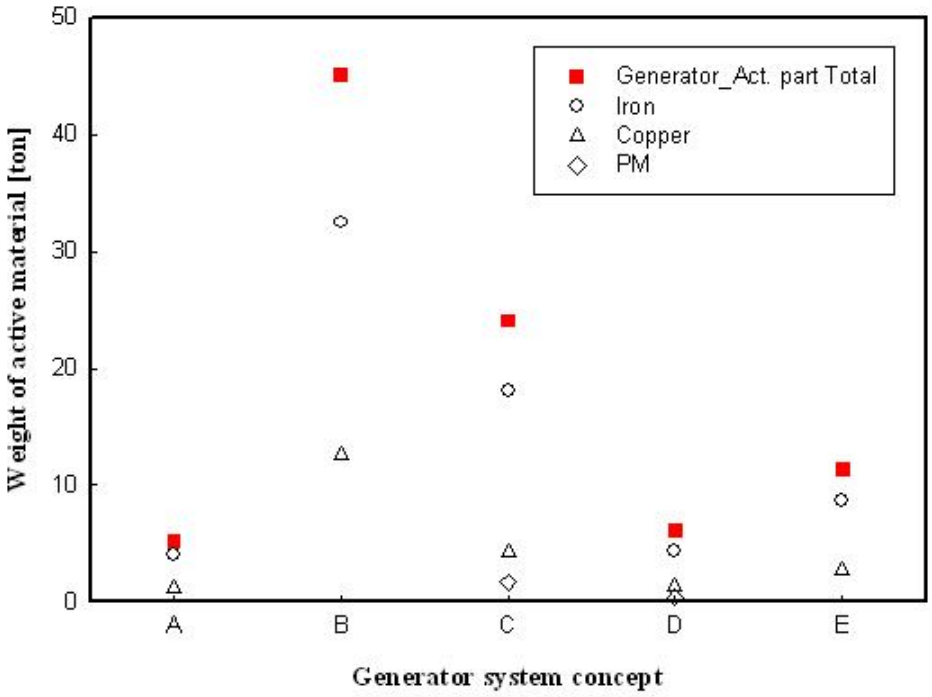

Fig. 4-1: *Weight of the active material of different generator systems*

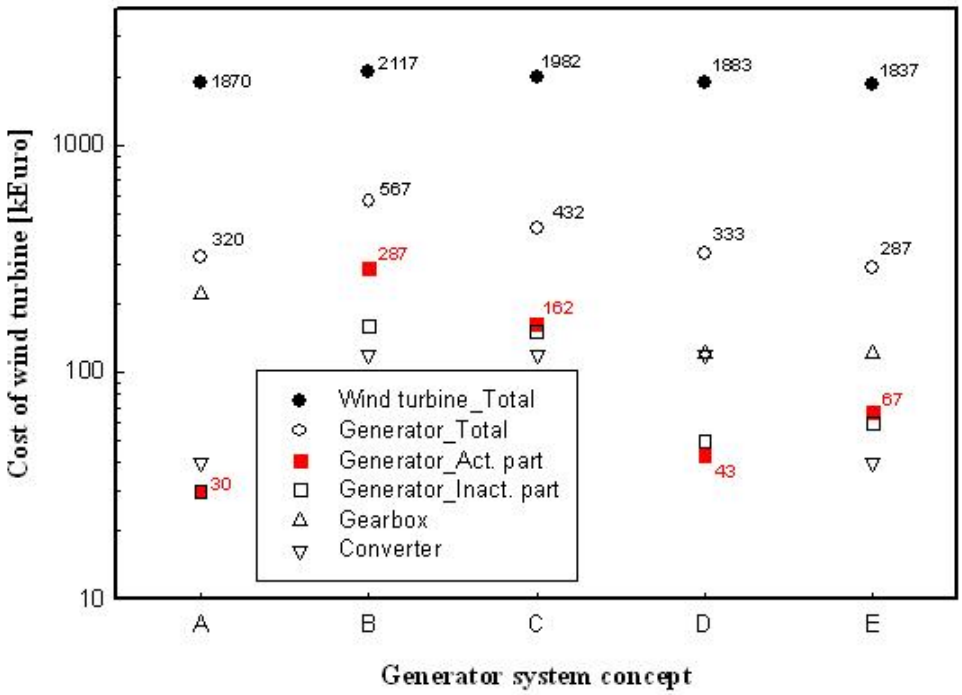

Fig. 4-2: *Cost of different wind turbines*

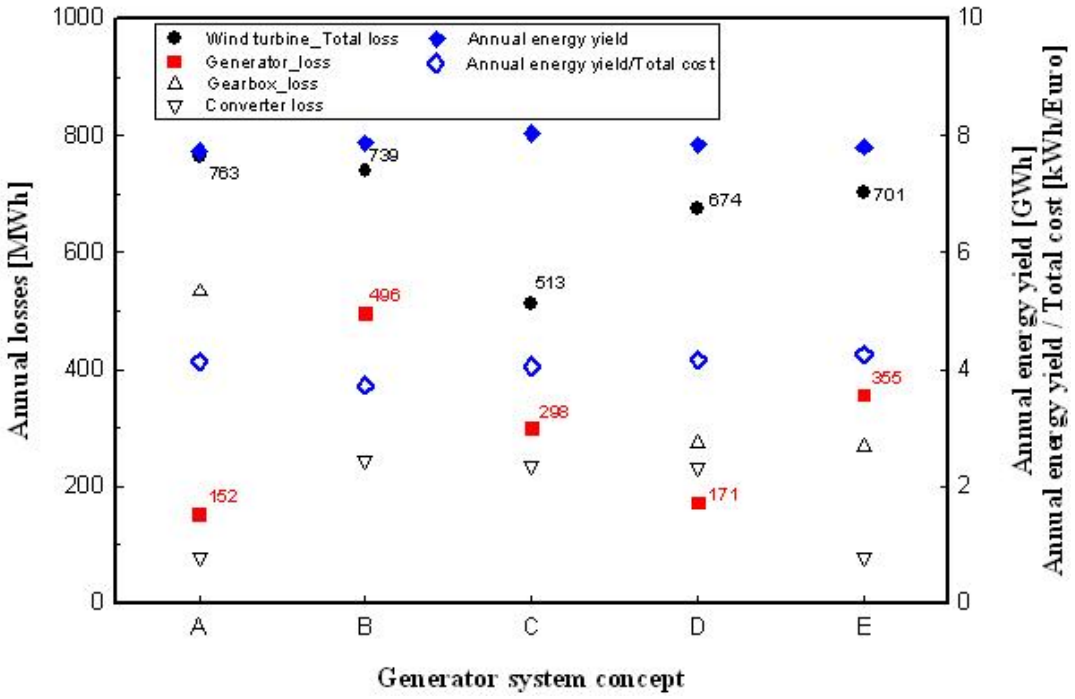

Fig. 4-3: *Annual losses and energy yield of different wind turbines*

Based on the above quantitative comparisons, some conclusion between the geared drive and the direct-drive wind generators can be drawn as follows.

- From the aspects of size and weight, the outer diameter of the direct-drive generator is usually larger than the geared-drive generator, but the total length is shorter. Considering the parts of wind turbine blade, the total system weight of wind turbines is almost similar between a three-stage geared-drive configuration and a direct-drive PMSG solution. As far as the costs are concerned, the direct-drive PMSG technology is almost in the same range as the geared-drive DFIG configuration, the direct-drive EESG is more expensive.
- The DFIG 1G is the most promising choice from the viewpoints of total generator cost and energy yield per cost.
- For direct-drive wind turbine topologies, PMSG DD is the better choice than EESG DD, but the Multibrid type of PMSG 1G has a better performance than PMSG DD from the viewpoints of total generator cost and energy yield per cost.

Lampola has investigated a variety of direct-drive wind generators [9]. The radial-flux machine is a better choice for gearless wind turbines than the axial-flux machine, if the machine output is more than 100kW. In a smaller machine, there is no significant difference between the two types of machines.
The TFPM machine has higher efficiency and a lower active weight, but it needs more PM material than the RFPM machine. Though both the AFPM and RFPM machine have high efficiency, the outer stator diameter of the AFPM machine is almost 1.82 times of the air-gap diameter of RFPM machine. On the other hand, it is mentioned in [137][140], for a generator diameter of 2.5m, the highest torque density per generator volume unity has been estimated at 75 kNm/m³ for the TFPM machine, and only 40 kNm/m³ for Torus and the RFPM machine designs. According to [140], torque densities generally increase with increasing generator diameter, up to 100 kNm/m³ for a Torus with 4.5 m diameter.
Recently, Y. Chen et al. have also provided some detailed comparisons among seven PM wind generator topologies based on the conditions of both high-speed and low-speed by the magnet-

circuit design. From the results presented in [50], the double-sided AFPM machine has a smaller volume and weight for a given power rating, making the power density and efficiency very high. The double side AFPM machine requires the least space, as in this configuration no rotor back yoke is needed and the axial length is very short. The outer-rotor RF construction is superior to the conventional inner-rotor RF construction. The radial-flux configurations have a smaller outer diameter and have a longer axial length than axial-flux constructions. The Torus construction is simple but it requires more magnet weight. For all axial-flux configurations except the Torus machine, the use of magnets is better than that for radial-flux constructions.
Dubois has also compared six different structures of PMSG by collecting data from the existing papers [140]. Two criteria used for the comparisons are torque density and cost per torque, as being critical for the integration of direct-drive generators for wind turbines. The results have shown that the TFPM machine and the double-sided AFPM machine have excellent characteristics.
Based on the above mentioned, the transverse-flux machine is small, efficient and light, but the mechanical design is very complicated. The RFPM machine has smaller outer diameter and it is cheaper than the axial-flux machine. The double-sided AF machines have higher torque density and efficiency than the others AF machine. Therefore, the configurations of outer-rotor RFPM machine, double-sided AFPM machine, and TFPM machine seem to be better choice to the direct-drive PMSG system.
TFPM machine has also been compared with RFPM machine in [8]. According to the comparison, TFPM machine with large air-gap seems to be no more attractive because its force density is a little high or even low compared to RFPM machine. Fig. 4-4 shows that TFPM machine provides a significant cost advantage in active material, over RFPM machine, for small air-gap. However, this advantage is reduced when the air-gap increases. TFPM cost advantage factor, K_{TFPM_Cost}, in Fig. 4-4 is defined as follow:

$$K_{TFPM\_Cost} = (Cost/Torque)_{RFPM} / (Cost/Torque)_{TFPM}$$

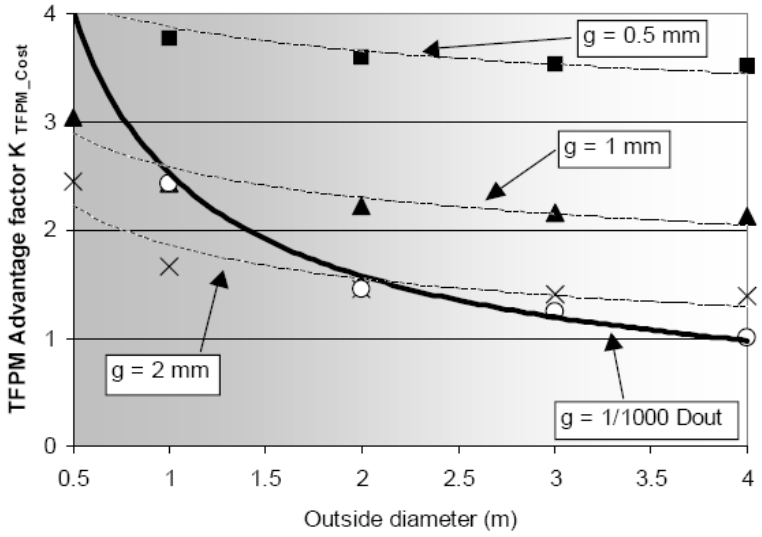

Fig. 4-4: *Cost advantage factor of TFPM machine over RFPM machine [8]*

4.2 Comparison criteria

In order to compare different wind generator topologies, various criteria may be used including the index of torque density, cost per torque, efficiency, active material weight, outer diameter, total length, total volume, total generator cost, annual energy yield and energy yield per cost,

and so on [1][3][7][148]. However, it may be relatively incomprehensive to make the comparison fair and reasonable by using a single aspect. For example, compared with the geared-drive technology, the advantages of the direct-drive technology actually available are usually less maintenance required, lower audible noise, higher efficiency at low wind speed. However, the advantages of the geared-drive technology are usually lower capital cost, ease of transportation and installation due to the smaller machine diameter, higher efficiency at higher wind speed. Though overall comparison criteria may be unpractical and impossible to obtain, with the development of wind power technology, some relatively comprehensive criteria including some more attractive factors need further investigation in the quantitative comparison of different wind generator topologies.

- Current trends of research and development of wind turbine concepts are mostly related to offshore wind energy. The most important difference between the requirements for onshore and offshore wind energy is that for offshore turbines it is much more important that they are robust and maintenance-free [143][144]. This is because it is extremely expensive and difficult and even impossible to do offshore maintenance and reparations under uncertain weather conditions. So the reliability and availability of large wind turbines may be more important aspects to be taken into consideration.
- With the increasing penetration of wind energy into the grid and the trends of wind farms be treated as the conventional plants, performances of interaction with weak grid, such as ride through capability, ability of flexible power control and advanced protection systems may be needed into the quantitative cost.
- Some performances referred to wind turbine blade and hub height are also worthwhile to be further considered, because a integral design of wind turbines and generator systems including manufacturing, transportation, and installation may considerably affect the price of wind turbines, especially with the increasing capacity of wind turbines, this aspect is more and more obvious.

Moreover, some performances (e.g. annual energy yield) of wind turbines are also usually related closely to the given wind distribution, e.g. annual wind speed and wind distribution. Therefore there are still many arguments to make a conclusion of most suitable generator system. An overall and practical comparison of different generator topologies including technical economy, control function, availability and reliability may be required in further investigation.

References

[1] H. Polinder, F.F.A. van der Pijl, G.J. de Vilder, P. Tavner, “Comparison of direct-drive and geared generator concepts for wind turbines”, IEEE Trans. Energy Conversion, Vol. 21, pp. 725-733, September 2006.

[2] H. Vihriälä, “Control of variable speed wind turbines”, Ph.D. dissertation Tampere University of Technology, Hervanta, Finland, 2002.

[3] S. Widyan, “Design, optimization, construction and test of rare-earth permanent-magnet electrical machines with new topology for wind energy applications”, Ph.D. dissertation Technische Universität Berlin, Berlin, Germany, 2006.

[4] R. Hoffmann, “A comparison of control concepts for wind turbines in terms of energy capture”, Ph.D. dissertation Darmstadt University of Technology, Darmstadt, Germany, 2002.

[5] J. Manwell, J. McGowan, A. Rogers, “Wind energy explained”, Wiley, 2002.

[6] G. Bywaters, V. John, J. Lynch, P. Mattila, G. Nortor, J. Stowell, M. Salata, O. Labath, A. Chertok and D. Hablanian, “Northern power systems windPACT drive train alternative design study report”, NREL, Golden, Colorado, report No. NREL/SR-500-35524, October 2004.

[7] A. Grauers, “Design of direct-driven permanent-magnet generators for wind turbines”, Ph.D. dissertation, Chalmers University of Technology, Göteborg, Sweden, 1996.

[8] M. Dubois, “Optimized permanent magnet generator topologies for direct drive wind turbines”, Ph.D. dissertation, Delft University of Technology, Delft, The Netherlands, 2004.

[9] P. Lampola, “Directly driven, low-speed permanent-magnet generators for wind power applications”, Ph.D. dissertation, Helsinki University of Technology, Finland, 2000.

[10] ENERCON GmbH, http://www.enercon.de/en/_home.htm, last accessed November 2006.

[11] Winwind Oy, http://www.winwind.fi/english/tuotteet.html, last accessed September 2006.

[12] Harakosan Europe BV, http://www.harakosan.nl/products/, last accessed November 2006.

[13] Vestas Wind Systems, http://www.vestas.com/vestas/global/en/Downloads/Downloads/Download_brochurer.htm, last accessed September 2006.

[14] Siemens AG, http://www.powergeneration.siemens.com/en/windpower/products/index.cfm, last accessed September 2006.

[15] Repower Systems AG, http://www.repower.de/index.php?id=12&L=1, last accessed September 2006.

[16] Nordex AG, http://www.nordex-online.com/en/products-services/wind-turbines.html, last accessed September 2006.

[17] Multibrid , http://www.multibrid.com/m5000/data.html, last accessed September 2006.

[18] GE Energy, http://www.gepower.com/prod_serv/products/wind_turbines/en/index.htm, last accessed September 2006.

[19] Gamesa Elórica, http://www.gamesa.es/gamesa/index.html, last accessed September 2006.

[20] Ecotècnia, http://www.ecotecnia.com/index_ing.htm, last accessed September 2006.

[21] DeWind, http://www.dewind.de, last accessed September 2006.

[22] Suzlon Energy, http://www.suzlon.com/product_overview.htm, last accessed September 2006.

[23] H. Weh, “Transverse-flux machines in drive and generator application”, in Proceedings of the IEEE Symposium on Electric Power Engineering (Stockholm Power Tech), Strockholm, Sweden, 1995, Vol. Invited speaker’ session, pp. 75-80.

[24] L. H. Hansen, L. Helle, et al. “Conceptual survey of generators and power electronics for wind turbines”, Risø-R-1205(EN), 2001.

[25] C. P. Maddison, “Transverse flux machines for high torque applications”, Ph.D. dissertation University of Newcastle upon Tyne, UK, 1999.

[26] E. Muljadi, C. P. Butterfield and Y. Wan, “Axial-flux modular permanent-magnet generator with a toroidal winding for wind-turbine applications”, IEEE Trans. Ind. Applicat., Vol. 35, No. 4, pp. 831-836, July/Aug. 1999.

[27] L. Söderlund, J-T. Eriksson, J. Salonen, H. Vihriälä and R. Perälä, “A permanent-magnet generator for wind power applications”, IEEE Trans. Magnetics, Vol. 32, No. 4, pp. 2389-2392, July 1996.
[28] L. Söderlund, A. Koski, H. Vihriälä, J-T. Eriksson and R. Perälä, “Design of an axial flux permanent magnet wind power generator”, in Proc. 1997 IEE Conf. Elec. Mach. And Drives, pp. 224-228.
[29] J. R. Bumby, R. Martin, “Axial-flux permanent-magnet air-cored generator for small-scale wind turbines”, IEE Proc.-Electr. Power Appl., Vol. 152, No. 5, pp. 1065-1075, September 2005.
[30] T. Okazaki, H. Sugimoto and T. Takeda, “Liquid nitrogen cooled HTS motor for ship propulsion”, in Proc. 2006 IEEE Con. Power Engineering Soc., pp. 1-6.
[31] C. Boccaletti, S. Elia and E. Nisticò, “Deterministic and stochastic optimization algorithms in conventional design of axial flux PM machines”, International Symposium on Power Electronics, Electrical Drives, Automation and Motion, Speedam 2006, pp. 111-115, May 2006.
[32] F. Caricchi, F. Crescimbini and E. Santini, “Basic principle and design criteria of axial-flux PM machines having counter-rotating rotors”, in Proc. 1994 IEEE Conf. Ind. Appl. Soc., pp. 247-253.
[33] B. J. Chalmers, W. Wu and E. Spooner, “An axial-flux permanent-magnet generator for a gearless wind energy system”, IEEE Trans. Energy Conversion, Vol. 14, No. 2, pp. 251-257, June 1999.
[34] J. F. Eastham, F. Profumo, A. Tenconi, R. Hill-Cottingham, P. Coles and G. Gianolio, “Novel axial flux machine for aircraft drive: Design and modeling”, IEEE Trans. Magnetics, Vol. 38, No. 5, pp. 3003-3005, September 2002.
[35] Y. Chen and P. Pillay, “Axial-flux PM wind generator with a soft magnetic composite core”, in Proc. 2005 IEEE Conf. Ind. Appl., pp. 231-237.
[36] A. Parviainen, “Design of axial-flux permanent-magnet low-speed machines and performance comparison between radial-flux and axial-flux machines”, Ph.D. dissertation Lappeenranta University of Technology, Lappeenranta, Finland, 2005.
[37] E. Spooner and B. J. Chalmers, “TORUS : A slotless, toroidal-stator, permanent-magnet generator”, IEE Proceedings-B, Vol. 139, No. 6, pp. 497-506, November 1992.
[38] W. Wu, E. Spooner and B. J. Chalmers, “Design of slotless TORUS generators with reduced voltage regulation”, IEE Proc.-Electr. Power Appl., Vol. 142, No. 5, pp. 337-343, September 1995.
[39] W. Wu, E. Spooner and B. J. Chalmers, “Reducing voltage regulation in toroidal permanent-magnet generators by stator saturation”, in Proc. 1995 IEE Conf. Elec. Mach. And Drives, pp.385-389.
[40] E. Spooner and A. C. Williamson, “Direct coupled, permanent magnet generators for wind turbine applications”, IEE Proc.-Electr. Power Appl., Vol. 143, No. 1, pp. 1-8, January 1996.
[41] Z. Chen and E. Spooner, “A modular, permanent-magnet generator for variable speed wind turbines”, in Proc. 1995 IEE Conf. Elec. Mach. And Drives, pp. 453-457.
[42] E. Spooner, A.C. Williamson and G. Catto, “Modular design of permanent-magnet generators for wind turbines”, IEE Proc.-Electr. Power Appl., Vol. 143, No. 5, pp. 388-395, September 1996.
[43] G. Geng and E. Spooner, “Cancellation of noise and vibration in modular permanent-magnet wind turbine generators”, in Proc. 1995 IEE Conf. Elec. Mach. And Drives, pp. 467-471.
[44] A.J.G. Westlake, J.R. Bumby and E. Spooner, “Damping the power-angle oscillations of a permanent-magnet synchronous generator with particular reference to wind turbine applications”, IEE Proc.-Electr. Power Appl., Vol. 143, No. 3, pp. 269-280, May 1996.
[45] E. Spooner and A. Williamson, “Modular, permanent-magnet wind-turbine generators”, in Proc. 1996 IEEE Conf. Ind. Appl., Vol. 1, pp. 497-502.
[46] E. Spooner and A.C. Williamson, “Parasitic losses in modular permanent-magnet generators”, IEE Proc.-Electr. Power Appl., Vol. 145, No. 6, pp. 485-496, November 1998.
[47] E. Spooner, P. Gordon, J.R. Bumby and C.D. French, “Lightweight, ironless-stator, PM generators for direct-drive wind turbines” , IEE Proc.-Electr. Power Appl., Vol. 152, No. 1, pp. 17-26, January 2005.

[48] P.J. Tavner and E. Spooner, “Light structures for large low-speed machines for direct-drive applications”, in Proc. of the International Conference on Electrical Machines(ICEM), pp. 421.1-6, September 2006.
[49] W. Wu, V.S. Ramsden, T. Crawford and G. Hill, “A low-speed, high-torque, direct-drive permanent magnet generator for wind turbine” , in Proc. 2000 IEEE Conf. Ind. Appl., Vol. 1, pp. 147-154.
[50] Y. Chen, P. Pillay and A. Khan, “PM wind generator topologies”, IEEE Transactions on Ind. App. Vol. 41, No. 6, pp. 1619-1626, November/December 2005.
[51] M.A. Mueller, “Design and performance of a 20kW, 100rpm, switched reluctance generator for a direct drive wind energy converter”, in Proc. 2005 IEEE Conf. Elec. Mach. and Drives, pp. 56-63.
[52] J. Chen, C.V. Nayar and L. Xu, “Design and finite-element analysis of an outer-rotor permanent-magnet generator for directly coupled wind turbines”, IEEE Transactions on Magnetics, Vol. 36, No. 5, pp. 3802-3809, September, 2000.
[53] K.C. Kim, S.B. Lim, K.B. Jang, S.G. Lee, J. Lee, Y.G. Son, Y.K. Yeo and S.H. Baek, “Analysis on the direct-driven high power permanent magnet generator for wind turbine”, in Proc. 2005 IEEE Conf. Elec. Mach. and Systems(ICEMS), Vol. 1, pp. 243-247.
[54] M.A. Mueller, A.S. McDonald and D.E. Macpherson, “Structural analysis of low-speed axial-flux permanent-magnet machines”, IEE Proc.-Electr. Power Appl., Vol. 152, No. 6, pp. 1417-1426, November 2005.
[55] A.S. McDonald, M.A. Mueller and H. Polinder, “Comparison of generator topologies for direct-drive wind turbines including structural mass”, in Proc. of the International Conference on Electrical Machines(ICEM), pp. 360.1-7, September 2006.
[56] P. Lampola and J. Perho, “Electromagnetic analysis of a low-speed permanent-magnet wind generator”, International Conference on Opportunities and Advances in International Electric Power Generation, pp. 55-58, March 1996.
[57] H. Polinder, “On the losses in a high-speed permanent-magnet generator with rectifier”, Ph.D. dissertation, Delft University of Technology, Delft, The Netherlands, 1998.
[58] G.R. Slemon and X. Liu, “Modeling and design optimization of permanent magnet motors”, Elec. Mach. And Power Syst., Vol. 20, pp. 71-92, 1992
[59] M.R. Dubois, H. Polinder and J.A. Ferreira, “Comparison of generator topologies for direct-drive wind turbines”, in Proc. 2000 Nordic Countries Pow. And Indust. Elec., pp. 22-26.
[60] M.R. Dubois, H. Polinder and J.A. Ferreira, “Axial and radial-flux PM generators for direct-drive wind turbines”, in Proc. 2001 Europ. Wind Energy Conf., pp. 1112-1115.
[61] F. Sahin, “Design and development of a high-speed axial-flux permanent-magnet machine”, Ph.D. dissertation, Eindhoven University of Technology, Eindhoven, The Netherlands, 2001.
[62] K. Sitapati and R. Krishnan, “Performance comparisons of radial and axial field, permanent magnet, brushless machines”, in Proc. 2000 IEEE Conf. Ind. Appl. Soc., pp. 228-234.
[63] F. Libert and J. Soulard, “Design Study of Different Direct-Driven Permanent-Magnet Motors for a Low Speed Application”, in Proceedings of the Nordic Workshop on Power and Industrial Electronics (NORpie), Trondheim, Norway, June 2004.
[64] D. Svechkarenko, J. Soulard and Chandur Sadarangani, “Analysis of a novel transverse flux generator in direct-driven wind turbines”, International Conference on Electrical Machines(ICEM), pp. 424.1-6, September 2006.
[65] D. Svechkarenko, J. Soulard and Chandur Sadarangani, “A Novel Transverse Flux Generator in Direct-Driven Wind Turbines”, in Proceedings Nordic Workshop on Power and Industrial Electronics, June 2006.
[66] D. Vizireanu, X. Kestelyn, S. Brisset, P. Brochet, Y. Milet and D. Laloy, “Polyphased modular direct-drive wind turbine generator”, in Proc. 2005 European Conference on Power Electronics and Applications, pp. 1-9.
[67] D. Vizireanu, S. Brisset and P. Brochet, “Design and optimization of a 9-phase axial-flux PM synchronous generator with concentrated winding for direct-drive wind turbine”, in Proc. 2006 IEEE Conf. Ind. Appl. Soc., Vol. 4, pp. 1912-1918.
[68] F. Wang, J. Bai, Q. Hou and J. Pan, “Design features of low speed permanent magnet generator direct driven by wind turbine”, in Proc. 2005 IEEE Conf. Elec. Mach. and Systems(ICEMS), Vol. 2, pp. 1017-1020.

[69] F. Wang, Q. Hou, J. Bo and J. Pan, “Study on control system of low speed PM generator direct driven by wind turbine”, in Proc. 2005 IEEE Conf. Elec. Mach. and Systems(ICEMS), Vol. 2, pp. 1009-1012.
[70] S. Evon and R. Schiferl, “Direct drive induction motors”, in Proc. 2004 IEEE the Pulp and Paper Industry Technical Conference, pp. 49-54.
[71] G. Böhmeke, R. Boldt and H. Beneke, “Geared drive intermediate solutions, comparisons of design features and operating economics”, in Proc. 1997 Europ. Wind Energy Conf., pp. 664-667.
[72] S. Siegfriedsen and G. Böhmeke, “Multibrid technology-a significant step to multi-megawatt wind turbines”, Wind Energy, Vol. 1, Issue 2, pp. 89-100, December 1998.
[73] G. Böhmeke, “Development and operational experience of the wind energy converter WWD-1”, in Proc. 2003 Europ. Wind Energy Conf.
[74] H. Weh, H. Hoffmann, J. Landrath, H. Mosebach and J. Poschadel, “Directly-driven permanent-magnet excited synchronous generator for variable speed operation”, in Proc. 1988 Europ. Wind Energy Conf., pp. 566-572.
[75] H. Weh, “Permanentmagneterregte Synchronmaschinen hoher Kraftdichte nach dem Transversalflusskonzept”, etzArchiv, Vol. 10, No. 5, pp. 143-149, 1988.
[76] H. Weh, “Synchronous machines with New Topologies”, in Proc. 1991 Int. Conf. on the Evolution and Modern Aspects of Sync. Mach., pp. C1-C9.
[77] M.R. Harris, G.H. Pajooman and S.M. Abu Sharkh, “Performance and design optimization of electric motors with heteropolar surface magnets and homopolar windings”, IEE Proc. Electr. Power Appl., Vol. 143, No. 6, pp. 429-436, Nov. 1996.
[78] T. Hartkopf, M. Hofmann and S. Jöckel, “Direct-drive generators for megawatt wind turbines”, in Proc. 1997 Europ. Wind Energy Conf., pp. 668-671.
[79] M.R. Harris, G.H. Pajooman, S.M. Abu Sharkh and B.C. Mecrow, “Comparison of flux-concentrated and surface-magnet configurations of the VRPM (Transverse-Flux) machine”, in Proc. 1998 Int. Conf. on Elec. Mach., pp. 1119-1122.
[80] G.H. Pajooman, “Performance assessment and design optimization of VRPM (Transverse Flux) machines by finite element computation”, Ph.D. dissertation, Southampton Univ., UK, 1997.
[81] H. Weh, “Transverse flux machines in drive and generator application”, in Proc. 1995 Stockholm Power Tech. Conf., pp. 75-80.
[82] A. Lange, W.-R. Canders, F. Laube and H. Mosebach, “Comparison of different drive systems for a 75kW electrical vehicle drive”, in Proc. 2000 Int. Conf. on Elec. Mach., pp. 1308-1312.
[83] B.C. Mecrow, A.G. Jack and C.P. Maddison, “Permanent magnet machines for high torque, low speed applications”, in Proc. 1996 Int. Conf. on Elec. Mach., pp. 461-466.
[84] A.J. Mitcham and J.J.A. Cullen, “Motors and drives for surface ship propulsion: comparison of technologies”, in Proc. 1995 Electric Propulsion Conf., paper 4.
[85] A.J. Mitcham, “Transverse flux motors for electric propulsion of ships”, in Proc. 1997 IEE Colloquium on New Topologies for PM Machines, pp. 3/1-3/6.
[86] J.E. Voyce, S.M. Husband and D.J. Mattick, “The PM propulsion motor: from infancy to adolescence”, in Proc. All Elec. Ship Conf., pp. 134-139.
[87] H. Weh, “Multiple track transversal flux machine with ring coils”, German patent DE 4 300 440, German patent Office, 1994.
[88] C.P. Maddison, B.C. Mecrow and A.G. Jack, “Claw pole geometries for high performance transverse flux machines”, in Proc. 1998 Int. Conf. on Elec. Mach., pp. 340-345.
[89] R. Blissenbach, G. Henneberger, U. Schäfer and W. Hackmann, “Development of a transverse flux traction motor in a direct drive system”, in Proc. 2000 Int. Conf. on Elec. Mach., pp. 1457-1460.
[90] P. Dickinson, A.G. Jack and B.C. Mecrow, “Improved permanent magnet machines with claw pole armatures”, in Proc. 2002 Int. Conf. on Elec. Mach., paper 245.
[91] S. Huang, J. Luo and T.A. Lipo, “Evaluation of the transverse flux circumferential current machine by the use of sizing equations”, in Proc. 1997 IEEE Conf. Elec. Mach. and Drives, pp. WB2/15.1-WB2/15.3.
[92] S. Huang, J. Luo and T.A. Lipo, “Analysis and evaluation of the transverse flux circumferential current machine”, in Proc. 1997 IEEE Conf. Ind. Appl. Soc., Vol. 1, pp. 378-384.

[93] G. Henneberger and M. Bork, “Development of a new transverse flux motor”, in Proc. 1997 IEE Colloquium on New Topologies for PM Machines, pp. 1/1-1/6.
[94] M.R. Harris, G.H. Pajooman and S.M.A. Sharkh, “Comparison of alternative topologies for VRPM(transverse-flux) electrical machines”, in Proc. 1997 IEE Colloquium on New Topologies for PM Machines, pp. 2/1-2/7.
[95] M.R. Harris, G.H. Pajooman and S.M.A. Sharkh, “The problem of power factor in VRPM (transverse-flux) machines”, in Proc. 1997 IEE Conf. Elec. Mach. and Drives, pp. 386-390.
[96] B.E. Hasubek and E.P. Nowicki, “Two dimensional finite element analysis of passive rotor transverse flux motors with slanted rotor design”, in Proc. 1999 IEEE Canadian Conf. Elec. and Computer Engineering, Vol. 2, pp. 1199-1204.
[97] B.E. Hasubek and E.P. Nowicki, “Design limitations of reduced magnet material passive rotor transverse flux motors investigated using 3D finite element analysis”, in Proc. 2000 IEEE Canadian Conf. Elec. and Computer Engineering, Vol. 1, pp. 365-369.
[98] W.M. Arshad, T. Bäckström and C. Sadarangani, “Analytical design and analysis procedure for a transverse flux machine”, in Proc. 2001 IEEE Conf. Elec. Mach. and Drives, pp. 115-121.
[99] C.D. French, C. Hodge and M. Husband, “Optimised torque control of marine transverse-flux propulsion machines”, in Proc. 2002 IEE Conf. Power Electronics, Mach. and Drives, pp. 1-6.
[100] B.S. Payne, S.M. Husband and A.D. Ball, “Development of condition monitoring techniques for a transverse flux motor”, in Proc. 2002 IEE Conf. Power Electronics, Mach. and Drives, pp. 139-144.
[101] M.R. Dubois, H. Polinder and J.A. Ferreira, “Transverse-flux permanent magnet (TFPM) machine with toothed rotor”, in Proc. 2002 IEE Conf. Power Electronics, Mach. and Drives, pp. 309-314.
[102] G. Kastinger and A. Schumacher, “Reducing torque ripple of transverse flux machines by structural designs”, in Proc. 2002 IEE Conf. Power Electronics, Mach. and Drives, pp. 320-324.
[103] W.M. Arshad, T. Bäckström and C. Sadarangani, “Investigating a transverse flux machine with intermediate poles”, in Proc. 2002 IEE Conf. Power Electronics, Mach. and Drives, pp. 325-328.
[104] Y. Rang, Chenglin Gu and H. Li, “Analytical design and modeling of a transverse flux permanent magnet machine”, in Proc. 2002 Conf. Power System Technology, Vol. 4, pp. 2164-2167.
[105] S.M. Husband and C.G. Hodge, “The Rolls-Royce transverse flux motor development”, in Proc. 2003 IEEE Conf. Elec. Mach. and Drives, Vol. 3, pp. 1435-1440.
[106] A. Njeh, A. Masmoudi and A. Elantably, “3D FEA based investigation of the cogging torque of a claw pole transverse flux permanent magnet machine”, in Proc. 2003 IEEE Conf. Elec. Mach. and Drives, Vol. 1, pp. 319-324.
[107] K.Y. Lu, E. Ritchie, P.O. Rasmussen and P. Sandholdt, “Modelling a single phase surface mounted permanent magnet transverse flux machine based on Fourier Series Method”, in Proc. 2003 IEEE Conf. Elec. Mach. and Drives, Vol. 1, pp. 340-345.
[108] K.Y. Lu, E. Ritchie, P.O. Rasmussen and P. Sandholdt, “General torque equation capable of including saturation effects for a single phase surface mounted permanent magnet transverse flux machine”, in Proc. 2003 IEEE Conf. Ind. Appl. Soc., Vol. 2, pp. 1382-1388.
[109] K.Y. Lu, E. Ritchie, P.O. Rasmussen and P. Sandholdt, “A simple method to estimate inductance profile of a surface mounted permanent magnet transverse flux machine”, in Proc. 2003 IEEE Conf. Power Electronics and Drive Systems(PEDS), Vol. 2, pp. 1334-1338.
[110] K.Y. Lu, E. Ritchie, P.O. Rasmussen and P. Sandholdt, “Modeling and power factor analysis of a single phase surface mounted permanent magnet transverse flux machine”, in Proc. 2003 IEEE Conf. Power Electronics and Drive Systems(PEDS), Vol. 2, pp. 1609-1613.
[111] J. Shi, Y. Li and W. Zheng, “Survey on the development of transverse flux machines”, in Proc. 2003 IEEE Conf. Elec. Mach. and Systems(ICEMS), Vol. 1, pp. 137-140.

[112] Y.G. Guo, J.G. Zhu, P.A. Watterson and W. Wu, “Design and analysis of a transverse flux machine with soft magnetic composite core”, in Proc. 2003 IEEE Conf. Elec. Mach. and Systems(ICEMS), Vol. 1, pp. 153-157.
[113] Y.G. Guo, J.G. Zhu, P.A. Watterson and W. Wu, “Development of a PM transverse flux motor with soft magnetic composite core”, IEEE Transactions on Energy Conversion, Vol. 21, No. 2, pp. 426-434, June 2006.
[114] A. Masmoudi, A. Njeh, A. Mansouri, H. Trabelsi and A. Elantably, “Optimizing the overlap between the stator teeth of a claw pole transverse-flux permanent-magnet machine”, IEEE Transactions on Magnetics, Vol. 40, No. 3, pp. 1573-1578, May 2004.
[115] G.Q. Bao, D. Zhang, J.H. Shi and J.Z. Jiang, “Optimal design for cogging torque reduction of transverse flux permanent motor using particle swarm optimization algorithm”, in Proc. 2004 IEEE Conf. Power Electronics and Motion Control(IPEMC), Vol. 1, pp. 260-263.
[116] G.Q. Bao and J.Z. Jiang, “A new transverse flux permanent motor for direct drive application”, in Proc. 2005 IEEE Conf. Elec. Mach. and Drives, pp. 1192-1195.
[117] G.Q. Bao, J.H. Shi and J.Z. Jiang, “Efficiency optimization of transverse flux permanent magnet machine using genetic algorithm”, in Proc. 2005 IEEE Conf. Elec. Mach. and Systems(ICEMS), Vol. 1, pp. 380-384.
[118] Z. Rahman, “Evaluating radial, axial and transverse flux topologies for ‘In-Wheel’ motors”, in Proc. 2004 IEEE Conf. Power Electronics in Transportation, pp. 75-81.
[119] E. Schmidt, “3-D finite element analysis of the cogging torque of a transverse flux machine”, IEEE Transactions on Magnetics, Vol. 41, No. 5, May 2005.
[120] J.F. Gieras, “Performance characteristics of a permanent magnet transverse flux generator”, in Proc. 2005 IEEE Conf. Elec. Mach. and Drives, pp. 1293-1299.
[121] Y. Zhao and J. Chai, “Power factor analysis of transverse flux permanent machines”, in Proc. 2005 IEEE Conf. Elec. Mach. and Systems(ICEMS), Vol. 1, pp. 450-459.
[122] U. Werner, J. Schüttler and B. Orlik, “Speed and torque control of a permanent magnet excited transverse flux motor for direct servo-drive applications”, in Proc. 2005 European Conference on Power Electronics and Applications, pp. 1-10.
[123] F. Caricchi, F. Crescimbini, F. Mezzetti and E. Santini, “Multi-stage axial-flux PM machine for wheel direct drive”, in Proc. 1995 IEEE Conf. Ind. Appl., Vol. 1, pp. 679-684.
[124] M.R. Harris and B.C. Mecrow, “Variable reluctance permanent magnet motors for high specific output”, in Proc. 1993 IEE Conf. Elec. Mach. and Drives, pp. 437-442.
[125] F. Caricchi, F. Crescimbini and O. Honorati, “Modular axial-flux permanent-magnet motor for ship propulsion drives”, IEEE Transactions on Energy Conversion, Vol. 14, No. 3, pp. 673-679, September 1999.
[126] R. Poore and T. Lettenmaier, “Alternative design study report: WindPACT advanced wind turbine drive train designs study”, NREL, Golden, Colorado, report No. NREL/SR-500-33196, August 2003.
[127] A.D. Hansen and L.H. Hansen, “Wind turbine concept market penetration over 10 years(1995-2004)”, Wind Energy, Vol.10, pp. 81-97, 2007.
[128] H. Polinder and J. Morren, “Developments in wind turbine generator systems”, Electrimacs 2005, Hammamet, Tunisia.
[129] Windflow Technology Ltd., http://www.windflow.co.nz/products/Windflow500/index.html, last accessed March 2007.
[130] Eize de Vries, “Drive and innovation: The DeWind D8.2 with Voith WinDrive”, Renewable Energy World, Vol. 10, Issue 2, pp. 55-65, March/April 2007.
[131] Chen, Z., Blaabjerg, F. “WIND ENERGY-The World's Fastest Growing Energy Source”, IEEE Power Electronics Society Newsletter, Volume18, Number 3, 2006, ISSN 1054-7231.
[132] Joseph Florence, “Global Wind Power Expands in 2006”, June 28, 2006. http://www.earth-policy.org/Indicators/Wind/2006.htm
[133] Chen, Z., Blaabjerg, F.,“Wind Turbines-A Cost Effective Power Source”, Przeglad Elektrotechniczny R. 80 NR 5/2004 pp 464-469 (ISSN 0033-2097).
[134] Blaabjerg, F., Chen Z., Kjaer S.B., “Power Electronics as Efficient Interface in Dispersed Power Generation Systems”, IEEE Trans. on Power Electronics, Vol. 19, No. 5, Sept. 2004, pp. 1184-1194.
[135] Robert Harrison, Erich Hau and Herman Snel, “Large wind turbines Design and Economics,” John Wiley & Sons Ltd, 2000, ISBN 0471-494569.

[136] Carlson O., Grauers A., Svensson J., Larsson A., “A comparison of electrical systems for variable speed operation of wind turbines”, European wind energy conf., pp.500-505, 1994.
[137] Joris Soens,“Impact of wind energy in a future”, Ph. D dissertation, ISBN 90-5682-652-2, Wettelijk depot,UDC 621.548, Dec., 2005.
[138] Chen, Z., “Issues of Connecting Wind Farms into Power Systems”, Proc. of 2005 IEEE/PES Transmission and Distribution Conference & Exhibition: Asia and Pacific. (Invited paper panel presentation paper).
[139] E. De Vries, “Global wind technology – overview of developments 2003 –2004,” Renewable Energy World, July 2004.
[140] Maxime R. Dubois, “Review of electromechanical conversion in wind turbines”, Repore EPP00.R03, April, 2000.
[141] Annon, “European wind turbine catalogue”, European commission, Brussels, Belgium, pp. 64-67, 1996.
[142] BTM Consults. “International Wind Energy Department—World Market Update 2004, Forecast 2005–2009”. A. Rasmussens, Ringkøbing, Denmark, 2005.
[143] P.J. Tavner and J. Xiang, “Wind turbine reliability, how does it compare with other embedded generation sources”, in Proc. IEE Rel. Transmission Distrib. Netw. Conf., London, U.K., Feb. 2005, pp. 243-248.
[144] H. Polinder, S.W.H. de Haan, M.R. Dubois, J.G. Slootweg, ‘Basic operation principles and electrical conversion systems of wind turbines'. In EPE Journal, December 2005 (vol. 15, no. 4), pp. 43-50.
[145] I. Boldea, Variable speed generators, Taylor&Francis, 2006.
[146] D. A. Torrey, “Switched Reluctance Generators and Their Control”, IEEE Transactions on Industrial Electronics, Vol.49, No. 1, February 2002, pp. 3-14.
[147] F. Runcos, R. Carlson, A. M. Oliveira, P. Kuo-Peng N. Sadowski, “Performance Analysis of a Brushless Double Fed Cage Induction Generator”, Nordic Wind Power Conference (NWPC04), Chalmers University of Technology, Göteborg, Sweden, March 1-2, 2004.
[148] R. Hanitsch and G. Korouji, “Design and constructing of a permanent magnet wind energy generator with a new topology,” KOMEL Conf., Poland, May 2004, pp. 63-66.

Project funded by the European Commission under the 6th (EC) RTD Framework Programme (2002- 2006) within the framework of the specific research and technological development programme “Integrating and strengthening the European Research Area”

Project UpWind

Contract No.:
019945 (SES6)

“Integrated Wind Turbine Design”

CONCEPT REPORT on GENERATOR TOPOLOGIES, MECHANICAL & ELECTROMAGNETIC OPTIMIZATION

(Deliverable No.: D 1B2.b.1)

Part 2

AUTHOR:	Dr. Markus Mueller; Alasdair McDonald
AFFILIATION:	Institute for Energy Systems, School of Engineering & Electronics, Joint Research Institute for Energy, University of Edinburgh
ADDRESS:	University of Edinburgh EH9 3JL, UK
TEL.:	
EMAIL:	Markus.Mueller@ed.ac.uk, Alasdair.McDonald@ed.ac.uk
FURTHER AUTHORS:	
REVIEWER:	Project members
APPROVER:	

Document Information

DOCUMENT TYPE	Deliverable
DOCUMENT NAME:	Deliverable_1B2.b.1.pdf
REVISION:	1
REV.DATE:	4/12/2007
CLASSIFICATION:	R1: Restricted to project members
STATUS:	

Abstract:

The output of MILESTONE 1 (part of DELIVERABLE D 1B2.b.1) for WP 1B2.b.4 “Structural Design Tools” is described in this report, namely the description of analytical tools for estimating the inactive mass or structural mass of low speed electrical generators for direct drive wind energy converters. Permanent magnet axial and radial flux generators are presented in the report, but the techniques are valid for other generator topologies. It should be stressed that these tools have been developed to provide a first order estimate of the structural mass to enable rapid comparison of different generator designs and topologies. Finite element analysis has been used to verify the design tools, and results are presented in the report.

CONTENTS

1. Introduction

Direct-drive electrical machines have received a lot of attention in recent years because of their potential for reliability and low maintenance. The removal of the gearbox from the drivetrain reduces the number of moving parts that can fail.

In large multi-MW wind turbines the turbine blades turn slowly (in the order of 10 rpm). The power of a generator is the product of the machine's torque, T and its speed, ω ($P = T\omega$) and so the directly-driven electrical machine must produce a very large peak torque. There are practical limits to electrical and magnetic loading in electrical machines and thus there is an upper limit to the shear stress that can be developed. Designers typically use shear stress of the range $\overline{\sigma}$ = 25 – 50 kN/m^2 [1].

The torque of a rotating electrical machine is given in equation (1),

$$T = 2\pi\overline{\sigma}R^2 l\,, \qquad (1)$$

where R is the machine radius and l is the axial length of the generator.

If a generator designed to run at 1500 rpm is connected to rotor blades rotating at 15 rpm (with a 1:100 gearbox) then the generator only has to develop 1/100th of the torque of the equivalent direct-drive electrical machine. If the two generators are of the same type (i.e. they generate the same shear stress, $\overline{\sigma}$ in the airgap) but have different dimensions R and l (where the aspect ratio $l/2R$ = constant), then the direct-drive electrical machine will have a radius and length approximately 4½ ($=\sqrt[3]{100}$) times greater than those of the original geared electrical machine. Direct-drive leads to large, heavy electrical machines which can be expensive to build, transport and install.

All directly-driven generators used in wind turbines are synchronous machines. One step to reducing the weight of the generator is to move from electrically excitation (so called "wound rotor") to permanent magnet excitation [2].

A further step in reducing the mass (and cost) of building these generators is to choose between the different permanent magnet synchronous machine topologies such as axial-flux, radial-flux and transverse-flux types. These can be compared on a torque density or cost per torque basis [3, 4]. Most studies concentrate on reducing the amount of permanent magnet material (typically NdFeB) because this has a higher specific cost than iron laminations and copper. In a 1996 study the specific cost of NdFeB was 25 times that of iron laminations [2]. The cost of these rare-earth type magnets is coming down – a recent study used a specific cost of NdFeB which is only 10 times that of iron laminations [5]. As the relative price of permanent magnets falls designers need to consider the whole of the electrical machine.

As well as the electromagnetically active material these electrical machines must contain material which is electromagnetically inactive. This material fulfils a structural role, maintaining the airgap clearance between the rotor and stator against a number of forces. These include normal stress (resulting from the magnetic field between the rotor and stator), gravity, thermal stresses and other forces discussed in section 2. The normal stress is the largest force in a conventional permanent magnet (PM) synchronous machine and is typically an order of magnitude greater than the torque-producing shear stress. It has been shown by the authors that the majority of machine mass in directly-driven conventional PM machines comes from this category [6, 7].

In this report the authors will introduce and comment on simple analytical design tools that can be used to estimate the structural mass of these generators early on in their design process. An integrated electro-mechanical design method will be outlined, showing how these tools can be used with traditional machine modeling, leading to whole machine optimization. Application of these tools can be found in references [6,7,10 & 22], which show that optimization of the design of direct drive electrical generator must include both the active and inactive mass.

2. Forces in an electrical machine

From a structural viewpoint maintaining the clearance between the rotor and stator is critical. While most of the forces described in this section are common for all electrical machines, it is only in these large direct-drive machines that they become so structurally demanding. The magnitude of these forces is small compared to those that are carried by similar sized structures (such as building elements and small bridges) but the allowable deflection is much more demanding. A typical design will have an airgap clearance of 1/1000th of the airgap diameter [2], meaning that a 2 MW machine with an airgap radius, r_g = 2.5m will have a clearance, g = 5mm. The allowable deflection should only be 10-20% of this clearance otherwise the airgap flux density will increase significantly [7, 8, 9]. This in turn will lead to an increase in normal stress, possibly leading to even greater deflection [10].

Figure 1 shows a view of a radial-flux permanent magnet generator. The inner rotor is spoked with permanent magnets mounted on the outside. Only part of the stator is shown for simplicity. A rectangular window is shown – this is used to examine forces at work in figures 2, 3 and 5 below.

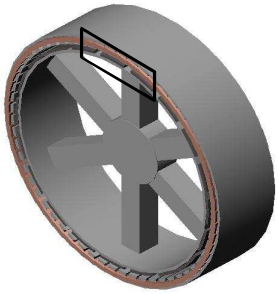

Figure 1: Radial-flux type permanent magnet generator

2.1 Shear stress

The shear stress is the useful force in an electrical machine, giving rise to torque as shown in equation (1). Designers have long tried to maximize this shear stress; hence the interest in transverse-flux permanent magnet machines which are characterized by high shear stresses [11]. If the distributions of flux density and electric loading are sinusoidal and are displaced by δ and the peak values are $\hat{B}$ and $\hat{K}$ then [12]

$$\overline{\sigma} = \frac{1}{2}\hat{B}\hat{K}\cos\delta\,. \qquad (2)$$

Because the shear stress is perpendicular to the airgap – as shown in figure 2 – it does not serve to close the airgap.

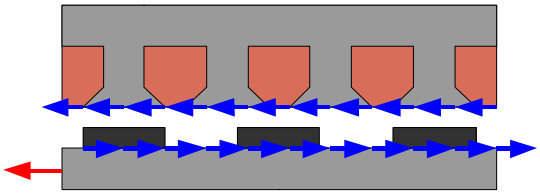

Figure 2: Section of radial-flux machine, with stator (top), rotor (bottom), direction of rotor movement (single arrow) and shear stress perpendicular to airgap (multiple arrows).

2.2 Normal stress

The normal stress, q is directed across the airgap, so that the outer iron surface (normally the stator) is attracted radially inwards and the inner iron surface (usually the rotor) is attracted radially outwards. This is shown for a section of the radial-flux machine in figure 3. When a large airgap flux density is used (e.g. $\hat{B}$ > 0.8 T) normal stress is about ten times than that of the shear stress.

The normal stress is a function of the square of the airgap flux density,

$$q = \frac{\hat{B}^2}{2\mu_o} \qquad (3)$$

where μ_o is the permeability of free space.

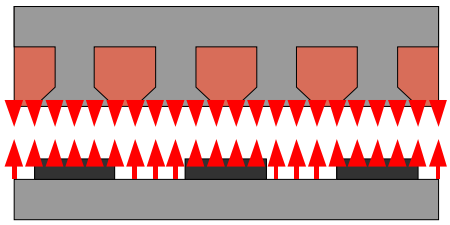

Figure 3: Section of radial-flux machine, with normal stress across airgap.

2.3 Gravity

The tilt angle, φ of the wind turbine rotor axis to the horizontal (typically about 5°) means that gravity acts on the generator in two ways: there is a major and a minor component as shown in figure 4(b).

The major component of gravity is of magnitude $g\cos\varphi$ and acts to deflect the rotor and stator back iron and structural members (such as spokes and support spiders). If the support is one sided then there will be a tipping moment – as in figure 4(c). Depending on their construction and the distribution of active material in the rotor and stator there may be different deflections, causing a narrowing or widening of the airgap.

The minor component of gravity is $g\sin\varphi$ and is axially directed leading to misalignment of the rotor and stator in the axial direction.

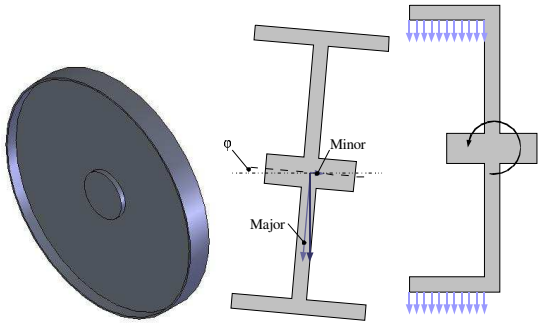

Figure 4: (a) Rotor, with cross sections: (b) Tilt angle, φ gives rise to a major and a minor component of gravity and deflection, (c) One sided or unsymmetrical support means that the major gravity component can lead to a tipping moment

2.4 Thermal expansion

Significant amounts of heat are generated in electrical machines leading to temperature rises in machine parts. These in turn give rise to expansion given by equation (4)

$$\Delta L = L_o \alpha \Delta T \,, \qquad (4)$$

where ΔL is the change in dimension, L_o is the original dimension, α is the thermal coefficient of expansion of the material and ΔT is the temperature rise. A difference in temperature rise in the rotor and the stator of a radial-flux machine will lead to a change in the airgap clearance.

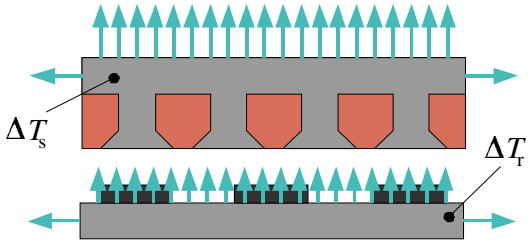

Figure 5: Section of radial-flux machine, with expansion due to temperature rises in the stator (ΔT_s) and rotor (ΔT_r).

2.5 Forces and moment from the rotor blades

These forces and moments include the weight of the rotor blades, horizontal and vertical wind shear, yaw error and inertial effects [13]. In a direct-drive wind turbine these forces may indeed be the biggest factor leading to airgap closure and can in turn lead to a change in the normal stress distribution. These forces will not be included in the design tool in section 3 as this work strays too far away from generator design and into the realm of wind turbine design. The authors acknowledge though that this is an area ripe for future investigation.

2.6 Centripetal force

Although the rotational speed of these direct-drive machines is low, the outer radius of the rotor is much larger than those found in typical multi-MW machines. The acceleration, a due to rotation is

$$a = \omega^2 r \qquad (5)$$

where ω is the rotational speed and r is the radius.

This leads to a force which is directed radially outwards (and into the airgap for an inner rotor). Figure 6 shows how this can deform an unsymmetrical rotor. In figure 6(a) the force on the rotor cylinder is shown by the arrows. This leads to a force and moment acting on the rotor disc or spokes – shown in figure 6(b) – giving rise to radial and axial deflections.

The rotor tip speed limit (≈75 m/s) means that as wind turbines grow larger the rotational speed, ω decreases. It can be proven that for a radial-flux generator with a constant aspect ratio ($l/2R$), the acceleration a falls as the machine gets bigger. The moment increases, the force stays fairly constant. This force will be neglected in section 3.

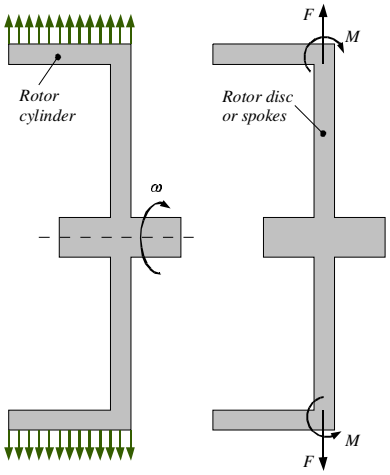

Figure 6: Section of radial-flux with centripetal force

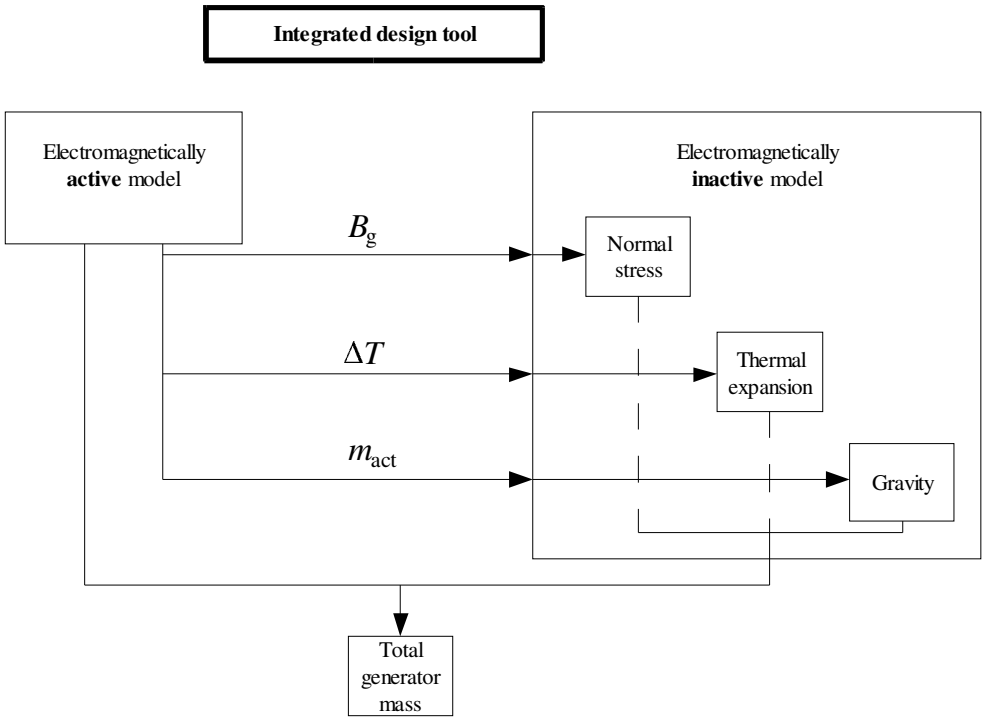

Figure 7: Integrated electromechanical design tool

3. An integrated electromechanical design tool

Figure 7 outlines an integrated approach to predicting machine mass (and by extension machine cost). Electrical machine designers are used to calculating the airgap flux density, temperature rise and active mass distribution. These can be fed into the models which predict airgap deflection based on the forces and inactive material. By limiting the airgap deflection the inactive mass can be found. Parts of this tool have been used in [6] and [7] to find the minimum mass for axial-flux and radial-flux topologies.

3.1 Machine structures

There are an infinite number of machine structures that could be possibly be used. Indeed a quick survey of direct-drive generator designs from companies [14, 15, 16, 17] and proposed designs [12, 18, 19, 20] illustrates the variation in machine structures. Any choice of structures will be a compromise between what is realistic and what can be modeled quickly and efficiently. Ultimately in the design process these structures will be analyzed with a finite element stress analysis package, but a simple analytical model can give us a reasonable indication of structure size early on in the design process. Simplified models are used here: figure 8 shows an axial-flux permanent magnet generator which is modeled as a set of circular discs, such as that shown in figure 9; figure 10 shows a simple symmetrical spoked rotor and stator which represents a radial-flux machine.

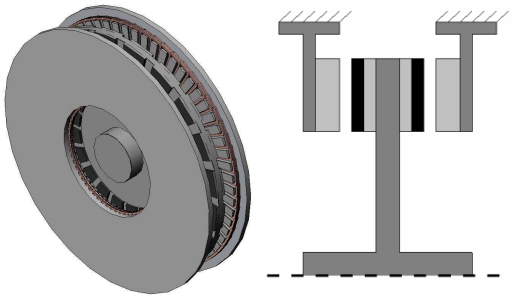

Figure 8: Axial-flux type permanent magnet generator (a) whole machine and (b) half cross section views

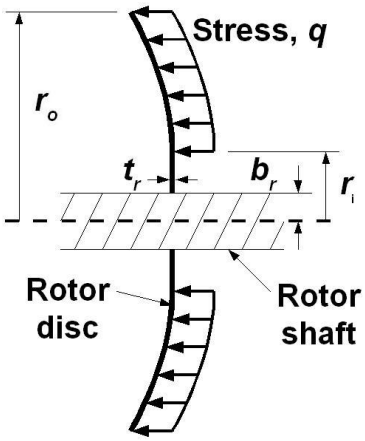

Figure 9: Circular plate model of axial-flux machine rotor

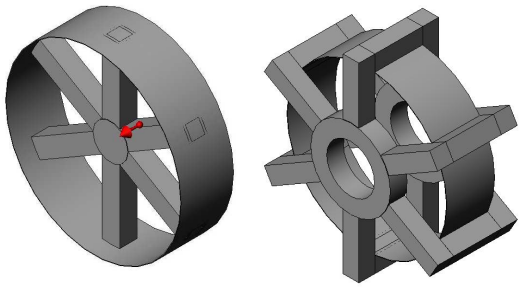

Figure 10: Simplified radial-flux structures (a) rotor and (b) stator.

3.2 Normal stress modeling

3.2.1 Axial-flux machine

For the axial-flux machine the airgap deflection, u can be found by using circular plate theory where the normal stress is applied between the inner and outer radii, r_i and r_o. The deflection of the rotor (figure 9) is found by

$$u = M_{rb}\frac{r_o^2}{D}C_2 + Q_b\frac{r_o^3}{D}C_3 - q\frac{r_o^4}{D}L_{11} \qquad (6)$$

where D is the plate constant, M_{rb} is the unit radial bending moment, Q_b is the per unit shear force at shaft and C_2, C_3 and L_{11} are circular plate and loading terms, details of which can be found in [6].

3.2.2 Radial-flux machine

A representation of a radial-flux rotor is shown in figure 11(a). Applying a normal stress, q to the outside surface of the rotor (described by a model taken from Pippard [21]) leads to the deflection, u_A at the midpoint, A (between two rotor arms) given in equation (7).

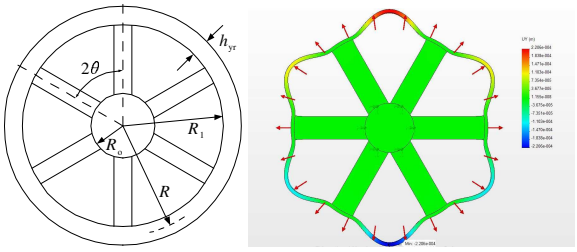

Figure 11: Rotor with spoked arms (a) analytical model and (b) finite element comparison.

$$u_A = \frac{qR^2}{Et}\left(1 + \frac{R^3\left[\frac{k_1(\sin\theta - \theta\cos\theta)}{4\sin^2\theta} - \frac{k_2}{2\sin\theta} + \frac{k_2^2}{2\theta}\right]}{I\left[\left(\frac{\theta}{\sin^2\theta} + \frac{1}{\tan\theta}\right)\left(\frac{R}{4A} + \frac{R^3}{4I}\right) - \frac{R^3}{2I\theta}\left(\frac{1}{m+1}\right) + \frac{R_1 - R_o}{a}\right]}\right) \qquad (7)$$

A detailed derivation will appear in [22]. The deflection for a 3 MW radial-flux machine with R = 3m, l = 0.8m and q = 280kN/m^2 is found (using equation (7)) to be 2.15 mm. Figure 11(b) shows a deflection of 2.21 mm as found using a mechanical finite element solver.

3.3 Gravity modeling

3.3.1 Major component

The major component of gravity acts to deflect both the rotor back iron (u_1) and the rotor arms (u_2) in the radial-flux machine. The largest deflection is at the midpoint between two arms (at the point below W in figure 12(a)). The deflection is found using Castigliano's second theorem (equation (8)) and by finding M_A, H_A, V_A (which can be found in Roark [23]) for a circular arch.

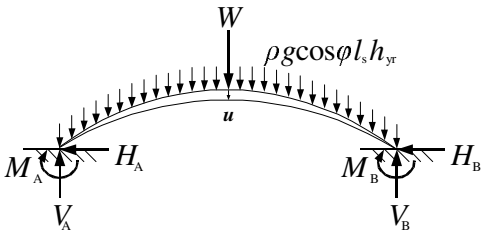

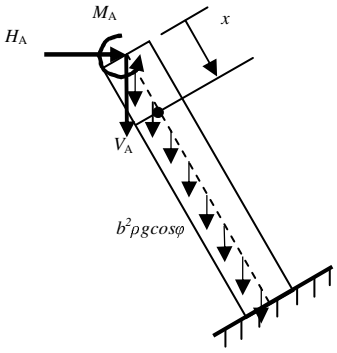

Figure 12: Deflection u of radial-flux rotor (a) rotor back iron and (b) support arm.

$$u_1 = \frac{\partial U}{\partial W} = \frac{2}{EI}\int_0^{\pi/6} M(\alpha)\frac{\partial M(\alpha)}{\partial W} R d\alpha \qquad (8)$$

$$u_2 = \frac{1}{EI}\left[\frac{V_A}{12}x^3 + b^2\rho g\cos\phi\frac{x^4}{32} - \frac{\sqrt{3}H_A}{12}x^3 + \frac{M_A}{4}x^2\right]_o^l \qquad (9)$$

A full deriviation will appear in [22]. The deflection of the rotor in 3.2.2 due to normal stress and gravity (as predicted by equations (7), (8) and (9)) is 2.59 mm. The deflection found using a finite element solver is 2.98 mm (figure 13).

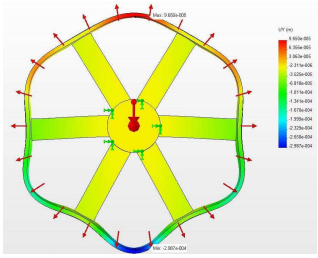

Figure 13: Deflection of 3 MW rotor found using finite element solver

3.4 Thermal modeling

In most permanent magnet generators an inner rotor is used (with the notable exception of the Vensys turbines [24]). Generally, it is the stator with its armature winding that heats up the most (because of the I^2R losses), although it is the outer stator that has the best cooling. Any temperature difference between the stator and the rotor is likely to lead to different thermal expansion. This temperature difference can be modeled using lumped parameter thermal networks, such as [2,25].

The machine described in 3.2.2 is run from cold (T = 20°C) and the temperature rises in the stator and the rotor are ΔT_s = 79.3°C and ΔT_r = 75°C. The rotor and stator back iron can be thought of as two concentric cylinders. Figure 14 shows the mean radius of these two cylinders: stator radius, R_s (= 3.15m) and the rotor radius, R_r (= 2.96m). Equation (4) can be adapted here for the change in radius,

$$\Delta R = R_o \alpha \Delta T \qquad (11)$$

where $\alpha = 13.2\times10^{-6}$/°C for steel. In this case, ΔR_r = 2.93 mm and ΔR_s = 3.30 mm so that the airgap opens by 0.37 mm.

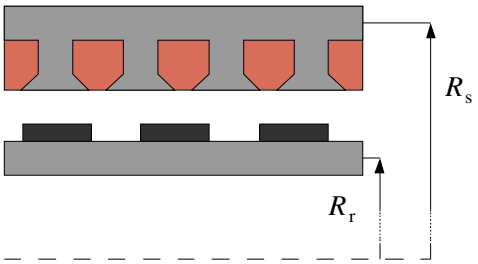

Figure 14: Mean radii of rotor and stator cylinders.

4. Structural analysis due to normal stress: full model descriptions.

4.1 Axial Flux Permanent Magnet Machines.

The electromagnetic and structural designs are linked by the magnetic attraction force acting between the stator and rotor, which is commonly referred to as the Maxwell Stress. Classical analysis of magnetic equivalent circuits can be used to determine the airgap flux density and hence the Maxwell Stress is given by:

$$q = \frac{B_g^2}{2\mu_o} \tag{12}$$

where B_g is the airgap flux density and μ_o is the permeability of free space.

The techniques for calculating B_g are well established and hence will not be repeated in this paper.

4.1.1 Rotor

There are two rotor discs in the single stage axial-flux permanent magnet machine shown in Figure 15. Mounted on a shaft with a radius, b_r, these discs have a number of magnets fixed between an inner radius, r_o, and outer radius, a_r (dimensions as in Figure 16). The parts covered by magnets experience a stress, q, given by eqn. (12). To simplify the analysis, it will be assumed that the stress, q, acts on the area bounded by r_o and a_r (i.e. spread across the pole pitch). The Maxwell Stress is thus modified by multiplying it by the magnet width/pitch ratio, so that the overall force acting on the rotor disc remains constant. Circular plate theory can be used to model the rotor disc as a flat circular plate of constant thickness, t_r, with its outer edge free and the inner edge fixed [23].

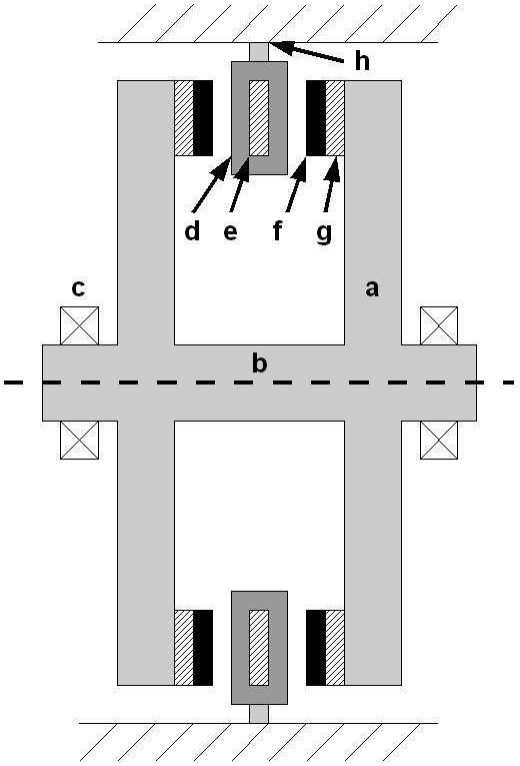

Fig. 15 Double rotor, single stator axial-flux machine. (a) rotor disc, (b) rotor shaft, (c) bearing, (d) copper winding, (e) stator iron core, (f) permanent magnet, (g) rotor iron core, (h) stator support structure.

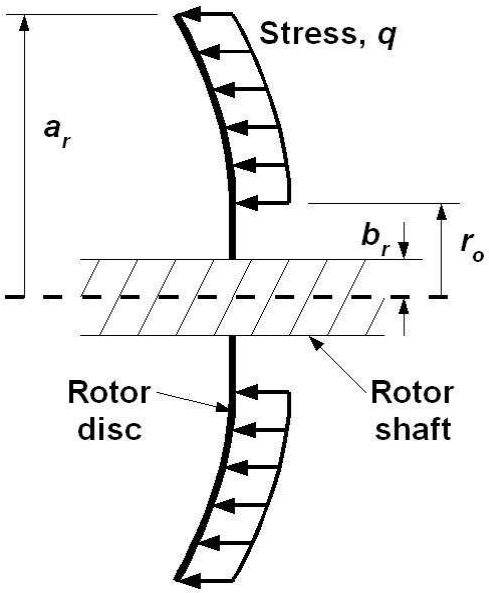

Fig. 16 Circular plate model of axial-flux rotor disc

The maximum deflection is at the outer radius, a_r. This deflection into the airgap, y_a, can be found from

$$y_a = M_{rb}\frac{a_r^2}{D}C_2 + Q_b\frac{a_r^3}{D}C_3 - q\frac{a_r^4}{D}L_{11}, \tag{13}$$

where the unit radial bending moment at the shaft, M_{rb}, is

$$M_{rb} = \frac{-qa_r^2}{C_8}\left[\frac{C_9}{2a_r b_r}\left(a_r^2 - r_o^2\right) - L_{17}\right], \tag{14}$$

and the unit shear force at the shaft, Q_b, is

$$Q_b = \frac{q}{2b_r}\left(a_r^2 - r_o^2\right). \tag{15}$$

Constants C_2, C_3, C_8, C_9, L_{11} and L_{17} are given in the appendix. The plate constant, D, is a function of plate thickness, t,

$$D = \frac{Et^3}{12\left(1-\nu^2\right)}. \tag{16}$$

By specifying the maximum allowable deflection at a, y_a, the rotor thickness, t_r, can be found,

$$t_r = \sqrt[3]{\frac{12a_r^2\left(1-\nu^2\right)}{Ey_a}\left[M_{rb}C_2 + Q_b a_r C_3 - qa_r^2 L_{11}\right]}. \tag{17}$$

Thus the mass of the rotor discs is expressed in eqn. (18).

$$m_r = n_{disc}\rho\pi\left(a_r^2 - b_r^2\right)\sqrt[3]{\frac{12a_r^2\left(1-\nu^2\right)}{Ey_a}\left[M_{rb}C_2 + Q_b a_r C_3 - qa_r^2 L_{11}\right]}, \tag{18}$$

where n_{disc} is the number of rotor discs.

4.1.2 Stator

The stator disc is modelled using circular plate theory in section 4.1.2.1. Its outer radius is attached to a multiple beam structure (analysed in section 4.1.2.2) or a cylindrical shell structure (analysed in section 4.1.2.3). These potential stator structures are based upon structures that have been observed in the published literature. To simplify the model the stator is modelled as one piece of iron connected directly to a structure (beams or casing) which is fixed at both ends to baseplates. Equations are developed to predict the thickness of the stator and supporting structures so that the deflection into the airgap is kept within defined limits when the largest Maxwell Stress, q, is applied, which occurs during assembly when the stator is moved into position opposite one rotor disc.

4.1.2.1 Stator disc

Flat circular plates with outer edge fixed and inner edge free are modelled in [23] as shown in the general case in Figure 17. A stress q (12) acts on the stator between r_o (which is equal to b_s in the case of the stator disc) and a_s which is equal to the rotor outer radius a_r plus a running clearance. This simplification (where q is applied over a greater area than that of the rotor as in section 4.1.1) leads to a conservative design.

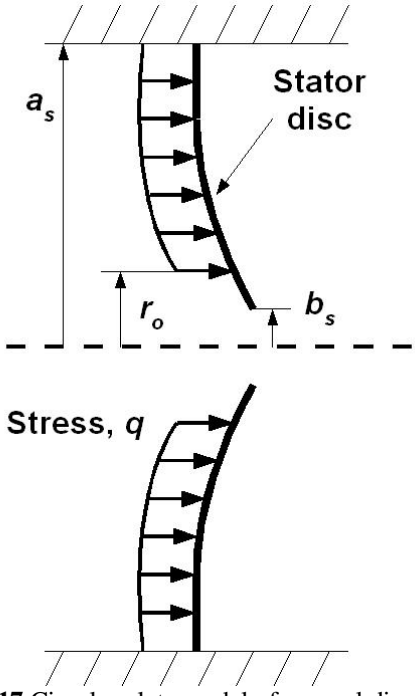

Fig. 17 Circular plate model of general disc case

The maximum deflection is at the inner radius and is given by

$$y_{b1} = \frac{-qa_s^4}{D}\left(\frac{C_1 L_{14}}{C_4} - L_{11}\right), \tag{19}$$

where C_1, C_4 and L_{14} are given in the appendix. By combining eqn. (16) with eqn. (19) and rearranging, the minimum stator thickness from a mechanical perspective can be determined and is given in eqn. (20).

$$t_s = \sqrt[3]{\frac{12qa_s^4\left(1-\nu^2\right)}{Ey_{b1}}\left(\frac{C_1 L_{14}}{C_4} - L_{11}\right)}. \tag{20}$$

It should be noted that magnetic circuit requirements may require a greater stator thickness. The mass of the stator disc due to structural needs is given in eqn. (21).

$$m_s = \rho\pi\left(a_s^2 - b_s^2\right)\sqrt[3]{\frac{12qa_s^4\left(1-\nu^2\right)}{Ey_{b1}}\left(\frac{C_1 L_{14}}{C_4} - L_{11}\right)}. \tag{21}$$

4.1.2.2 Beam structure

The model of the stator disc assumes a solid structure that can react the moment per circumferential length given in eqn. (11) and hold the stator core in position.

$$M_{ra} = -qa_s^2\left(L_{17} - \frac{C_7}{C_4}L_{14}\right). \tag{22}$$

Several configurations have been used [26], [27]. In this analysis, the iron core is made up of two toroidal halves fixed to a toroidal plate sandwiched between them. This plate has several tabs which are held in position by beams, the ends of which are fixed to two baseplates (Figure 18 (a)). Assuming that the total circumferential moment is equally shared by all the n_b beams, then the moment on each beam is expressed in eqn. (23).

$$M_o = \frac{2\pi a_s M_{ra}}{n_b}. \tag{23}$$

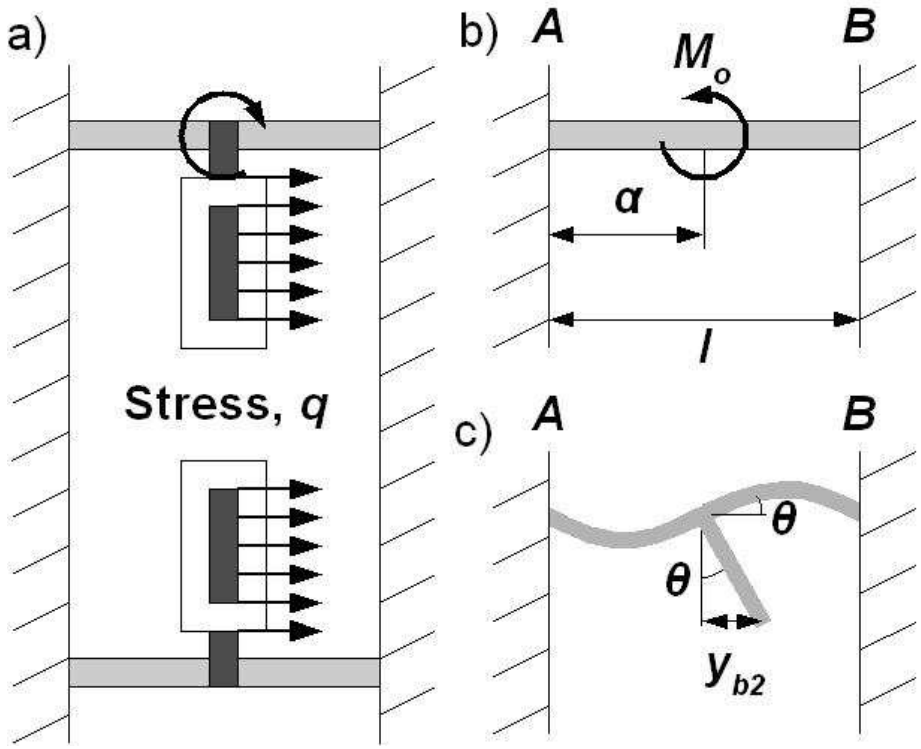

Fig. 18 a) Stator and beam model b) Beam reacting moment M_o at mid point c) Deflection, y_{b2}, due to beam bending

Modelling the beams (Figure 18 (b)) as elastic straight beams with both ends fixed, this moment is applied at $\alpha=l/2$ m along the beam and leads to an angular displacement at distance x along the beam [14] given in eqn. (24)

$$\theta = \frac{M_A x}{EI} + \frac{R_A x^2}{2EI}, \tag{24}$$

where

$$M_A = \frac{-M_o}{l^2}\left(l^2 - 4\alpha l + 3\alpha^2\right), \tag{25}$$

and

$$R_A = \frac{-6M_o\alpha}{l^3}(l-\alpha). \tag{26}$$

If the beams have a circular cross section then the second moment of area $I = \pi R^4/4$. By combining (24-26), the beam radius (to give a specified angular displacement θ at $x=\alpha$) is given in eqn. (27).

$$R = \left(\frac{-4M_o\alpha}{\pi l^2 E\theta}\left[l^2 - 4\alpha l + 3\alpha^2 + \frac{6(l-\alpha)\alpha}{2l}\right]\right)^{1/4}. \tag{27}$$

Figure 18(c) shows how this angular displacement produces a deflection into the airgap. For a given y_{b2} the angular displacement is expressed in eqn. (28).

$$\theta = \tan^{-1}\frac{y_{b2}}{b_s - a_s}. \tag{28}$$

Thus the mass of the structural support beams follows,

$$m_b = n_b \rho l \pi \sqrt{\frac{-4M_o\alpha}{\pi l^2 E\theta}\left[l^2 - 4\alpha l + 3\alpha^2 + \frac{6(l-\alpha)\alpha}{2l}\right]}. \tag{29}$$

4.1.2.3 Cylindrical casing

Instead of attaching the stator to beams, the stator could be hung off the machine casing. This casing can be modelled as a short thin-walled cylindrical shell with an intermediate applied moment shown in Figure 19 [23]. As in the beam case, the angular displacement must be limited to keep the deflection into the airgap less than y_{b2} given by eqn. (28).

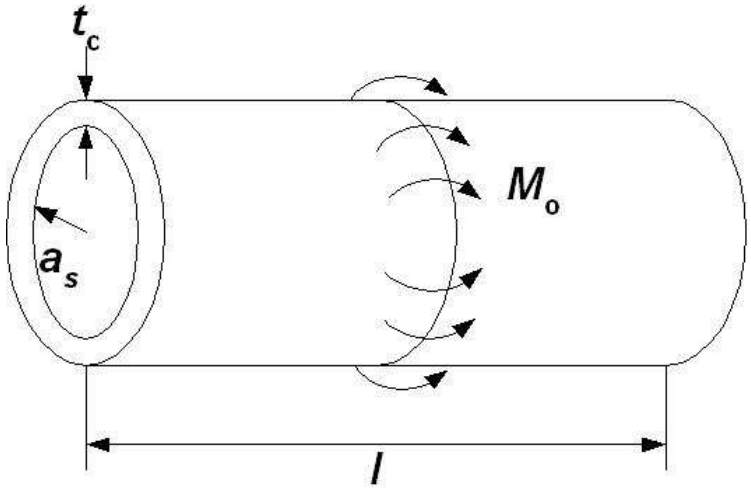

Fig. 19 Cylindrical shell model of machine casing

For cylindrical shells, the angular displacement (meridional slope) halfway along the cylinder is

$$\psi = \psi_A F_1 - y_A \lambda F_4, \tag{30}$$

where

$$\psi_A = \frac{-M_o}{D\lambda} \frac{K_2 K_{a1} + K_3 K_{a4}}{K_{11}}, \tag{31}$$

$$y_A = \frac{M_o}{2D\lambda} \frac{2K_3 K_{a1} + K_4 K_{a4}}{K_{11}}, \tag{32}$$

$$\lambda = \left(\frac{3(1-\nu^2)}{a_s^2 t_c^2} \right)^{1/4}. \tag{33}$$

Cylindrical shell constants K_2, K_3, K_4, K_{11}, K_{a1}, K_{a4} and functions F_1 and F_4 are given in the appendix. The thickness of the cylinder t_c can be altered so that $\psi=\theta$. Thus the mass of the machine casing is

$$m_c = \rho l \pi \left(t_c^2 + 2 a_s t_c \right). \tag{34}$$

4.1.3 Finite Element Models

Structural finite element analysis is used in this section to model the maximum deflection due to the stress q. These deflections will be compared with those predicted by the analytical equations in section 2. Table 1 gives the relevant dimensions for a number of different iron-cored machines based on the design by Söderlund *et al.* in [28], each of which have been modelled using finite element analysis and the analytical expressions developed in section 2. Finite element results have been previously reported for a double rotor, coreless stator machine built by Wang *et al.* [29]. Commercial finite element software was used to develop the structural models in this paper [30].

Rotor				***Stator***			***Support structures***		
a_r, m	b_r, m	r_o, m	t_r, mm	a_s, m	b_s, m	t_s, mm	l, m	R, mm	t_c, mm
1.20	0.240	1.09	37.4	1.26	1.09	4.74	0.173	5.34	3.13
2.39	0.477	2.17	74.3	2.50	2.17	9.44	0.288	10.2	6.43
3.26	0.651	2.96	101	3.42	2.96	12.9	0.366	13.6	9.04
5.14	1.03	4.67	160	5.40	4.67	20.3	0.520	20.9	15.3
7.66	1.53	6.96	238	8.04	6.96	30.3	0.717	30.6	24.8

Table 1 **Parameters of iron-cored machines**

4.1.3.1 Rotor disc

Coreless machine

Full details and results of a finite element model developed by Wang *et al.* are given in [29]. Briefly, they constructed a one sixteenth model with 4 node shell elements with symmetry conditions. Results from the model were used to calculate the maximum deflection of a rotor disc with a_r=360mm, b_r=165mm, r_o=250mm, t_r=17mm and q=69.8kPa machined from steel with mechanical properties E=200GPa and v=0.3. This result is used later by the authors to verify the analytical method.

Iron-cored machine

A similar one sixteenth shell element model was created in a finite element solver by the authors for a number of sample machines based on the Söderlund machine design in [28]. The relevant dimensions used in the finite element and analytical models are presented in Table 1. In the finite element model the inner edge was constrained (no translation or rotation) and a stress q=28kPa (equivalent to B_g=0.33T with a magnet width/pitch ratio of 0.653) was applied to find the deflection at the outer rotor disc radius (Figure 20) for all machine cases in Table 1. The Söderlund machine uses rotor discs made of an aluminium alloy with mechanical properties E=69GPa and v=0.33 for the structural part of the rotor.

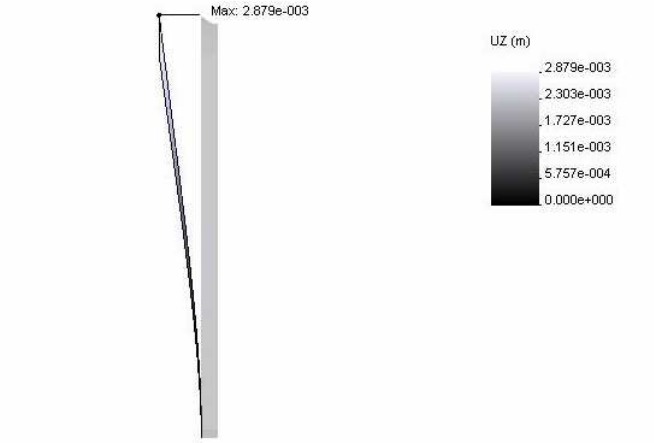

Fig. 20 One sixteenth finite element model of rotor disc showing deflection when a_r = 1.2m

4.1.3.2 Stator

Stator disc

Again, a one sixteenth model with 4 node shell elements and symmetry conditions was created (Figure 21), this time constrained at its outer edge. The same stress q was applied to find the deflection at the inner stator disc radius for the stator parameters in Table 1.

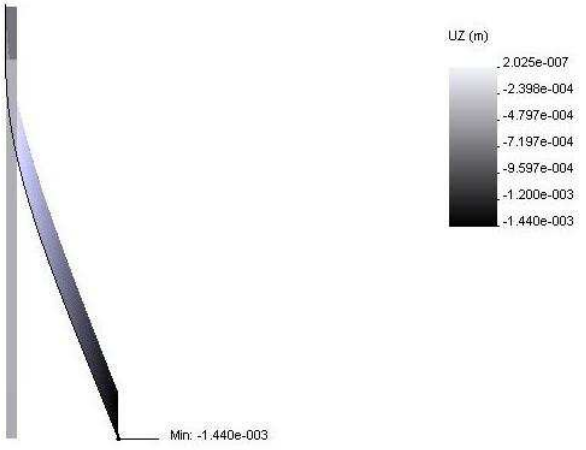

Fig. 21 One sixteenth finite element model of stator disc showing deflection when a_s=1.26m

Beam structure

A one thirtieth (n_b=30) model – with 4 node solid mesh and symmetry conditions – of a section of the stator disc with a beam of radius R (Table 1) joined midway along at radius a_s was created (Figure 22(a)). The ends of the beam were constrained and the deflection at the inner stator disc radius was found when q was applied to the stator disc.

Fig. 22(a) One thirtieth finite element model of stator disc and beam support showing deflection when R=5.34mm

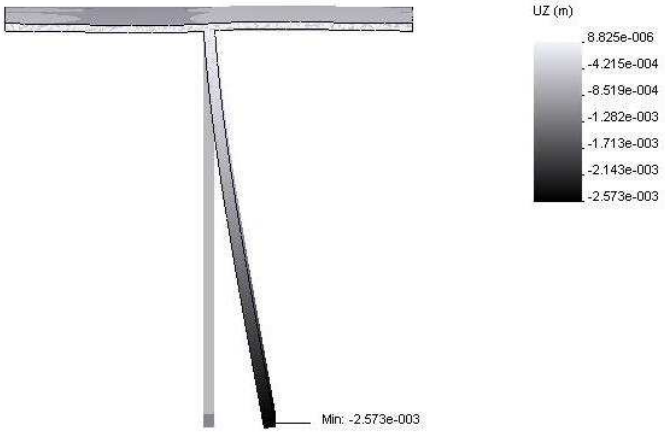

Fig. 22(b)One thirtieth finite element model of stator disc and cylindrical casing showing deflection when t_c=3.13mm

Cylindrical casing

In this case the one thirtieth model with 4 node solid mesh consisted of a section of the stator disc and the cylindrical casing with thickness t_c from Table 1. The ends of the cylinder were constrained and the deflection was found (Figure 22(b)).

4.1.4 Results

4.1.4.1 Rotor disc

By rearranging eqn. (6) the maximum deflection y_a can be found in terms of rotor thickness, t_r. For the coreless machine y_a=0.1475mm if the plate thickness t_r=17mm, which compares favourably to the

deflection of 0.145mm reported by Wang *et al.* The analytic and finite element deflections for the iron-cored machine designs in Table 1 are given in Table 2, which show excellent agreement.

Case	*Rotor disc deflection,* mm		*Stator disc (only) deflection,* mm		*Stator disc (with beams) deflection,* mm		*Stator disc (with cylinder) deflection,* mm	
	FE	Analytic	FE	Analytic	FE	Analytic	FE	Analytic
1	2.85	2.85	1.44	1.43 (-1%)	5.00	2.85 (-43%)	2.57	2.85 (11%)
2	5.68	5.66	2.87	2.83 (-1%)	10.1	5.66 (-44%)	4.66	5.66 (22%)
3	7.75	7.73	3.93	3.87 (-2%)	14.1	7.73 (-45%)	6.04	7.73 (28%)
4	12.2	12.2	6.17	6.10 (-1%)	22.3	12.2 (-45%)	8.66	12.2 (41%)
5	18.2	18.2	9.21	9.10 (-1%)	33.6	18.2 (-46%)	12.0	18.2 (52%)

Table 2 **Analytical and finite element deflection and percentage difference**

4.1.4.2 Stator

Rearranging eqn. (18) gives the maximum deflection at the inner stator core radius with stator thickness, t_s. Combining eqn. (27) and eqn. (28) gives the radius, R of the support beams needed to limit the maximum combined deflection, y_b. Using equations (28) and (30-33) the maximum combined defection, y_b can be found when the casing has a thickness of t_c. The analytic and finite element deflections of the stator for the iron-cored machines are given in Table 2.

4.1.3 Discussion

4.1.3.1 Cylinder plate theory for rotor and stator discs

Both the analytical models for the rotor and stator discs give maximum deflections that are within 2% of those produced in the finite element analysis reported in this paper and elsewhere. These disc models can be applied to all axial-flux topologies, not just the double rotor, single stator configuration.

4.1.3.2 Beam vs. cylindrical shell model

The stator plate model assumes that the outer radius is constrained. The applied stress q produces a moment per circumferential length. In the beam model this constraint is badly approximated by the beams, giving a much larger deflection in the finite element analysis than predicted by the analytical model. A cylindrical shell model with an intermediate moment per circumferential length (at the point that the stator is fixed to the casing) predicts the deflection more closely than the beam equations, although the model over-predicts the required cylinder thickness, particularly at large radii.

4.2 Radial Flux Machines – Polynomial Model

4.2.1 Theory behind modelling

Polynomial modelling has been used before to model a number of parameters in a range of electrical machines in the past [11,31]. One could generate a look-up table from preanalysed models, but a polynomial approach needs fewer input data points (particularly as the number of variables increases). This method also has the advantage that the analytical function can be optimised.

4.2.2 Identify parameters to describe the essential features of the machine

In the radial-flux machine model used, there is an inner rotor (shown in Fig. 23 and an outer stator (Fig. 24). The rotor is fully described by four parameters: length l_s, outer radius R_{rot}, rotor disc thickness t_r

and rotor back thickness h_{yr}. All of the other dimensions are fixed ratios of these parameters. The stator is similarly described by the following parameters: length l, the airgap radius R, support arm thickness t_{sa} and stator back thickness h_{ys}. Again, other stator dimensions are fixed ratios of these base parameters (e.g. the support arm height $h_{sa} = 2t_{sa}$). A direct stress q is applied to the outside of the cylinder for the rotor and to the inside of the cylinder for the stator.

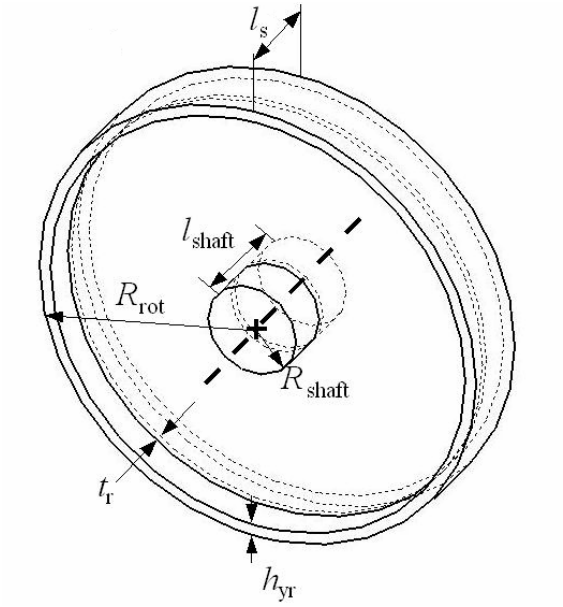

Figure 23: Rotor model

4.2.3 Identify performance quantity

In this case the machine designer is interested in the deflection u into the airgap given the dimensions of the machine structure. The designer usually stipulates beforehand the permissible deflection as a percentage of the airgap clearance c.

4.2.4 Establish range of interest for each parameter

This research is interested in multi-MW direct drive machines so the following ranges of parameters were chosen:

- R = 0.5-5.5m
- l_s = 0.5-1.5m
- q = 40-700 kPa (corresponds to B_g = 0.3-1.3T)
- h_{yr} = 0.002-0.03m
- h_{ys} = 0.002-0.28 m
- t_r = 0.01-0.14 m
- t_{sa} = 0.03-0.7 m

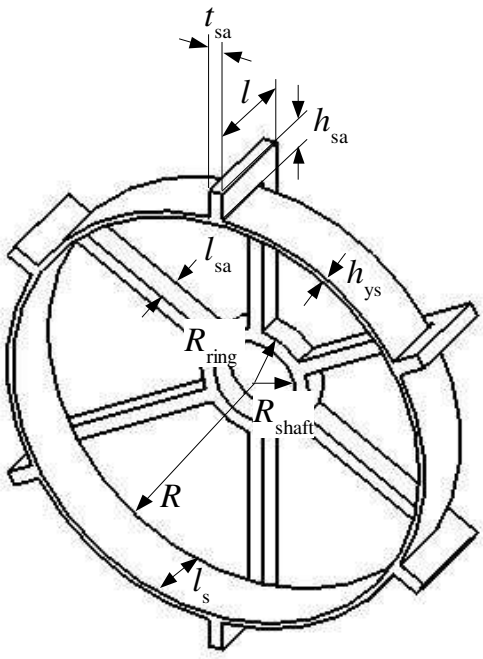

Figure 14: Stator model

4.2.5 Create generalised model

Generalised models of the rotor and stator were created in a 3D CAD program (SolidWorks) and then transferred to a finite element package (COSMOSWorks). Here the appropriate constraints and forces (normal stress q and gravity g) were applied and material constants were assigned. In this case the axis of the machine is set at 5° to the horizontal (this models the tilt which is found in most wind turbines).

4.2.6 Run model for range of parameters and extract performance quantity

486 models (for both the rotor and stator) were analysed using the FE package. The results were extracted and saved.

4.2.7 Derive analytical function for performance quantity

In this case a polynomial is used to model the results. The deflection u is a multiple sum of products of a set of coefficients and the 5 design parameters along with a dummy parameter $x_0 = 1$. In the rotor case then $x_1 = q$, $x_2 = R$, $x_3 = l_s$, $x_4 = t_r$ and $x_5 = h_{yr}$. The quadratic function is shown in Equation (35).

$$u_p = \sum_{i=0}^{5} \sum_{j=i}^{5} a_{i,j} x_i x_j \qquad (35)$$

Similar expressions can be found for cubic and other higher order polynomial functions.

At this stage the coefficients (denoted in Equation (35) by $a_{i,j}$) are unknown. The method of least squares is used to find the polynomial which gives the best fit to the results.

First the square of the difference between the input data point u and the value given by the polynomial u_p is calculated. We sum all these 'errors' in Equation (36), differentiate the sum by the polynomial coefficients and in turn set these differentials to zero (Equation (37)). The polynomial coefficients $a_{i,j}$ can then be easily calculated using matrix algebra as in [31].

$$S = \sum_{n} (u_p - u)^2 \qquad (36)$$

$$\frac{\partial S}{\partial a_{i,j}} = 0 \qquad (37)$$

4.2.8 Choice of polynomial

With 5 input variables, the number of coefficients for each polynomial is given in Table 3:

Polynomial order	Number of coefficients
Linear	6
Quadratic	21
Cubic	56
4th order	126
5th order	252
6th order	462

Table 3: Number of coefficients for 5 variable polynomials

To ensure a good fit it is necessary to use about twice as many input data points as there are coefficients [31]. So for example, to produce a 5 variable quadratic 2 x 21 = 42 input data points should be used. With 486 input data points it is possible to model up to a 5th order 5 variable polynomial.

4.2.9 Use polynomial coefficients to evaluate new machine designs

With the order and coefficients of the polynomial established, the polynomial function coefficients can be used in a spreadsheet to quickly analyse the performance of the machine structure.

As an example this method has been applied to a design similar to that in [15]: a 1.6MW machine with R =2.1m, l_s = 1.2m, q = 174kPa rated at f = 9.25Hz and n = 18.5rpm.

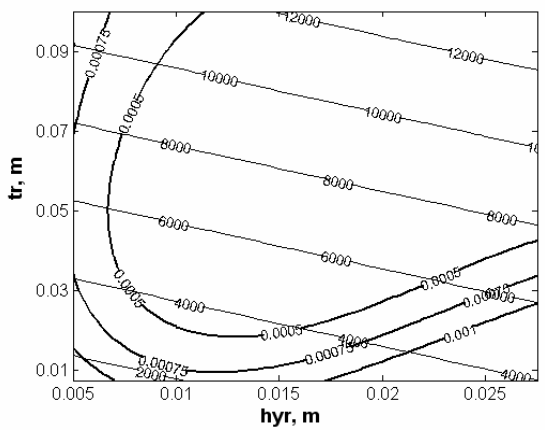

Figure 25: Rotor cubic t_{sa} plotted against h_{ys} for R = 0.5, 1.5, 2.5, 3.5, 4.5 and 5.5m.

The thick lines in Fig. 25 model the deflection of the rotor into the airgap (produced by a cubic function). Thinner contours show the inactive mass of the structure given the values of h_{yr} and t_r. For a 0.003m airgap clearance a deflection of 0.00075m gives a minimum mass of 2.3 tonnes.

With the appropriate R, l_s and q values a number of simulations can be run with a range of h_{yr} and t_r values. Fig. 26 is a contour map of the deflection produced when 100 such models are simulated. The inactive mass here is about 3 tonnes.

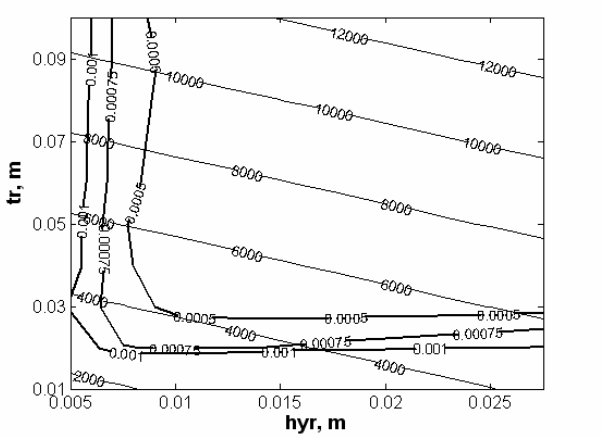

Figure 26: Actual deflection found by interpolation between 100 points

4.2.10 Discussion

For electromagnetic quantities the machine designer uses quick and simple analytical tools during the design study stage and advances to more accurate – but more involved – numerical and finite element techniques later on in the design study. The mechanical design tools presented here are also for the early stages of the design process; the results can be refined with more involved finite element analysis when the design space becomes narrower.

Although not perfect – see the differences between Figs. 3 and 4 – the polynomial modelling technique used in the radial-flux case gives useful results for estimating the inactive mass of the rotor and stator. The method presented in [5] for the axial-flux case is more accurate but the majority of large direct-drive machines are radial-flux and so the techniques described here are more valuable.

A large amount of work is required in running the finite element models before the polynomial technique is used. However once the results are produced the analysis is very quick and the polynomials can be used to explore an extremely large design space.

The analysis of airgap deflection for both the axial- and radial-flux topologies can be improved by considering the effect of this deflection on the airgap flux density and therefore the normal stress. An iterative calculation shows that the final deflection is greater than that predicted by the basic design equations. An adjustment factor (to the disc thickness, t_r or the support arm thickness, t_{sa}) can be quickly found to counter this effect. In the cases examined here, this factor is in the region of 10% [10]

5. Summary

The report describes the analytical tools developed for estimating the structural mass of electrical generators. These tools have been developed to be used within a design office environment, where a first order estimate is required rapidly. Any further design refinement can be achieved using more sophisticated modelling tools such as finite element analysis. The design tools have been verified using results in the public domain (where available) and also using finite element analysis. Overall the verification was very good, better for axial flux machines than radial flux. The latter made use of a polynomial model. A more analytic model is still being developed, and once fully verified will be published in reference [22].

References

[1] H. Polinder, S.W.H. de Haan, M.R. Dubois, J.G.H. Slootweg, "Basic operation principles and electrical conversion systems of wind turbines," *EPE Journal*, vol. 15, no. 4, 2005.

[2] A. Grauers, "Design of direct-driven permanent-magnet generators for wind turbines," Ph.D dissertation, Department of Electric Power Engineering, Chalmers University of Technology, Göteborg, Sweden, 1996.

[3] Dubois, M.R., Polinder, H., and Ferreira, J.A., "Comparison of generator topologies for direct-drive wind turbines," in *Proc. of the Nordic Countries Power & Ind. Electronics Conf. (NORPIE)*, Aalborg, Denmark, 2000, pp. 22-26.

[4] Yicheng Chen, P. Pillay, and A. Khan, "PM wind generator topologies," *IEEE Trans. on Ind. Appl.*, vol. 41, no. 6, pp. 1619- 1626, 2005.

[5] H. Polinder, B.C. Mecrow, A.G. Jack, P.G. Dickinson, and M.A. Mueller, "Conventional and TFPM linear generators for direct-drive wave energy conversion," *IEEE Trans. on Energy Conversion*, vol. 20, no. 2, pp. 260-267, 2005.

[6] M.A. Mueller, A.S. McDonald, and D.E. Macpherson, "Structural analysis of low-speed axial-flux permanent-magnet machines," *IEE Proc. Electr. Power Appl.*, vol. 152, no. 6, pp. 1417-1426, 2005.

[7] A.S. McDonald, M.A. Mueller and H. Polinder, "Comparison of generator topologies for direct-drive wind turbines including structural mass," in *Proceedings of the International Conference on Electrical Machines (ICEM06)*, Chania, Crete, 2-5 September 2006.

[8] T. Hartkopf, M. Hofmann and S. Jöckel, "Direct-drive generators for megawatt wind turbines," in *Proc. European Wind Energy Conf.*, Dublin, Ireland, 1997, pp. 668-671.

[9] H. Polinder, D.-J. Bang, R.P.J.O.M. van Rooij, A.S. McDonald and M.A. Mueller, "10 MW wind turbine direct-drive generator with pitch or active speed stall," *IEEE Int. Electric Machines and Drives Conf.*, Antalya, Turkey, May 3-5 2007.

[10] A.S. McDonald and M.A. Mueller, "Mechanical design tools for low speed high torque electrical machines", in *Proc. 3rd IET International Conference on Power Electronics, Machines and Drives (PEMD 2006)*, Dublin, Ireland, 2-6 April 2006, pp. 666-670.

[11] M.R. Dubois, "Optimized permanent magnet generator topologies for direct-drive wind turbines," Ph.D dissertation, Department of Electrical Engineering, Delft University of Technology, Delft, Netherlands, 2004.

[12] E. Spooner, P. Gordon, J.R. Bumby and C.D. French, "Lightweight ironless-stator PM generators for direct-drive wind turbines," *IEE Proc. Electr. Power Appl.*, vol. 152, no.1, pp. 17-26, 2005.

[13] T. Burton, D. Sharpe, N. Jenkins and E. Bossanyi, "Wind Energy Handbook," John Wiley & Sons, Chichester, 2001.

[14] http://www.enercon.de, last accessed January 2007.

[15] C.J.A. Versteegh, "Low speed direct drive PM generator for application in the Zephyros Z72 wind turbine" in *IEE Seminar on Electr. Aspects of Offshore Renewable Energy Systems*, NaREC, Blyth, Northumberland, UK, 2004

[16] http://www.leitwind.com, last accessed January 2007.

[17] J. Pyrhönen, P. Kurronen and A. Parviainen, "Permanent magnet 3 MW low-speed generator development, " in *Proceedings of the International Conference on Electrical Machines (ICEM06)*, Chania, Crete, 2-5 September 2006.

[18] G. Bywaters, V. John, J. Lynch, P. Mattila, G. Norton, J. Stowell, M. Salata, O. Labath, A. Chertok, and D. Hablanian, "Northern Power Systems WindPACT drive train alternative design study report," National Renewable Energy Laboratory, 1617 Cole Boulevard, Golden, CO, report NREL/SR-500-35524, October 2004. Available at http://www.nrel.gov/wind/windpact/drivetrain.html

[19] Corus UK Ltd, "Direct drive: a potential breakthrough technology in wind power generation," *Feasibility Study Report to DTI New & Renewable Energy Programme*, 2004.

[20] S. Engström, "NewGen a new direct drive wind turbine generator," *Nordic Wind Power Conference (NWPC'2006)*, Hanasaari, Espoo, Finland, 22-23 May 2006. http://nwpc.vtt.fi/presentations/engstrom_slides.pdf.

[21] A.J.S. Pippard, "Studies in Elastic Structures," Edward Arnold & Co., London, 1952.

[22] McDonald & Mueller, "Structural analysis of low-speed radial-flux permanent-magnet machines," *to be published in IET Journal of Electric Power Applications*

[23] R.J. Roark, and W.C. Young, "Roark's Formulas for Stress and Strain," McGraw-Hill International Editions, Singapore, 1989, 6th edn.

[24] S. Jöckel, A. Herrmann, and J. Rink, "High energy production plus built-in reliability – the new Vensys 70/77 gearless wind turbines in the 1.5 MW class," in *Technical Track of the European Wind Energy Conference*, Athens, 27th February to 2nd March, 2006.

[25] E. Spooner, and B.J. Chalmers, "'TORUS': a slotless, toroidal-stator, permanent-magnet generator," *IEE Proc. B. Electr. Power Appl.*, vol.139, no.6, pp. 497-506, 1992.

[26] Caricchi, F., Chalmers, B.J., Crescimbini, F., and Spooner, E.: 'Advances in the design of torus machines'. Proc. Int. Conf. on Power Electronic Drives and Energy Systems for Ind. Growth (PEDES), Perth, Australia, 1998, **2**, pp. 516-522

[27] Bumby, J.R., Martin, R., Mueller, M.A., Spooner, E., Brown, N.L., and Chalmers, B.J.: 'Electromagnetic design of axial-flux permanent magnet machines', *IEE Proc. Electr. Power Appl.*, 2004, **151**, (2), pp. 151-160

[28] Söderlund, L., Koski, A., Vihriälä, H., Eriksson, J.-T., and Perälä, R.: 'Design of an axial flux permanent magnet wind power generator'. IEE 8th Int. Conf. on Electr. Mach. and Drives (EMD), Cambridge, UK, 1997, Conf. Publ. no. 444, pp. 224-228

[29] Wang, R.-J., Kamper, M.J., VanderWesthuizen, K., and Gieras, J.F.: 'Optimal design of a coreless stator axial flux permanent-magnet generator', *IEEE Trans. on Magn.*, 2005, **141**, (1), pp. 55-64

[30] COSMOSWorks, SolidWorks Corporation, 300 Baker Avenue, Concord, MA 01742, www.cosmosworks.com

[31] M.N. Hamlaoui, M.A. Mueller, J.R. Bumby, E. Spooner. "Polynomial modelling of electromechanical devices: an efficient alternative to look-up tables", *IEE Proc. – Electrical Power Applications*, **151**, (6), pp. 758-768, (2004).

Appendix

Flat circular plates

Flat circular plate constants

$$C_1 = \tfrac{1+\nu}{2}\left(\tfrac{b}{a}\right)\ln\left(\tfrac{a}{b}\right) + \tfrac{1-\nu}{4}\left(\tfrac{a}{b} - \tfrac{b}{a}\right) \quad (1)$$

$$C_2 = \tfrac{1}{4}\left[1 - \left(\tfrac{b}{a}\right)^2\left(1 + 2\ln\left(\tfrac{a}{b}\right)\right)\right] \quad (2)$$

$$C_3 = \tfrac{b}{4a}\left\{\left[\left(\tfrac{b}{a}\right)^2 + 1\right]\ln\left(\tfrac{a}{b}\right) + \left(\tfrac{b}{a}\right)^2 - 1\right\} \quad (3)$$

$$C_4 = \tfrac{1}{2}\left[(1+\nu)\tfrac{b}{a} + (1-\nu)\tfrac{a}{b}\right] \quad (4)$$

$$C_7 = \tfrac{1}{2}\left(1+\nu^2\right)\left(\tfrac{a}{b} - \tfrac{b}{a}\right) \quad (5)$$

$$C_8 = \tfrac{1}{2}\left[1 + \nu + (1-\nu)\left(\tfrac{b}{a}\right)^2\right] \quad (6)$$

$$C_9 = \tfrac{b}{a}\left\{\tfrac{1+\nu}{2}\ln\left(\tfrac{a}{b}\right) + \tfrac{1-\nu}{4}\left[1 - \left(\tfrac{b}{a}\right)^2\right]\right\} \quad (7)$$

Flat circular plate loading constants

$$L_{11} = \tfrac{1}{64}\left\{1 + 4\left(\tfrac{r_o}{a}\right)^2 - 5\left(\tfrac{r_o}{a}\right)^4 - 4\left(\tfrac{r_o}{a}\right)^2\left[2 + \left(\tfrac{r_o}{a}\right)^2\right]\ln\left(\tfrac{a}{r_o}\right)\right\} \quad (8)$$

$$L_{14} = \tfrac{1}{16}\left\{1 - \left(\tfrac{r_o}{a}\right)^4 - 4\left(\tfrac{r_o}{a}\right)^2\ln\left(\tfrac{a}{r_o}\right)\right\} \quad (9)$$

$$L_{17} = \tfrac{1}{4}\left\{1 - \tfrac{1-\nu}{4}\left[1 - \left(\tfrac{r_o}{a}\right)^4\right] - \left(\tfrac{r_o}{a}\right)^2\left[1 + (1+\nu)\ln\left(\tfrac{a}{r_o}\right)\right]\right\} \quad (10)$$

Cylindrical shells

Cylindrical shell functions

$$F_1 = \cosh(\lambda x)\cos(\lambda x) \quad (11)$$

$$F_4 = \cosh(\lambda x)\sin(\lambda x) - \sinh(\lambda x)\cos(\lambda x) \quad (12)$$

Cylindrical shell constants

$$K_2 = \cosh(\lambda l)\sin(\lambda l) + \sinh(\lambda l)\cos(\lambda l) \quad (13)$$

$$K_3 = \sinh(\lambda l)\sin(\lambda l) \quad (14)$$

$$K_4 = \cosh(\lambda l)\sin(\lambda l) - \sinh(\lambda l)\cos(\lambda l) \quad (15)$$

$$K_{11} = \sinh^2(\lambda l) - \sin^2(\lambda l) \quad (16)$$

$$K_{a1} = \cosh[\lambda(l-a)]\cos[\lambda(l-a)] \quad (17)$$

$$K_{a4} = \cosh[\lambda(l-a)]\sin[\lambda(l-a)] - \sinh[\lambda(l-a)]\cos[\lambda(l-a)] \quad (18)$$